



DELFT UNIVERSITY OF TECHNOLOGY

MSC THESIS REPORT

*Research into the application of
undrained analysis with critical state
soil mechanics approach for the design
of a quay wall*

Author:

F.H. Leferink

Graduation Committee:

Prof. Dr. Ir. S.N. Jonkman

Ir. J.H. van Dalen

Dr. Ir. J.G. de Gijt

Dr. Ir. T. Schweckendiek

Ir. H.E. Pacejka

Delft University of Technology

Delft University of Technology

Delft University of Technology

Delft University of Technology

Municipality of Rotterdam

February 3, 2020

Abstract

The design and construction of quay walls are processes that exist for many centuries and have become more complex and challenging in current engineering practice.

For the design of quay walls a number of guidelines and design codes have been developed over the years. These give the requirements that a quay wall structure should meet, but do also provide some guidance in which steps to take in order to arrive at a proper final design. The relevance of undrained soil behavior, described using critical state soil mechanics, for the analysis of quay wall stability is yet unknown. The main objective of this research is to investigate the possibilities to use the alternative design approach for modelling soil behavior in the design processes of a quay wall. For this, three case studies have been elaborated. The three case studies represents soil profiles consisting 1) predominantly sandy soils, 2) normally consolidated clay and 3) overconsolidated clay. The differences between the analyses and outcomes of the conventional approach and the new approach have been compared for each case study.

Based on the quantitative results of case study 1 and 3, the difference in outcome between the conventional and alternative design approaches is between 0 and 10% for both displacements and sectional forces. The outcome of case study 2 is not in line with the results of case 1 and 3.

Based on the results of the first case study with sandy soil profile, the alternative design approach applied in this report is not a valid option for the design of a quay wall due to the absence of undrained soil conditions. For a soil profile consisting clay, the magnitude of preconsolidation of the soil plays an important role. For the alternative design approach, increasing values of pre-loading results in decreasing values of sectional forces and displacements of the wall. This effect is stronger in comparison to the conventional design approach. In further research the aim should be to increase the reliability of the alternative design approach. This can be done by using in-situ measurements of the displacements of the wall to validate if the model represents the reality accurately.

Contents

Abstract	3
1 Introduction	8
1.1 Problem description & research questions	9
1.2 Method and scope	9
2 Theoretical background	10
2.1 Design of quay walls	10
2.2 Soil mechanics	12
2.2.1 Stress-strain relations	12
2.2.2 Shear strength	12
2.2.3 Horizontal soil stresses	13
2.2.4 Undrained soil behavior	14
2.3 Design methods for quay walls	15
2.3.1 Method of Blum	15
2.3.2 Spring-supported elastic beam model	17
2.3.3 FEM - Plaxis	18
2.4 Developments in dike safety assessment	20
2.4.1 Design process for a dike vs quay wall	20
2.4.2 New design approach for dikes based on critical state soil mechanics	21
2.5 Material models for describing soil behavior	23
2.5.1 Mohr-Coulomb	23
2.5.2 Hardening Soil	23
2.5.3 Soft Soil	24
2.5.4 NGI-ADP	24
2.5.5 Shansep NGI-ADP	26
3 Method	27
3.1 Framework case studies	27
3.1.1 General modelling choices	29
3.1.2 Specific modelling choices per case	31
3.2 Framework for determining soil parameters	32
3.2.1 General soil parameters	32
3.2.2 Shansep model parameters	33

3.2.3	NGI-ADP model parameters	34
4	Case study 1 - Quay wall Amazonehaven	36
4.1	Introduction	36
4.2	Parameters / Boundary conditions	39
4.2.1	Soil profile	40
4.3	Design verification calculation based on theory of Blum	44
4.4	Designs based on conventional design approach	45
4.5	Design based on alternative design approach using cssm	48
4.5.1	Design using D-Sheet	48
4.5.2	Design using Plaxis	49
4.6	Results	50
4.6.1	Discussion	54
4.6.2	Conclusion	54
5	Case study 2 - Amazonehaven modified with normally consolidated clay layer	55
5.1	Parameters / Boundary conditions	56
5.1.1	Type of soil response	56
5.1.2	Soil profile	57
5.1.3	Different scenarios regarding the timing of construction and loading of the wall	57
5.2	Designs based on conventional design approach	59
5.2.1	Design using Plaxis	59
5.3	Design based on alternative design approach using undrained analysis combined with cssm	61
5.4	Results	63
5.4.1	Discussion	65
5.4.2	Conclusion	66
6	Case study 3 - Quay wall situated in overconsolidated clay layer	67
6.1	Introduction	67
6.2	Parameters and Boundary conditions	68
6.2.1	Type of soil response	68
6.2.2	Soil profile	70
6.3	Designs based on conventional design approach	70
6.3.1	Preliminary design based on theory of Blum	71
6.3.2	Design using Plaxis	72
6.4	Design based on alternative design approach using undrained analysis combined with cssm	74
6.5	Sensitivity analysis for historic loads	76
6.6	Results	78
6.6.1	Discussion	80
6.6.2	Conclusion	81
7	Discussion	82
8	Conclusion	84

List of Figures	86
List of Tables	88
A Info about current practise CSSM in dikes and embankments	92
A.1 Approach for determining the critical state friction angle	92
B Finite Element Method	95
C Additional information case study 1: Amazonehaven	97
C.1 D-Sheet calculations	97
D Additional information case study 2: soft soil consisting of clay and peat	98
D.1 Soil investigation data	98
E Additional information case study 3: Boulder clay	105
E.1 Soil investigation data	105

CHAPTER 1

Introduction

The design, construction and use of quay walls are processes that exist already for many centuries. In time, more and more knowledge and experience about quay walls has developed, like the strength, safety, reliability and structural behavior of the wall and the surrounding soil, to name a few. Research into these topics is still being conducted up to this day. One of these research areas is the soil-structure interaction between quay walls and the surrounding soil, and how soil behavior affects this interaction. Sufficient knowledge about the modelling of this interaction will contribute to a safe and cost-efficient design.

In 2017, an alternative approach has been introduced in the Netherlands for the assessment of slope stability of dikes. The prevailing approach based on the theory of Mohr-Coulomb (MC) has been replaced by a new method considering an undrained soil response and using critical state soil mechanics theory (CSSM). Research of several case studies has shown that the application of CSSM in combination with undrained analysis of the soil gives a more accurate description of the behaviour of soft organic clay and peat compared to the conventional approach (van Duinen and van Hemert, 2013). Also, using effective stress shear strength parameters based on triaxial tests often produces high stability factors, which did not always comply with reality (van Duinen, 2013).

Research into this subject is still ongoing, for instance in the Dutch research project *Projectoverstijgende Verkenning Macrostabieliteit* (POVM). One of the research areas is the development and improvement of design tools for assessing the slope stability of the dikes, also taking into account possible structural elements in the dike. The structural elements, for instance sheet pile walls, contribute to the resistance of several failure mechanisms, including slope stability of the dike. To model this soil-structure interaction, often a Finite Element Method is used.

With respect to the slope stability of the dike, the sheet pile wall has two objectives: 1) decreasing the amount of seepage through the dike and 2) soil retention in case of shearing of the soil. In the last case, the sheet pile wall intersects the potential sliding plane of the soil, and the bending stiffness of the structural element will prevent the soil body from sliding. The second objective mentioned above is one of the primary functions of a quay wall. Despite of differences between a dike body and a quay wall in for instance geometry and load cases, there are also similarities. For example, in both cases a difference in horizontal pressure across the structure is present which greatly affects the functioning

of the structure. To gain further insight in the slope stability of quay walls, different constitutive models for describing soil behavior will be investigated.

1.1 Problem description & research questions

For the design of quay walls a number of guidelines and design codes have been developed over the years. These give the requirements that a quay wall structure should meet, but do also provide some guidance in which steps to take in order to arrive at a proper final design. The relevance of undrained soil behavior, described using CSSM, for the analysis of quay wall stability is yet unknown.

The main objective of this research is to investigate the possibilities to use the alternative design approach for modelling soil behavior in the design processes of a quay wall. This objective can be summarized in the following research question:

Can critical state soil mechanics in combination with undrained analysis of the soil be applied for the design of quay walls, and what are the effects for the prediction of strength and stability?

In order to be able to answer the research question, the following sub questions have to be addressed:

1. For which situations / conditions is the new assessment approach for dikes developed, and do these conditions also occur in case of retaining structures?
2. Which failure mechanisms of quay walls can be analyzed using the new approach?
3. How do the results of the new approach compare to the conventional design approach?

1.2 Method and scope

To identify the possibilities for application of this approach for quay walls, three case studies have been elaborated. For each case study, two designs are elaborated. The first design is based on the conventional design approach, following the guidelines and design rules CUR166 (2008) and CUR211 (2014). For the second design the new approach is applied, following the regulations and guidelines prescribed in WBI2017. The scope of this research is the soil characteristics and loading situations for which the new approach could be applied. The three case studies represents soil profiles consisting 1) predominantly sandy soils, 2) normally consolidated clay and 3) overconsolidated clay.

Using different material models in Plaxis, quantities such as the strength and stability of a soil body, the displacements of soil bodies or structures and structural forces can be calculated. Also, this program is able to take into account the effects of pore water pressures and therefore suited to model undrained soil behavior.

The differences between the analyses and outcomes of the conventional approach and the new approach will be compared for each case study.

In this chapter, general background information regarding the design of quay walls is presented. This entails the general characteristics and types of quay walls (section 2.1), basic soil mechanics (section 2.2) and different methods to design and calculate a quay wall structure (section 2.3). Besides this, the new design approach for dikes in the Netherlands is briefly explained in section 2.4. Lastly, in section 2.5 some technical information about the material models used in the FEM software plaxis is presented.

2.1 Design of quay walls

This section provides general background information about quay walls, i.e. functions of quay walls, different types of quay wall structures and different failure mechanisms that can occur. Most part of this section is based on the design guidelines CUR166 and CUR211.

Functions of quay walls

Quay walls are structural elements that enable ships to moor and to exchange cargo and passengers with the land. This can be inside an harbour, along a river or navigation canal but also along canals inside city centres. The quay structure must meet all kind of requirements based on functionality, user demands, soil conditions, water levels, size of the vessels, magnitude of external loads due to mooring and transferring cargo. The main functions of quay walls are (CUR211, 2014):

- Providing berthing facilities for ships
- Retaining the soil body located behind the quay
- Providing the bearing capacity to carry the loads imposed by transshipment of cargo, presence of cranes, other equipment and freight storage facilities
- Act as flood defense for the area behind the quay during periods of high water

Types of quay walls

Given a set of specific functions and boundary conditions that have to be fulfilled, a choice can be made for the design between different types of quay walls. Each type (or combi-

nation of types) has certain characteristics which makes it more suitable for particular design conditions. The main types of quay walls are being described below.

Gravity walls

These structures ensure stability by their self weight, possibly added with the pressure of the soil on top of the structure.

Sheet pile walls

Sheet pile walls ensure stability from the bending capacity of the vertical elements making up the wall, which are fixated deep inside the soil. The elements are connected using interlocks, to ensure soil-tightness. The wall often consists of a combined wall of steel tubular piles with sheet piles in between. The wall can also be anchored to create a support at the top. This type is most common for quay walls in the Netherlands.

Structures with relieving platforms

In this type of quay wall a concrete superstructure is constructed on top of the combined wall at the waterside, and additional support is created by applying concrete bearing piles and anchorages. The structure will reduce the amount of soil behind the quay wall, and will transfer the surcharge loads effectively to the load bearing soil layers, thereby significantly reducing the horizontal soil pressures behind the wall.

Open berth quays (jetties)

In this type of structure, the soil is not retained by a vertical wall but by a slope beneath the berthing platform, covered with revetment. The platform is supported by vertical or inclined bearing piles, and possibly anchorages. This type has the advantage that the soil pressures on the structure are much lower compared to the other types, but more space is required.

Failure mechanisms of quay walls

Depending on the type of quay wall structure, multiple failure mechanisms can occur. For each of these, the requirements for structural safety (ultimate limit state, ULS) or usability (serviceability limit state, SLS) of the structure have fallen short. The most relevant failure mechanisms of a quay wall structure are:

- Exceeding of the horizontal or vertical bearing resistance of the soil
- Exceeding of the resistance for shearing of the soil
- Exceeding of the strength of the wall due to (a combination of) bending moment, normal forces and shear forces
- Exceeding of the strength of anchorage
- Exceeding of the strength of bearing piles
- Loss of global stability of the structure
- Exceeding of the allowable deformations of the wall

The design standards *Eurocode* provide a set of requirements for both ULS and SLS to ensure a certain safety level for the structure. Design guidelines such as CUR166 and CUR211 are based on the Eurocode and have at some points extended requirements. Also, for most designs of quay walls specific requirements have been established in agreement with the client, based on the desired functionality and usability.

2.2 Soil mechanics

2.2.1 Stress–strain relations

In general, a soil consist of a mixture of soil particles, water and air. The space between the soil particles are called pores, and in case of a saturated soil the pores are filled with water. The magnitude of pores of a soil is expressed in the variable of porosity n , and this is an essential property of soils and soil behavior.

The deformations of soils are determined by the effective stresses, which are a measure for the contact forces transmitted between the particles. If the ratio of shear force and normal force exceeds a certain value (the *friction coefficient* of the particles), the particles will start to slide over each other, which will lead to deformations. The deformations caused by shearing of the soil are usually much larger than the deformations in compression. Also, in compression the material becomes gradually stiffer, whereas in shear it becomes gradually softer. This is the stress-dependency of stiffness, and is an essential property of granular soils.

Deformations of soils are irreversible. After a full cycle of loading and unloading of a soil, a permanent deformation is observed. The behavior in unloading and reloading, below the maximum load sustained before, often seems practically elastic, with some additional plastic deformation after each cycle. A soil is said to be overconsolidated if it has been loaded before, by a certain preload. Up to the stresses of the preload, the soil will behave relatively stiff. When the stresses exceed the stress of the preload, the soil will behave relatively soft again.

A very characteristic property of relatively dense soils is the ability to increase in volume if loaded in shear. This is called dilatancy. If dilatancy occurs in a saturated soil, water must be attracted to fill the additional pore space. If this process cannot occur fast enough, an under pressure in the pores can occur, resulting in temporary higher effective stresses. The reverse effect can occur in case of very loosely packed sand, and this is called contractancy. At continuing deformations both dense and loose sand will tend towards a state of average density, sometimes denoted as the critical density. At high stresses the critical density is somewhat smaller than at small stress.

2.2.2 Shear strength

The shear strength of a soil is generally defined by Coulomb:

$$\tau = c' + \sigma'_v \cdot \tan \phi' \quad (2.1)$$

Combined with Mohr's circle this results in the Mohr-Coulomb (MC) failure criteria. The MC-failure criteria are used in several models for describing soil behavior. Equation 2.2 gives the definition of the failure criterion for one principle direction.

$$\frac{(\sigma'_1 - \sigma'_3)}{2} - \frac{(\sigma'_1 + \sigma'_3)}{2} \sin \phi' - c' \cot \phi' = 0 \quad (2.2)$$

where:

ϕ' = friction angle

c' = cohesion

σ'_1 = major principal effective stress

σ'_3 = minor principal effective stress

The strength parameters c' and ϕ' are not constants, but are dependent on several factors such as effective stresses, relative density and compaction. For clays the Mohr-Coulomb criterion is reasonably well applicable, provided that the influence of the pore pressures is taken into account.

2.2.3 Horizontal soil stresses

The horizontal soil pressure can be expressed as a function of the cohesion and the vertical soil pressure by means of applying a *coefficient for lateral earth pressure* K . If the soil is not subjected to lateral movement and there are no external horizontal forces action on the soil, the neutral soil pressure is present. The relation for the coefficient of neutral soil pressure found by Jáký (1948) is often used, which reads:

$$K_0 = (1 - \sin \phi)OCR^{\sin \phi} \quad (2.3)$$

If the soil is subjected to horizontal displacements, the horizontal soil pressures changes. In case of a retaining wall moving away from the soil, the horizontal pressure reduces. When the extreme value is reached, this is called the active soil pressure. When the retaining wall moves towards the soil, the horizontal soil pressure increases until the passive soil pressure is reached. Several relations have been derived to determine the coefficients for active and passive soil pressure, for instance by Rankine, Coulomb, Müller-Breslau or Culmann and Kötter. Primary difference between the methods is the way the slip surface is determined, and if this sliding plane is either straight or curved.

Stress paths

Stress paths are diagrams that represent the stresses in a specific point by two characteristic parameters. Important aspect is what parameters to choose for drawing stress paths, for instance:

- average stress (isotropic stress) $\frac{1}{3}(\sigma_1 + \sigma_2 + \sigma_3)$ versus the difference of major and minor principal stress $\sigma_1 - \sigma_3$
- mean effective (plane strain) stress $\frac{1}{2}(\sigma_1 + \sigma_3)$ versus deviatoric stress $\frac{1}{2}(\sigma_1 - \sigma_3)$

If effective stress parameters are used, the stress path is called an *effective stress path* (ESP). The effective stress paths for dilatant and contractant material show a different graph, see Figure 2.1. Here, for both a dilatant and a contractant soil the stress paths are drawn. The upper blue line represents the shear strength of the soil (Equation 2.1). For a dilatant soil, the ESP moves to the right which means that the shear strength increases with increasing normal stresses. For a contractant soil, the ESP bends slightly to the left, which means that after only a very small increase in normal stress (σ) the shear strength of the soil is reached.

The distance between effective stress path and total stress path represents the pore pressure. Besides dilatant or contractant behavior, stress paths can be used to visualize many more features of soil behavior, for example drained soil behavior versus undrained soil behavior.

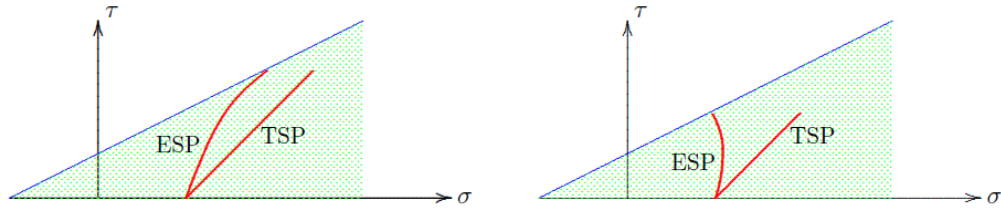


Figure 2.1: The left figure shows stress paths of a dilatant soil, the right figure shows stress paths of a contractant soil. (Verruijt, 2012)

2.2.4 Undrained soil behavior

For modelling the behavior of soils and the response of a soil to an external load and/or displacements or settlements of the soil, a good understanding of the interaction between soil particles and pore water is essential. When a soil is subjected to compression, the porosity of the soil decreases and in case of shear the porosity can either decrease (contractant behavior) or increase (dilatant behavior). In case of a small permeability of the soil, it will take time for the pore water to adjust to the new situation and reinstate equilibrium conditions (hydrostatic pore pressures). This process is called consolidation.

Undrained behavior of a soil takes place when there is no sufficient time for the inflow of water into the pores, or outflow of water from the pores as a reaction to new boundary conditions. The change in pore pressures will affect the effective soil stresses and therefore the strength and stiffness of the soil, until the soil is consolidated again.

When only considering the total soil stresses, the strength of the soil can be characterized by a cohesion only, which is denoted as c_u , the undrained shear strength of the soil. Assuming isotropic effective stress conditions and using the MC failure criterion (Equation 2.2), as a first approximation the undrained shear strength can be estimated by equation 2.4.

$$c_u = \frac{\sigma'_1 - \sigma'_3}{2} = c' \frac{\cos \phi'}{1 - \frac{1}{3} \sin \phi'} + \sigma'_0 \frac{\sin \phi'}{1 - \frac{1}{3} \sin \phi'} \quad (2.4)$$

where: σ'_0 = initial mean effective stress

This equation indicates that if $\phi' > 0$ the undrained shear strength c_u increases with increasing initial mean effective stress σ'_0 .

However, this formula is derived under the assumption that a volume change can be produced only by a change of the average effective stress. So anisotropy, dilatancy/contractancy etc. are not accounted for, and the formula is only a first approximation!

Hydrodynamic period

To quantify if a soil layer responds predominantly in a drained or undrained way, Vermeer and Meier (1998) have derived the hydrodynamic period T :

$$T = \frac{kE_{oed}t}{\gamma_w L^2} \quad (2.5)$$

where:

k = permeability of the soil

E_{oed} = Oedometer stiffness
 γ_w = volumetric weight of pore water
 L = drainage length
 t = time

Limit values are given for this parameter, indicating drained or undrained behavior considering one-dimensional consolidation. It is stated that for values of $T < 0.01$ a loading situation can be considered undrained. For $T > 0.4$, sufficient consolidation can take place and the situation can be modelled as drained. For values of T in between these limits, the most unfavourable situation should be considered.

In practice this means that the type of soil response is determined by the physical properties of the soil, but also by the thickness of the soil layer, the duration of the load, and the speed at which displacements or changes in pore pressures occur.

2.3 Design methods for quay walls

In this section the theoretical background of the design methods is given. First the method of Blum is explained, which entails a basic, conservative approximation of the minimum required sheet pile length and the cross-sectional forces in the wall.

Secondly, a more accurate model based on the Euler-Bernoulli beam theory is covered. Here the retaining wall is modelled as a spring-supported beam where the soil behaves linear elastic. The software program D-Sheet Piling is used for this method.

Lastly, the approach using the Finite Element Method is described. This method has the advantage of offering possibilities to describe the behavior of the soil in more detail and more accurately, using a variety of material models. The software program Plaxis is used for this method.

2.3.1 Method of Blum

To ensure the horizontal and rotational equilibrium of a sheet pile wall, Blum has developed an approach in which the required length of the sheet pile can be calculated in an analytic way. The basic principle of Blums method of analysis is that the sheet pile wall is considered as fully clamped at its toe, with the additional condition that the bending moment at the toe is zero. A shear force R can be present at the level of the assumed clamped edge. It is assumed that during failure the deformations are sufficient to generate full active or passive soil pressures on each side of the wall.

By analyzing all forces acting on the wall and using the condition that the displacement of the top of the wall has to be zero (due to an horizontal ground anchor), the required embedded depth of the wall and thereby the required length of the wall can be calculated. In Figure 2.2 a schematization of the situation with the acting forces on the wall are presented.

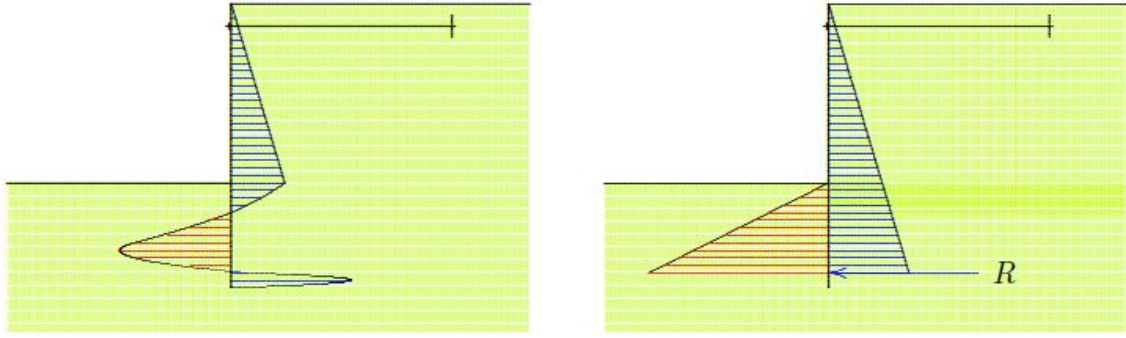


Figure 2.2: Schematization of Blum for a situation with homogeneous soil profile. In the left figure the internal stresses in the wall are shown. The right figure shows the pressures due to soil and groundwater, acting on the wall. (Verruijt, 2012)

To enable the generation of the concentrated force R , the wall should be given some additional length. This is done by choosing the length of the wall somewhat larger than the theoretical value computed in the analysis. Schematizing the structure in this way results in somewhat lower bending moments in the wall, but a larger length of the wall is required.

The Blum calculation is performed using a script which is based on the examples given in Verruijt (2012). The coefficients of lateral soil pressure are determined using the Müller-Breslau method, see also 2.2.

Müller-Breslau assumes straight slip surfaces, but also takes into account the wall friction δ (Deltares, 2017);

$$K_a = \frac{\cos^2 \phi'}{\left(1 + \sqrt{\frac{\sin \phi' \sin(\phi' + \delta)}{\cos \delta}}\right)} \quad (2.6)$$

$$K_p = \frac{\cos^2 \phi'}{\left(1 - \sqrt{\frac{\sin \phi' \sin(\phi' + \delta)}{\cos \delta}}\right)} \quad (2.7)$$

with: ϕ' = effective friction angle of the soil

δ = friction angle between soil and wall

Modelling undrained soil behavior with the method of Blum

The method of Blum does not take into account undrained soil behavior.

Also, the way Blum's theory schematizes the soil stresses on the wall neglects certain features of real soil behavior, i.e. stiffness properties and stress-dependency. This makes the results only a first estimate of the required length of the wall and forces that are being generated.

2.3.2 Spring-supported elastic beam model

The spring-supported elastic beam model is a design method which enables the implementation of more complicated boundary conditions. In this model the behavior of the soil is modelled by uncoupled elasto-plastic springs. The reaction forces of the soil depend on the properties of the soil, the geometry of the elastic supported beam and the magnitude of the displacements. The reaction forces of the soil are expressed in terms of force per meter length, and can be determined using the following relationship:

$$p = k \cdot w \quad (2.8)$$

with:

p = soil pressure per unit area [kN/m^2]

k = modulus of subgrade reaction [kN/m^3]

w = displacement [m]

For the elasto-plastic analysis of the soil a schematization has to be made of the horizontal soil pressures as function of the displacement of the wall. As already described in Chapter 2.3.1, the simplistic model of Blum states that the soil immediately behaves as fully plastic. Based on the direction of the deformation of the wall the soil reaches either the active or passive soil pressure. The spring-supported elastic beam model however, states that the soil reaches the active or passive soil pressure only after a certain displacement takes place. In between these two extreme values, the soil behaves linear elastic and the soil pressure depends on the magnitude of the displacement of the wall. When no displacement has occurred yet, the soil is in the neutral state and the horizontal stresses in the soil equals the neutral soil pressure.

The software D-Sheet Piling calculates the soil pressures for many points along the wall. Because the soil pressures, displacements, water pressures and internal forces in the wall are all correlated, the calculations are performed in an iterative manner.

Also, multiple construction stages can be defined, taking into account the stress and strain history from previous steps. The effects of creep and arching of the soil are neglected (CUR166, 2008).

The coefficients of active and passive soil pressure can be determined with several methods. In D-Sheet, three approaches are available: the method of Culmann and method of Müller-Breslau which both use straight sliding planes, and the method of Kötter which uses a curved sliding plane. It is also possible to enter the coefficients, and other parameters, manually. An example of the interface of D-Sheet is given in Figure 2.3.

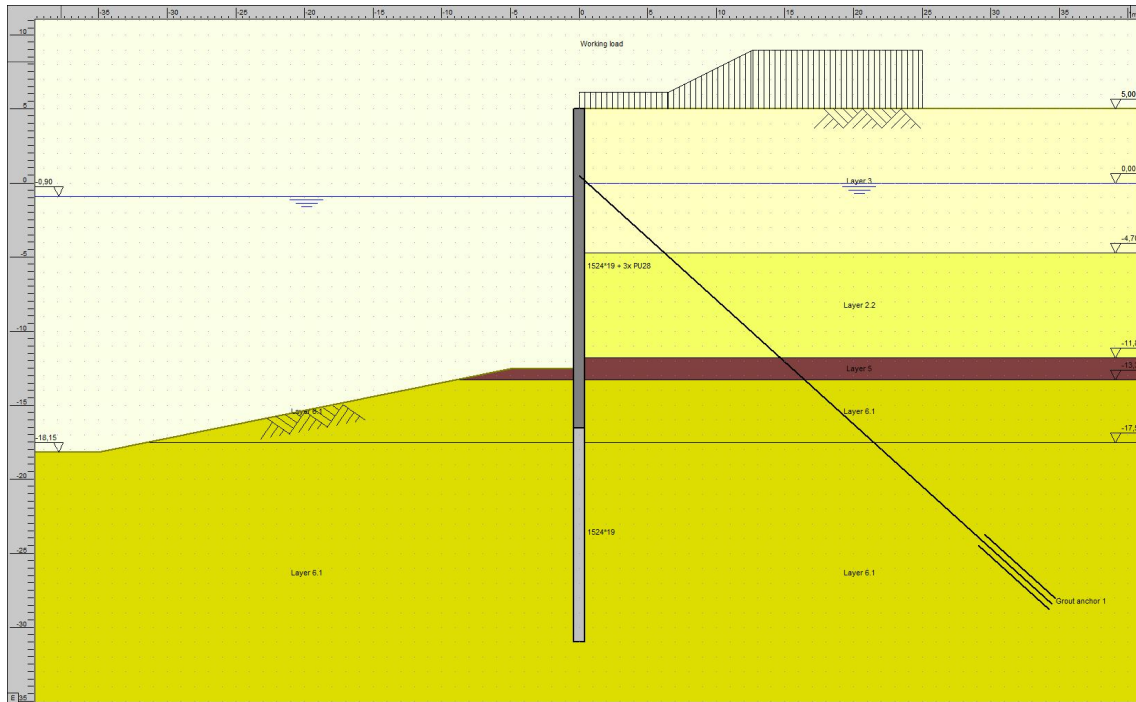


Figure 2.3: Example of a retaining wall in D-Sheet Piling

Undrained soil behavior in D-Sheet Piling

D-Sheet Piling does not take into account undrained conditions and undrained soil behavior. The undrained shear strength could be determined by stating that in undrained conditions $\phi' = 0$ and the undrained cohesion c_u represents the undrained shear strength. The analysis, in which the friction of the material and the pore pressures are neglected, is called an undrained analysis. In general the following relation holds:

$$s_u = \frac{1}{2}(\sigma_1 - \sigma_3) \quad (2.9)$$

When assuming that in a saturated soil there can be practically no volume change in undrained conditions, the isotropic effective stress remains constant. In case of failure, the major and minor principle stresses σ'_1 and σ'_3 must satisfy the Mohr-Coulomb failure criterion. Combining this information with Equation 2.9 results in the following relation for the undrained shear strength (Verruijt, 2012):

$$s_u = \frac{\sigma'_1 - \sigma'_3}{2} = c \frac{\cos \phi}{1 - \frac{1}{3} \sin \phi} + \sigma'_0 \frac{\sin \phi}{1 - \frac{1}{3} \sin \phi} \quad (2.10)$$

This formula does not take into account the effects of anisotropy and dilatancy, and is therefore only a first approximation. Also, when the situation occurs that the excess pore pressures in the soil can dissipate without a decrease in loading, this relation is not valid anymore.

2.3.3 FEM - Plaxis

Plaxis is a software package that uses a finite element method that enables the analysis of deformation, stability and groundwater flow in geotechnical engineering. It is widely

used in practice for a variety of design and engineering problems. The software offers a variety of models to describe the mechanical behavior of soils and rocks, both very basic models which serve as crude approximations, but also more advanced models which take into account essential properties of soil behavior such as stress-dependency of stiffness, anisotropy and time dependencies.

The Plaxis software will divide the model space into a number of elements (mesh). For each element, both stresses and strains are calculated using predefined constitutive relations. These relations differ for each material model that can be assigned to a certain soil layer in the program. The material models which are used in this research, along with their essential properties, are briefly covered in section 2.5.

2.4 Developments in dike safety assessment

In this section the main properties and characteristics of a dike are presented, and how this relates to the properties of a quay wall. Also, the new design approach for dikes is explained.

2.4.1 Design process for a dike vs quay wall

The primary function of a dike is to retain water. A dike should therefore be sufficiently high, and also be able to withstand the horizontal water pressures and possible wave attacks. Figure 2.4 shows an example of a typical dike with its most important elements.

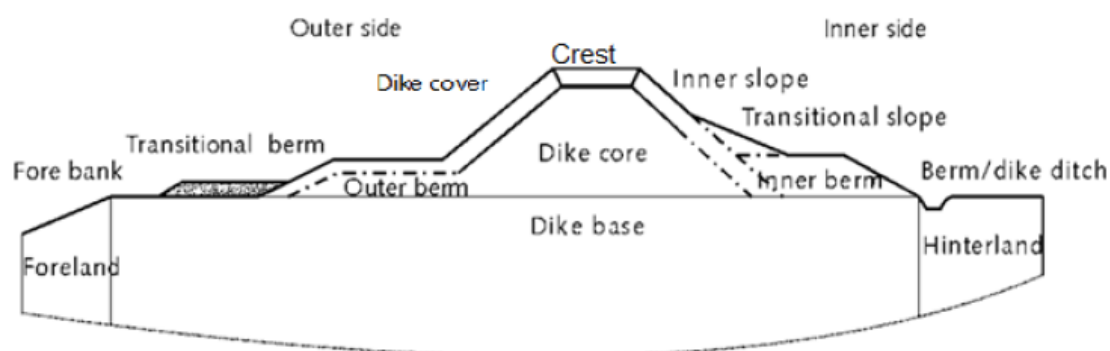


Figure 2.4: General overview of dike showing the most important elements. Source: Jonkman et al. (2018)

Due to the difference in water levels between the inner and outer side of the dike, seepage through (and underneath) the dike will occur. To prevent this, the dike body should be constructed to be sufficiently impermeable for the water to flow through. Often the dike core or dike cover is constructed of clayey soil with a low permeability. This will prevent seepage and possible outflow of soil from the dike. However, due to the increased hydrostatic pressure acting on the dike at times of high water, the pore water pressures inside the dike core and dike cover will increase as well, which results in a decrease of the effective soil pressure. Most importantly, a lower effective soil pressure results in a lower shear strength of the soil (see equation 2.1) and hence can result in slope instability.

This effect can be countered in several ways, the most commonly used is increasing the dike width, i.e. reducing the slope steepness of the dike. At places with limited available space other strength increasing measures are applied, such as inserting stability screens inside the dike body. Figure 2.5 gives an example of a sheet pile wall constructed inside the dike body, connected with grout anchors.

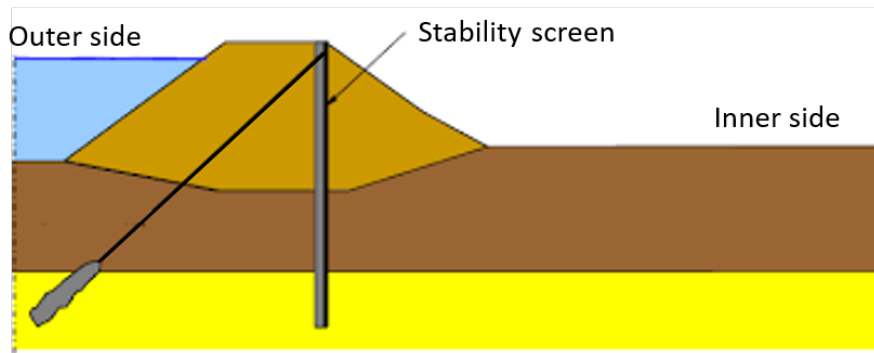


Figure 2.5: Example of a dike with a stability screen. In this case there are grout anchors applied along the screen, to provide more horizontal support if the soil body starts shearing. Source: POVM

The assessment regarding strength and stability of a dike with stability screen shows some similarities with that of a quay wall. Most important, in both cases there are one or more structural elements situated inside the geotechnical body to prevent large deformations and sliding of the soil, in the case the shear resistance of the soil is exceeded. However, the new design approach is developed for the specific situation where there is a high water level on one side of the dike. So the external load is caused by a horizontal (hydrostatic) water pressure. In case of a quay wall, the external load working on the wall is caused by a difference in retaining height in combination with surcharge loads. This has consequences for the development of soil stresses when the structure is experiencing the expected loads.

During a high water wave the dike is loaded by horizontal pressures in the form of a hydrostatic water table. The dominant phenomenon here is thus that the total soil pressures are increased due to an increase in water pressures. Because of the low permeability of the dike body this will result in excess pore pressures.

For the quay wall holds that the total soil pressure increases due to additional surcharge at the surface level. Difference here is that the surcharge acts as effective vertical soil pressure at the surface level of the retaining side of the wall. However, if the permeability of the soil is relatively small compared to the load duration or speed of loading, the pore water pressures cannot follow the new stress situation and excess / deficit pore water pressures will occur.

2.4.2 New design approach for dikes based on critical state soil mechanics

With respect to the previous assessment round of primary flood defences several changes have been implemented regarding the modelling of soil behavior. The most important changes are (Rijkswaterstaat, 2017):

1. the switch of the Mohr-Coulomb model to Critical State Soil Mechanics theory for describing the soil behavior.
2. differentiate between drained and undrained behavior of the soil during failure and using the SHANSEP method to determine the undrained shear strength during the critical loading situation. Section 2.5 will give more information about how the undrained behavior of the soil is modelled with this new approach.

Introduction of cssm framework

The critical state is defined as the density state where the granular materials shear at a constant volume and stress state. At this state, the dilatancy rate diminishes and approaches zero. The critical state framework determines the shear strength of the soil based on the ultimate strength instead of the peak strength of the soil, distinguishing between normally consolidated and overconsolidated soils (Rijkswaterstaat, 2017).

In the normally consolidated phase of the soil, the failure envelope is described using the following formula:

$$t_{max} = s' \sin \phi'_{cv} \quad (2.11)$$

where:

- t_{max} the maximum mobilized shear strength,
- s' the mean effective stress $\frac{1}{2}(\sigma_v + \sigma_h)$,
- ϕ'_{cv} the critical state friction angle

The shear strength of the soil is based on the mean effective stress in the soil (s') and the critical state friction angle ϕ'_{cv} . Connecting the values of t_{max} for different stress states will give a line with slope $\sin \phi'_{cv}$. This line represents the critical state line and connects the peaks of the Mohr's circles at failure of the soil. See Figure 2.6 for a graphical representation. In this approach the cohesion is not explicitly taken into account, but is incorporated in the over consolidation ratio (OCR).

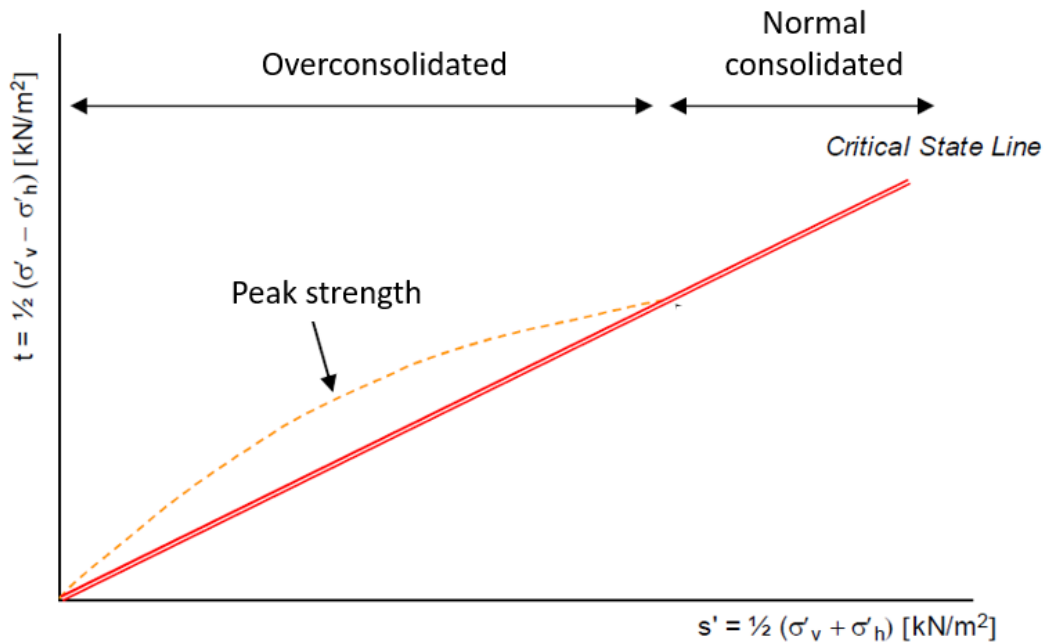


Figure 2.6: Shear strength according to CSSM. (Rijkswaterstaat, 2017)

In the normally consolidated state of the soil, there is no cohesion. In the overconsolidated state, the cohesion provides the additional strength resulting in the peak strength. The behavior of soil during undrained loading situations is determined by the local conditions

of the soil. These are expressed in terms of the yield stress σ_{vy} and the OCR.

Next to the critical state framework, also the soil behavior based on an undrained response is introduced for the assessment of slope stability. The primary and most essential change is the use of the NGI-ADP model Grimstad (2011). This model aims to predict and describe the undrained soil behavior based on undrained strength and stiffness parameters, and taking into account anisotropy of the soil. For the detailed calculations at the stage near failure, the model is adjusted to determine a new stress state based on the SHANSEP theory. More information about these models can be found in section 2.5.

2.5 Material models for describing soil behavior

In this section a number of models are described which are used in the FEM software PLAXIS to model essential features of soil behavior. Each model has different characteristics and has its own advantages and limitations for various applications.

2.5.1 Mohr-Coulomb

The Mohr-Coulomb soil model describes the soil behavior as linear elastic perfectly plastic and can be used to obtain a first estimate of the deformations. Because it is perfectly plastic, there is no hardening or softening of the soil taken into account in this model. Mohr-Coulomb can not model the critical state of the soil, because the dilatancy continues forever during plastic shearing.

In the Mohr-Coulomb model, undrained behavior could be modelled by setting the friction angle ϕ equal to zero and the cohesion c to c_u , the undrained shear strength. However, when using this approach only the undrained shear strength is taken into account. Regarding the stiffness of the soil, still the drained situation is assumed. Also, this model does not take into account the process of consolidation, and therefore with this approach caution is required for loads of longer duration (Plaxis, 2018).

2.5.2 Hardening Soil

The Hardening Soil (HS) material model takes into account the stress dependent stiffness behavior of soils, by using a power-law formulation for the stiffness parameters. It also has multiple stiffness parameters: for primary loading the secant stiffness E_{50} and the unloading/reloading stiffness E_{ur} . These properties are visualized in Figure 2.7. HS takes into account the compression hardening and the shear hardening of the soil. *Compaction hardening* is used to model plastic strains that are generated during primary compression. The *shear hardening* includes the generation of plastic deviatoric strains by mobilizing the materials internal friction. During this process the stiffness of the soil slowly decreases.

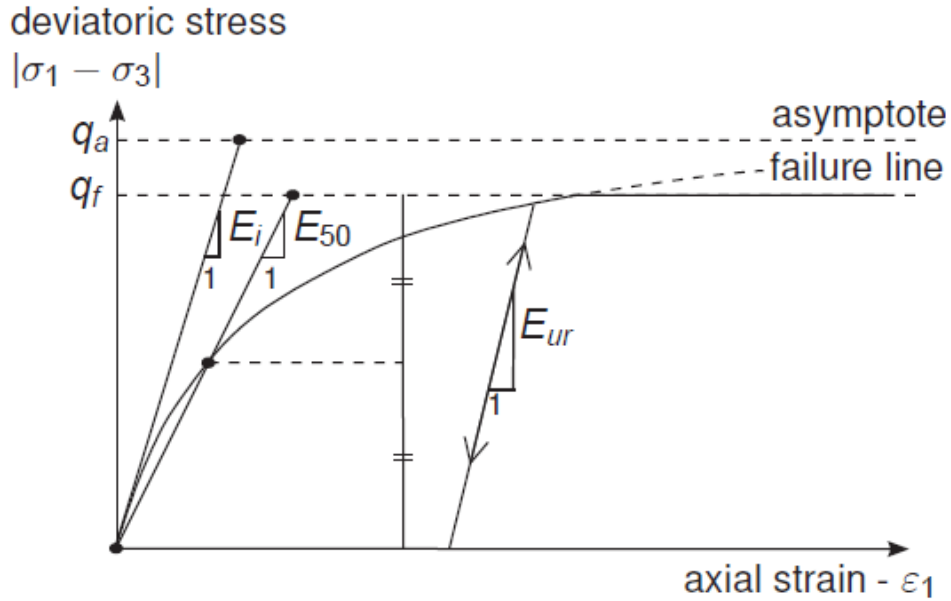


Figure 2.7: Hyperbolic stress-strain relation of sand in primary loading for a standard drained triaxial test. (Plaxis, 2018)

In 2.7 it is shown that the Hardening Soil model takes into account the stress- and strain dependency of the stiffness. The initial stiffness E_i for instance has a larger value than the secant stiffness E_{50} at 50% of the maximum strength of the soil. The Hardening Soil small strains (HSss) material model is particularly suited for situations where small strains occur. The application of cssm however, considers the critical state where very large strains are present. Therefore the HSss model is not taken into account in this study.

2.5.3 Soft Soil

The Soft Soil (SS) material model may be used for near normally consolidated clay-type soils (Plaxis, 2018). This class of materials is best characterized by their high degree of compressibility. Compared to normally consolidated sands, the normally consolidated clays behave up to ten times softer. For these extreme compressibility the Soft Soil model is suitable.

This model takes into account the stress-dependency of soil stiffness, distinction between primary loading and unloading-reloading and uses the Mohr-Coulomb failure criterion, similar to the Hardening Soil model. Important difference is the logarithmic dependency between stresses and strains, compared to the hyperbolic relation in the HS model.

2.5.4 NGI-ADP

The NGI-ADP model may be used for bearing capacity, deformation and soil-structure interaction analyses involving undrained loading of clay (Plaxis, 2018). Distinction is made between three different stress states; compression (Active mode), neutral (Direct Simple Shear mode) and extension (Passive mode). For each mode, both the undrained shear

strength and the shear strain at failure are defined. This way the model takes into account the anisotropy of undrained shear strength and stiffness of the soil.

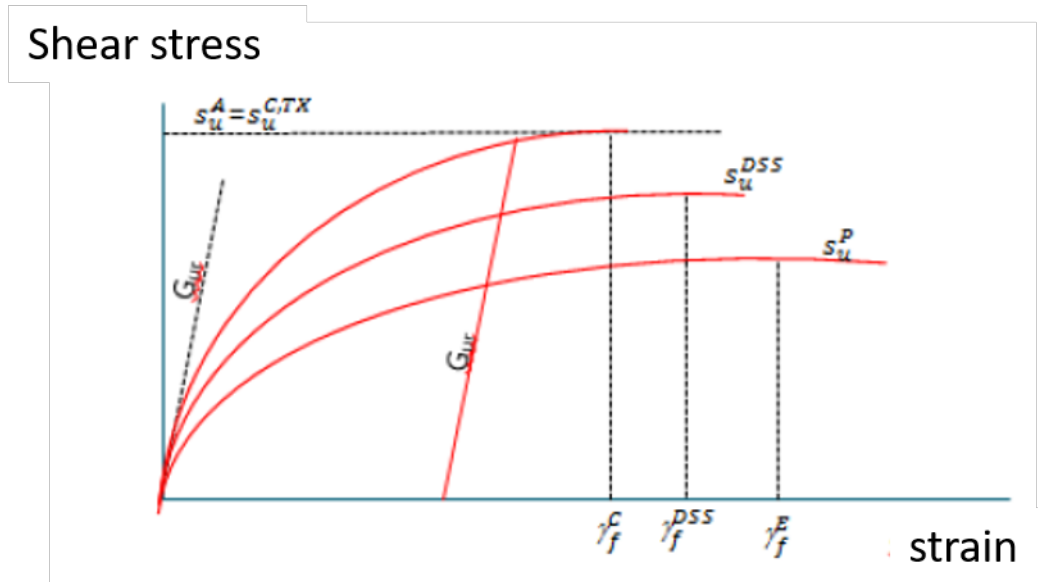


Figure 2.8: Stress-strain relation of clay and peat. The three curves represent the results of an undrained triaxial compression test (s_u^A), an undrained triaxial extension test (s_u^P) and a Direct Simple Shear test (s_u^{DSS}). G_{ur} defines the isotropic elasticity of the soil. (Naves and Lengkeek, 2017)

A list of the model variables of the NGI-ADP model is given in Table 2.1.

Symbol	Description
G/s_u^A	Ratio unloading/reloading shear modulus over (plane strain) active shear strength
γ_f^C	Shear strain at failure in triaxial compression
γ_f^E	Shear strain at failure in triaxial extension
γ_f^{DSS}	Shear strain at failure in direct simple shear
$s_{u,ref}^A$	Reference (plane strain) active shear strength
$vert_{ref}$	Reference depth
$s_{u,inc}^A$	Increase of shear strength with depth
s_u^P/s_u^A	Ratio of (plane strain) passive shear strength over (plane strain) active shear strength
τ_0/s_u^A	Initial mobilized shear resistance
s_u^{DSS}/s_u^A	Ratio of direct simple shear strength over (plane strain) active shear strength
ν	Poisson's ratio
ν_u	Undrained Poisson's ratio

Table 2.1: Shansep NGI-ADP model variables. (Brinkgreve and Panagoulas, 2017)

2.5.5 Shansep NGI-ADP

The Shansep NGI-ADP material model is a user defined material model which combines the NGI-ADP material model with the SHANSEP (Stress History And Normalized Soil Engineering Properties) concept. The advantage of this model is that it is able to simulate potential changes of the undrained shear strength based on the effective stress state of the soil (Brinkgreve and Panagoulas, 2017).

The undrained shear strength of the soil is determined using the SHANSEP method (Ladd, 1974):

$$s_u = \sigma'_{vi} \cdot S \cdot OCR^m \quad (2.12)$$

S and m are normalized soil parameters. The variable S determines how fast and to which extend the stress path bends away from the vertical to the left, and reaches the CSL. The power m determines to what extend the effect of the load history (σ'_{vy} and OCR) influences the undrained shear strength. The value of m can be between 0.5 and 1.0 where $m = 1.0$ represents linear elastic soil behavior.

The over consolidation ratio OCR depends on the site characteristics, actual stresses and loading history.

$$OCR = \frac{\sigma'_{vy}}{\sigma'_{vi}} \quad (2.13)$$

where:

σ'_{vy} yield stress,
 σ'_{vi} in-situ effective stress.

This material model is developed such that at first it models the soil using the properties of the NGI-ADP model. Only after the user activates a switch, the Shansep - MC material model is being activated and the new soil stresses are calculated according the relation given in equation 2.12. The value of σ'_{vi} in equation 2.12 is being extracted from the output of the last calculation step, and the yield stress (or pre-consolidation stress) is the highest stress level the soil has experienced until that moment.

This chapter describes the procedure that has been used to elaborate the case studies. This includes the specific applications of the different design methods for the case studies, important modelling choices and assumptions that have been made.

3.1 Framework case studies

To help answer the main research question ” *Can critical state soil mechanics in combination with undrained analysis of the soil be applied for the design of quay walls, and what are the effects for the prediction of strength and stability?*”, three different case studies of a quay wall are elaborated. The primary difference between the case studies is the soil profile surrounding the quay wall. All other variables such as different loading types, the retaining height and the geometry of the quay wall, the strength and stiffness of the structural elements, and the construction phases are all kept constant across the case studies. Each case study covers a different type of soil profile for the Holocene part of the soil, namely:

- Case study 1: soil profile consisting of mainly sandy soils.
- Case study 2: soil profile where the Holocene part of the subsoil contains a normal consolidated clay layer. In this case study the effects of the alternative design method on soft soils are investigated. The anisotropy of the soil along the sliding plane will be taken into account in this case study.
- Case study 3: soil profile where the Holocene part of the subsoil contains an over-consolidated clay layer. In this case study, both the anisotropy of the soil along the sliding plane and the stress history of the clay layer are taken into account.

An overview of the three case studies is presented in Figures 3.1 up to Figure 3.3. The figures are adapted from the Plaxis user interface.

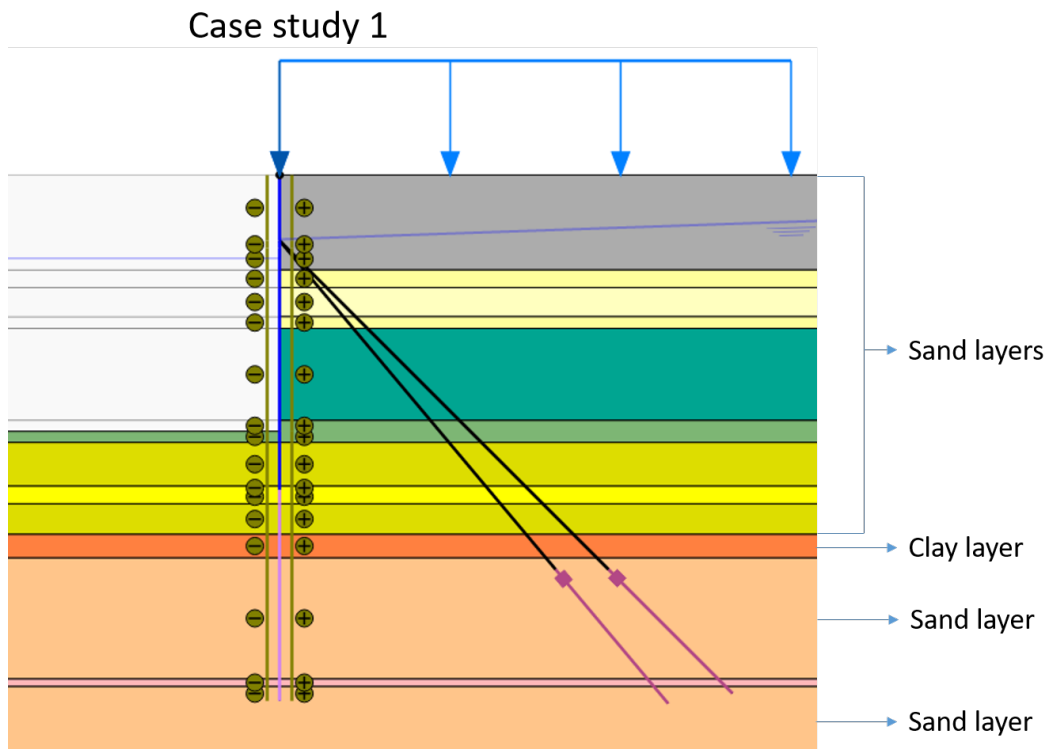


Figure 3.1: Overview of soil layers and soil types for case study 1.

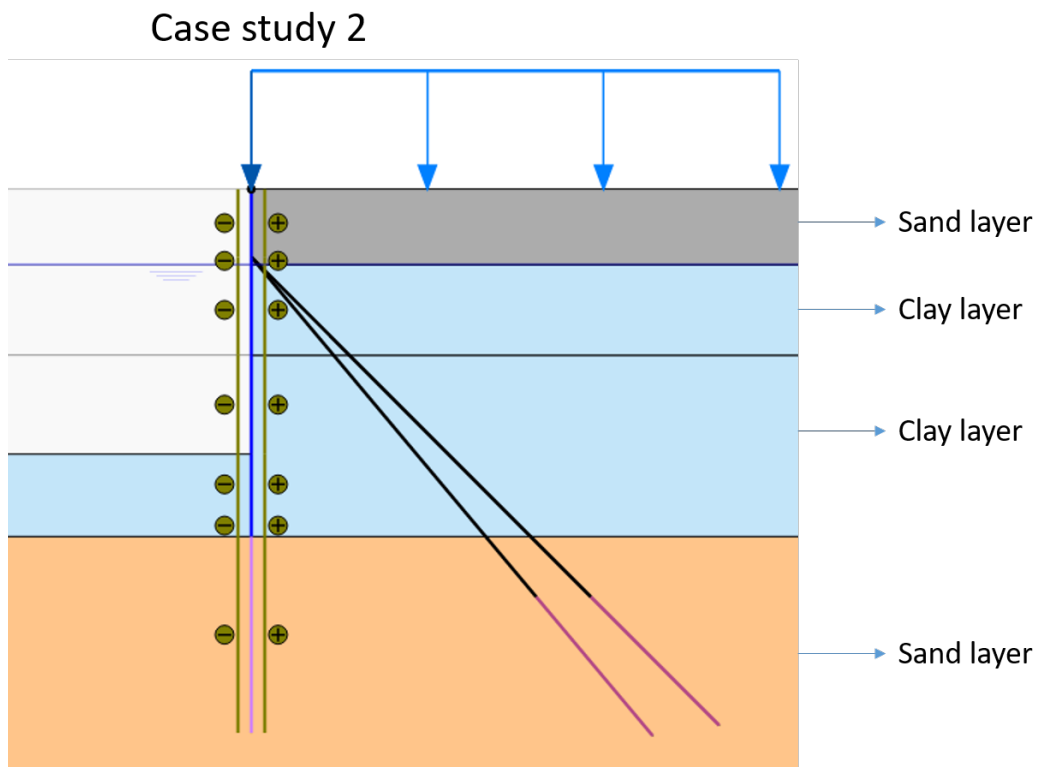


Figure 3.2: Overview of soil layers and soil types for case study 2.

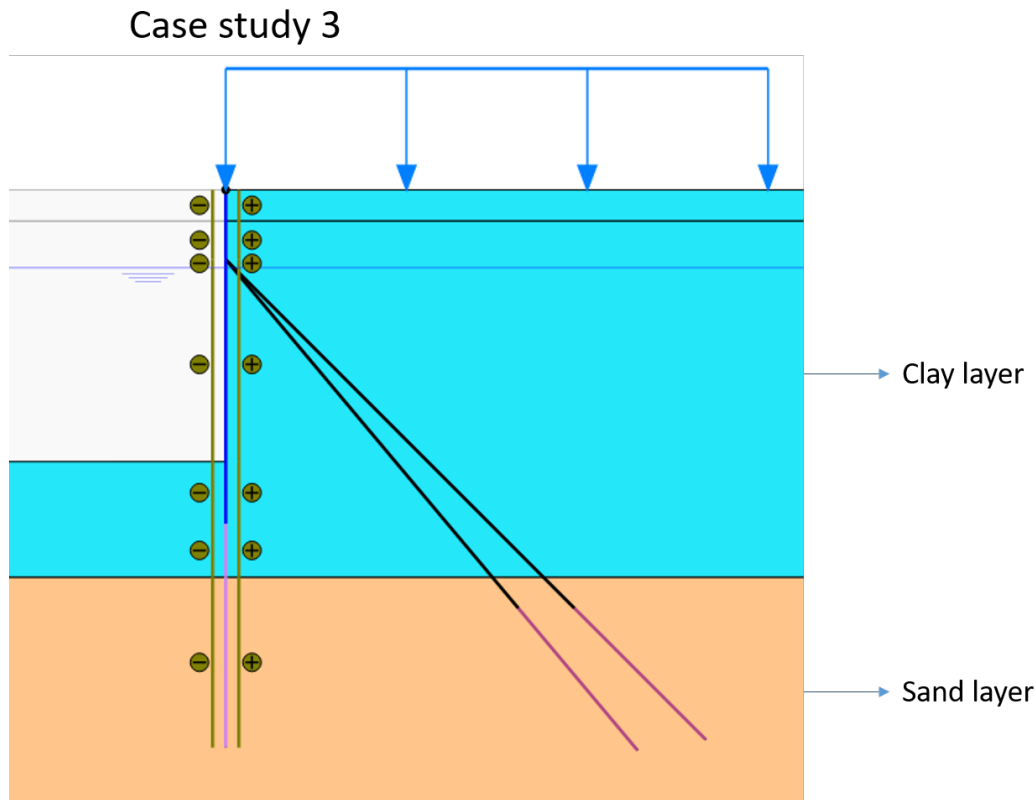


Figure 3.3: Overview of soil layers and soil types for case study 3.

For each case study, two different design calculations will be performed.

1. Design calculations based on the **conventional design approach**. For the detailed calculations D-Sheet or Plaxis are used, in accordance with the guidelines presented by CUR166 (2008) and CUR211 (2014).
2. Design calculations based on the **alternative design approach**. Here the Plaxis material model NGI-ADP Shansep model is recommended by POVM when analyzing a stability screen inside a dike body. Therefore this material model will be applied in the plaxis calculations, when performing an undrained analysis of a quay wall using the alternative design approach.

3.1.1 General modelling choices

Characteristic values versus mean values

For the alternative design approach, no partial safety factors are deduced for quay walls so far. Therefore, in this research the mean value for each of the design parameters will be used for both the conventional and alternative design approach. This approach ensures that the input used for the calculations is identical.

The results of the design calculations are quantified using the maximum displacements of the quay wall and the sectional forces of the quay wall. A comparison is made between the values of these quantities found using both design approaches. The relative difference between the results will give an indication whether the alternative design approach shows any promising results.

Software used for the conventional design approach

The results of the conventional design approach are generated using the software programs D-Sheet Piling and Plaxis. For D-Sheet Piling, the strength parameters are obtained from triaxial compression tests, and the stiffness parameters are obtained from design calculations of the reference project.

For the plaxis calculations, the material model Hardening Soil is used for both sand and clay layers. Specific correlations that are used to determine the model parameters are given in appendix B.

Also, a preliminary calculation is performed using the method of Blum. The result of this calculation is used as starting point for the detailed design.

Software used for the alternative design approach

For the alternative design approach only calculations in Plaxis are performed. Essential for this approach is the modelling of undrained soil behavior. Both D-Sheet Piling and the method of Blum do not have the ability to perform this.

For every soil layer, an analysis is made whether an undrained response of the soil is expected. In that case, soil layers below the phreatic surface consisting of clay are modelled using the NGI-ADP-Shansep material model. Sand layers as well as clay layers above the phreatic surface have to be modelled using a drained analysis where the strength parameters at the critical state are used. (POVM BEEM, 2018). For the calculations, different construction phases have been defined.

An overview of these phases is presented in Figure 3.4

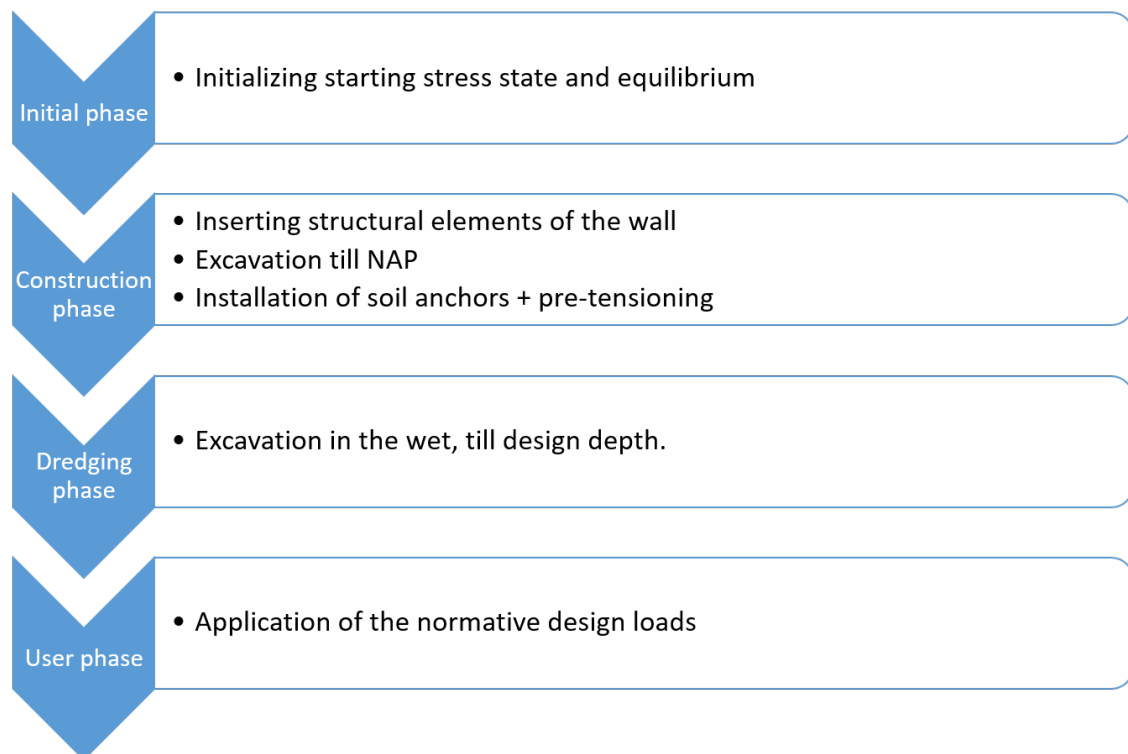


Figure 3.4: Overview of construction phases used in the calculations

3.1.2 Specific modelling choices per case

Case study 1 - quay wall Amazonehaven

For the first case study, the Amazonehaven quay wall is used as reference project. This project provides a large set of soil investigation data, technical drawings and structural properties of the quay wall.

The results of the calculations performed by Blum & D-Sheet Piling are used as benchmark values and will indicate whether the Plaxis calculations are reasonably accurate.

Since this case study does not include undrained analysis of the soil, both conventional and alternative design methods use effective strength and stiffness parameters. For the alternative design approach, new strength parameters are derived to represent the critical state of the soil. More detailed information about parameter derivation for the critical state is given in Appendix A.1.

Case study 2 - quay wall Alblasserdam Container Terminal

In this case study the development of the Alblasserdam Container Terminal is used as reference project. This project provides a set of soil investigation data that consists among others information about soft soils, in particular normal consolidated clay. The available information of these soils is used to construct an alternative soil profile for the quay wall structure. In this profile a large clay layer with the aforementioned properties is present. The structural properties of the quay wall, geometry and loading types are identical to those of case study 1.

Case study 3 - quay wall Groningen

In this case study the development of a deep foundation pit in the province of Groningen is used as reference project. Characteristic for this location is the presence of boulder clay, large layers of fine clay which are overconsolidated as a result of large ice loads in the past. Again, the available soil investigation data is used to create a representative soil profile. The structural properties of the quay wall, geometry and loading types are identical to those of case study 1.

The similarities and differences of modelling choices and boundary conditions between the case studies are summarized in Table 7.1.

	Soil types	Retaining height [m]	User load [kN/m ²]	Wall type
Case 1	Sand	17.55	20-70	1524*19 + 3PU28
Case 2	NC clay & sand	17.55	20-70	1524*19 + 3PU28
Case 3	OC clay & sand	17.55	20-70	1524*19 + 3PU28

Table 3.1: Similarities and differences of modelling choices and boundary conditions for the case studies

3.2 Framework for determining soil parameters

In this section background information is provided about the various soil parameters used in the analysis. The most important parameters for each design method are briefly exemplified, and it is explained how these parameters can be derived from soil investigation data.

3.2.1 General soil parameters

Friction angle

The friction angle ϕ represents the amount of friction between the soil particles. Together with the cohesion it determined the shear strength of the soil, according to Equation 2.1. To determine its value, triaxial tests (drained for sand, undrained for clay) or direct simple shear tests (for peat) are used. In general, ϕ is related to the peak strength of the soil, at 2% axial strain.

For the application of the new design approach, the critical state friction angle ϕ_{cv} is used. The standards for the new design approach for dikes prescribe the following conditions and set up for triaxial tests (Rijkswaterstaat, 2017):

- Anisotropic consolidation on either undisturbed or prepared soil specimen.
- The prepared soil specimen should have a void ratio close to the in-situ value of the soil.
- The consolidation stress is chosen to be higher than the preconsolidation pressure or equal to the in situ vertical effective stress, so that yielding of the soil is assured.
- The specimen has to be sheared up to at least 25% axial strain in case of sand or clay, and to at least 40% axial strain in case of peat. These strain levels ensure that it is safe to assume that the critical state of the soil is reached.

Cohesion

Cohesion c encloses the Van der Waals-forces, the effect of cementation and the capillary forces in (partly) saturated soils. The value for the cohesion is related to the peak strength of the soil, at 2% axial strain. In the critical state at normally consolidated state, the cohesion of the soil is assumed to be zero.

Dilatancy angle

The dilatancy angle ψ quantifies the amount of volume expansion during shearing of the soil. For normally consolidated clay and for peat, the dilatancy angle is equal to zero. For quartz sand it can be specified using the following relation (Plaxis, 2018):

$$\psi = \phi' - 30^\circ \quad (3.1)$$

Undrained shear strength

The undrained shear strength quantifies the resistance of the soil during shearing at undrained conditions. Values can be obtained directly from undrained triaxial tests, or using correlations. Relation between undrained shear strength and cone resistance of CPT:

$$s_u = q_{net}/N_{kt} \quad (3.2)$$

Here q_{net} represents the cone resistance, corrected for pore water pressure effects and total stresses. N_{kt} is an empirical factor, generally around 20.

Yield stress

The last parameter that is important for cssm is the yield stress σ'_{vy} , a measure for the loading history of the soil. The relation between the yield stress and the in-situ effective vertical stress can be presented in two ways:

- $\sigma'_{vy} = \sigma'_{vi} + POP$
- $\sigma'_{vy} = \sigma'_{vi} \cdot OCR$

where POP is the pre-overburden pressure.

3.2.2 Shansep model parameters

Undrained shear strength ratio S

The undrained shear strength ratio S gives an indication of the magnitude of the undrained shear strength in relation to the stress state of the soil. The parameter S has to be determined using the relation:

$$S = \frac{q_{cv}}{\sigma_{vc}} \quad (3.3)$$

The soil specimen has to be consolidated undrained triaxial test, using a consolidation stress σ_{vc} . This value corresponds with the stress at the point in a sigma-epsilon diagram of a CRS test, where the tangent of the primary loading branch first touches the settlement curve. This point is represented by arrow B in Figure 3.5.

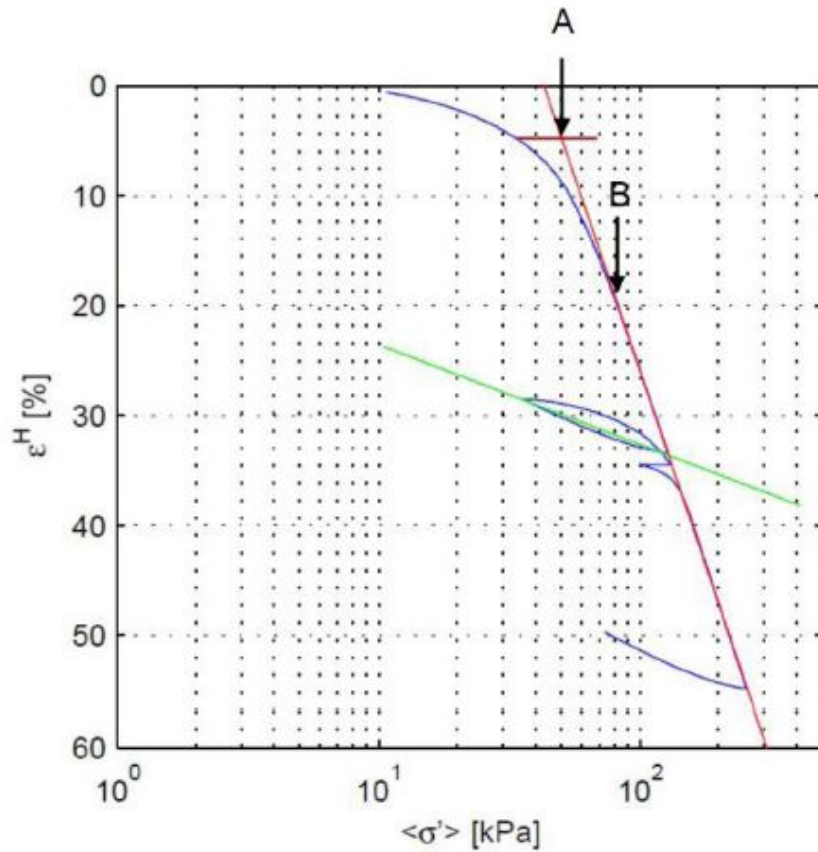


Figure 3.5: Stress-strain diagram of an CRS test. The blue line represents the test results. The red line through points A and B represents the tangent line of the primary loading branch of the diagram. Source: Rijkswaterstaat (2017)

Here q_{cv} is the deviator stress at constant volume of the soil, and follows from the triaxial test mentioned above. In case of overconsolidated soil, S can be determined using the same approach where the soil specimen is now consolidated at the estimated in-situ vertical effective stress σ_{vi} . Overall, the value of S increases with decreasing volumetric weight of the soil.

Power coefficient

The power m determines to what extent the stress history of the soil (σ'_{vy}) influences the undrained shear strength. The value of m can be between 0.5 and 1.0 where $m = 1.0$ represents linear elastic soil behavior. Typical values are between 0.7 and 0.8.

To determine this parameter, the following relationship can be used;

$$m = \frac{b - a}{b} \quad (3.4)$$

where a and b are the isotachen parameters from an oedometer test or CRS test.

3.2.3 NGI-ADP model parameters

Parameter determination according to Post and Lujendijk (2018) and (POVM BEEM, 2018). The following correlations and default values have been used for the calculations

using the Shansep NGI-ADP material model;

$$S \approx \frac{\sin \phi_{cv}}{2} \quad (3.5)$$

$$m \approx 1 - \frac{C_s}{C_c} \quad (3.6)$$

C_c and C_s are the primary and secondary compression indices. They take into account the effect of virgin loading and creep on the one-dimensional compression of a soil.

$$s_u^P / s_u^A = e^{-2\beta} \quad (3.7)$$

$$\beta = \frac{\sqrt{3}\eta_0\Lambda}{2M} \quad (3.8)$$

$$\eta_0 = \frac{3(1 - K_0)}{1 + 2K_0} \quad (3.9)$$

$$\Lambda = m \quad (3.10)$$

$$M = \frac{6 \sin \phi'}{3 - \sin \phi'} \quad (3.11)$$

$$s_u^{DSS} / s_u^A \approx \frac{1}{2} \cdot (1 + s_u^P / s_u^A) \quad (3.12)$$

$$G \approx \frac{E_{50}^u}{3} \quad (3.13)$$

$$\gamma_f^C = \frac{3}{2} \varepsilon_1^C \quad (3.14)$$

Parameter	Symbol	Value	Unit
Reference interface stiffness	E_{oed}^{ref}	15.0 E3	kN/m ²
Reference interface cohesion	c'_{ref}	1.0	kN/m ²
Friction angle	ϕ	8.0	°
Dilatancy angle	ψ	0	°
Power coefficient determining stress-dependency of stiffness	UD-Power	1.0	-
Reference stress level	UD-P ref	100	kN/m ²

Table 3.2: Strength and stiffness parameters of the interface of boulder clay for the Shansep NGI-ADP model

Case study 1 - Quay wall Amazonehaven

In this chapter the first case study is elaborated. In section 4.1 a brief, general introduction of the case study is given. Specific characteristics for this case study and several boundary conditions and technical specifications are given in section 4.2. The designs based on the conventional design approach and the new design approach are presented in sections 4.4 and 4.5. Finally, section 4.6 gives an overview of the results of both designs and analysis of the outcome.

4.1 Introduction

The first case study includes the quay wall of the Amazonehaven in the Port of Rotterdam. This quay wall structure is constructed in 2011-2012, and has replaced the existing quay wall to create a larger entrance of the Amazonehaven harbour branch. In Figure 4.1 the location of the Amazonehaven in the Port of Rotterdam is given.

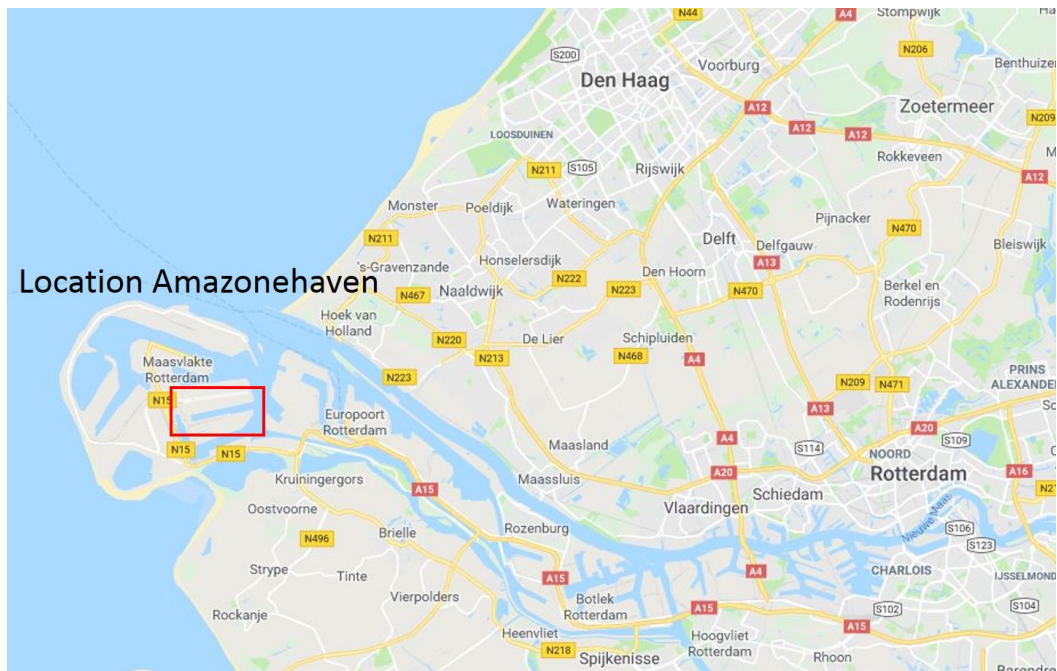


Figure 4.1: Location of the Amazonehaven in the Port of Rotterdam. Source: Google Inc.

The quay wall is designed using several sections, each having different dimensions based on their specific requirements and boundary conditions. Taking into account the available data and information from CPT's and lab tests of the different sections, the first part of the quay wall (Kade A1 in Figure 4.2) is used for this research. This quay wall and area behind it serve for the transshipment and storage of coal.

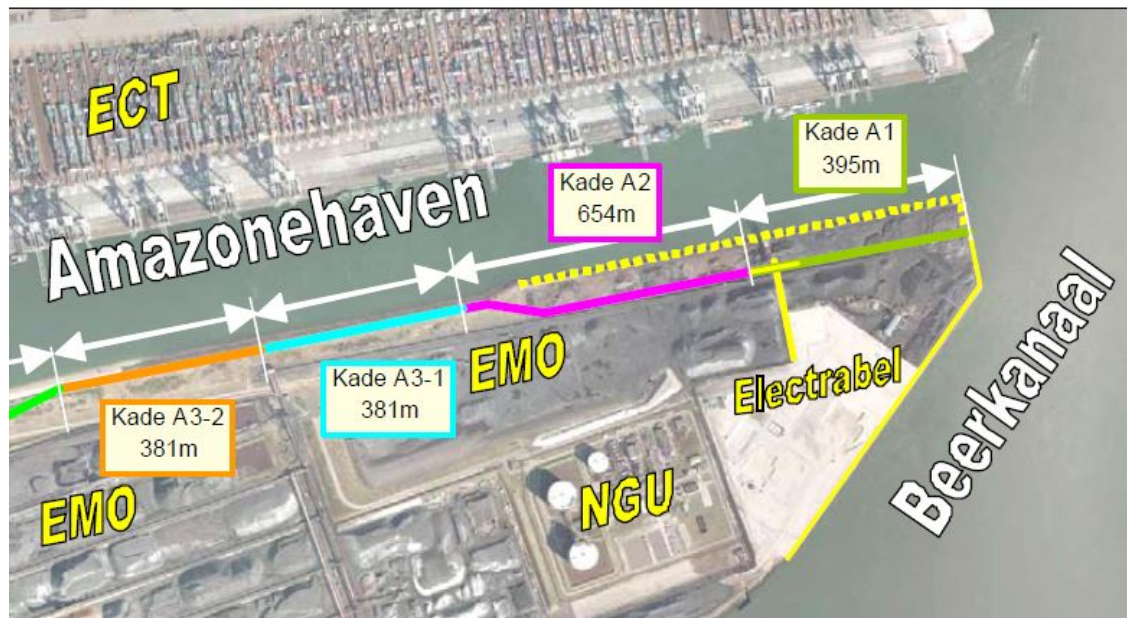


Figure 4.2: Overview Amazonehaven with different quay walls. 'Kade A1' and 'Kade A2' are indicated with the solid green respectively purple line. The dotted yellow line indicates the old quay wall, which has been demolished afterwards. Source: Gemeentewerken Rotterdam (2011a)

The soil profile consists of mainly sandy soils with good permeability. Therefore for this case study the new design approach is only partially applied. The critical state approach is used for the design of this quay wall, but the undrained analysis is not. This new design is further elaborated in the following sections.

Primary sources of data used in the design calculations are the (geo-)technical reports of BAM Infra (2009), Fugro GeoServices B.V. (2011) and Gemeentewerken Rotterdam (2011a).

4.2 Parameters / Boundary conditions

Quay wall structure

The quay structure consists of a combined wall of tubular piles with interconnecting sheet piles. On top of the combined wall a large capping beam of reinforced concrete is constructed. This beam will distribute the forces over the wall, and also provides support for the mooring bollards. The beam has a width of 2.5m and a height of 5.0m.

The wall is anchored by two rows of grout anchors connected to each tubular pile. The tubular piles are the main structural elements and transfer the loads induced by the ships, the soil and additional surcharge loads to the subsoil. The piles are placed every 3.38m in longitudinal direction of the quay wall. A cross-section of the quay wall including some dimensions is given in Figure 4.3.

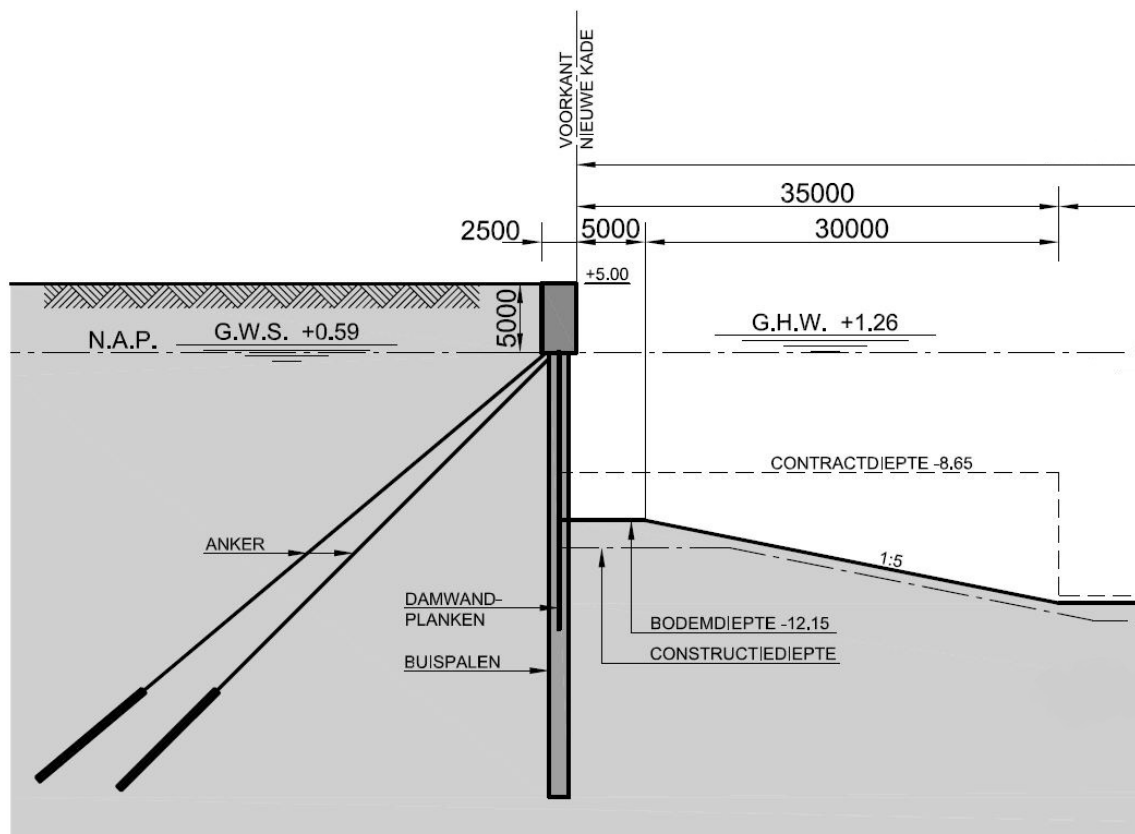


Figure 4.3: Cross section of quay wall A1. Source: Gemeentewerken Rotterdam

Structural and geometric properties

The following list shows the characteristic values used for modelling the quay wall. All structural parameters are averaged per meter length of the wall.

- Final surface level behind the quay wall: NAP + 5.0m
- Embedded depth of tubular piles: NAP - 31.0m
- Embedded depth of sheet pile elements between the tubular piles: NAP - 16.55 m
- Normative depth of the bottom in front of the wall: NAP - 12.55m

- Normative depth at center of harbour branch Amazonehaven: NAP - 18.15m
- Normative low water level: NAP - 0.68m
- Normative hydraulic head behind quay wall, in case of poor drainage: NAP + 0.59m
- Stiffness of combined wall: $EI = 1.649 \cdot 10^6$ [kNm²/m]
- Stiffness of tubular piles: $EI = 1.579 \cdot 10^6$ [kNm²/m]
- Young's modulus steel: $E = 2.1 \cdot 10^5$ [=N/mm²]
- Anchor 1: angle 40°, length 47m of which the last 12m consists of the grout body.
- Anchor 2: angle 45°, length 44m of which the last 12m consists of the grout body.
- Anchor bar cross section $1.59 \cdot 10^{-3}$ [m²/m], design yield force 896 [kN/m]
- Grout body diameter 0.38m.
- Axial skin resistance of the anchor: 400kN
- Both wall and anchor have elastoplastic material behavior

Loads

During the lifetime of the structure, it is subjected to several external loads. The loads that result in the normative loading situation are listed below:

- Vertical point load representing the weight of the capping beam: 270 [kN/m]
- Distributed surface load: 20 - 70 [kN/m²], see Figure 4.4
- Pre-tension in anchors: 350 [kN/m]

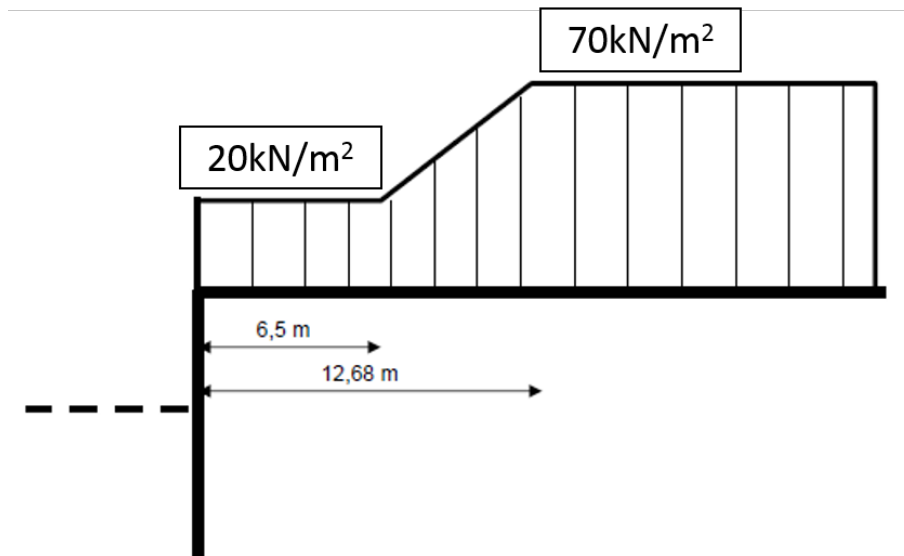


Figure 4.4: Schematization of the variable load behind the quay wall

4.2.1 Soil profile

Along the existing quay wall and around the center line of the newly build quay wall, multiple CPT's and boreholes have been executed. Based on the data from the soil investigations, a soil profile has been constructed. This geotechnical length profile varies along the quay wall. For each section of the quay wall a normative soil profile has been determined which is representative for the entire section.

For this report, part 1 of section A1 of the quay wall is used. The geotechnical length profile of this section, based on both recent and historical soil investigation data plus en-

gineering experience in Rotterdam, is presented in Figure 4.5.

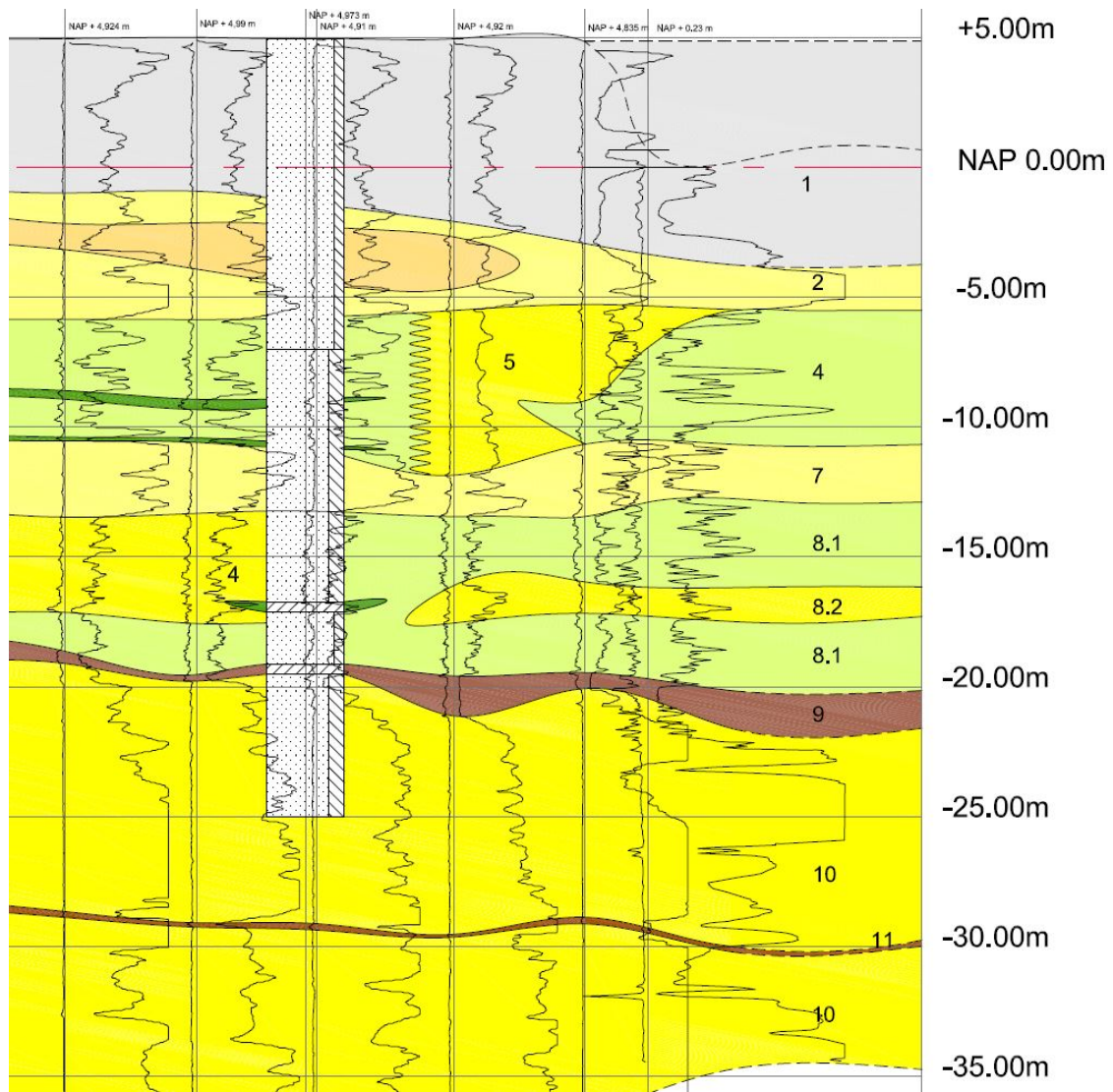


Figure 4.5: Geotechnical length profile of the Amazonehaven quay wall part A1. Source: Gemeentewerken Rotterdam

The normative soil profile that is used for the design calculations is presented in Table 4.1. The layer numbers correspond to those of Figure 4.5. The values for the soil parameters γ , ϕ and c are used as input parameters for the various design calculations.

Layer	Top of layer [m NAP]	Soil type	$\gamma_{dry}/\gamma_{sat}$ [kN/m ³]	ϕ [°]	C [kPa]
1	+5.0	Sand, anthropogenic	17.2 / 19.2	30	0
2	-1.5	Sand, beach sand formation	17.4 / 19.4	32.5	0
3	-2.7	Sand, beachsand, low q_c	17.2 / 19.2	30.0	0
2	-4.7	Sand, beach sand formation	17.4 / 19.4	32.5	0
5	-5.5	Sand, 'wadzand' formation, with few thin clay layers	17.2 / 19.2	30.0	0
7	-11.8	Sand, 'wadzand' formation, high q_c	17.2 / 19.2	32.5	0
8.1	-13.3	Sand, deep 'wadzand' formation, with many thin clay layers	17.0 / 19.0	27.5	0
8.2	-16.3	Sand, deep 'wadzand' formation	17.2 / 19.2	30.0	0
8.1	-17.5	Sand, deep 'wadzand' formation, with many thin clay layers	17.0 / 19.0	27.5	0
9	-19.6	Clay, occasionally thin peat layers	15.0 / 15.0	17.5	10
10	-21.2	Sand, Pleistocene	18.0 / 20.0	32.5	0
11	-29.5	Silty clay / clay	17.0 / 17.0	22.5	5
10	-30.0	Sand, Pleistocene	18.0 / 20.0	32.5	0

Table 4.1: Normative soil profile and parameters of quay wall part A1, profile1. In the 3rd column the volumetric weights of the soil in both dry and saturated state are given. The 4th and 5th column give the friction angle and cohesion of the soil for an axial strain level of 2%, based on historical data & triaxial tests.

Model parameters	Symbol	Value	Unit
Axial stiffness of combined wall	EA_1	4.05E+06	kN/m
Bending stiffness of combined wall	EI_1	1.65E+06	kN/m ² /m
Moment capacity combined wall	$M_{p,wall}$	5076	kNm/m
Bending stiffness of tubular piles	EI_2	1.579E+06	kN/m ² /m
Moment capacity of tubular piles	$M_{p,tube}$	4031	kNm/m
Axial capacity of tubular piles	$N_{p,tube}$	1638	kN/m

Table 4.2: Structural parameters of quay wall used in Plaxis models

Model parameters	Symbol	Value	Unit
center to center distance	$L_{spacing}$	3.38	m
Axial stiffness bar	EA_{bar}	1.129E+06	kN
Axial capacity in tension	$F_{max,tens}$	3028	kN
Young's modulus of grout body	E_{grout}	7.07E+06	kN/m ²
Diameter grout body	D_{grout}	0.38	m
Plastic moment capacity anchor	M_p	1000	kNm/m
Plastic axial capacity anchor	N_p	4000	kN/m
Axial skin resistance	-	Linear	-
Skin resistance start	$T_{skin,start,max}$	286.5	kN/m
Skin resistance end	$T_{skin,end,max}$	286.5	kN/m

Table 4.3: Structural parameters of grout anchor used in Plaxis models

4.3 Design verification calculation based on theory of Blum

In this section the calculation based on the theory of Blum is presented. Blum is used to check the required embedding depth of the wall to ensure stability of the wall. It is assumed that all soil layers show a drained response. Therefore the effective strength parameters ϕ' and c' are used. As already discussed in chapter 2.3.1, the coefficients of lateral earth pressure are determined using the theory of Müller-Breslau.

Because the first 5 soil layers (from NAP + 5.0m till NAP - 13.3m) have almost the same volumetric weights and strength parameters, they are combined to one representative layer to simplify the calculation.

Parameters

The input parameters used for the calculation are given in Table 4.4.

Top of layer [m NAP]	Bottom of layer [m NAP]	$\gamma_{dry}/\gamma_{sat}$ [kN/m ³]	ϕ' [°]	c' [kPa]	δ [°]
+5.0	-13.3	17.2 / 19.2	30	0	20
-13.3	-16.3	17 / 19	27.5	0	18.3
-16.3	-17.5	17.2 / 19.2	30	0	20
-17.5	-19.6	17 / 19	27.5	0	18.3
-19.6	-21.2	15 / 15	17.5	10	5.83
-21.2	-29.5	18 / 20	30.0	0	16.6
-29.5	-30.0	17 / 17	22.5	5	7.5
-30.0	-35.0	18 / 20	30.0	0	16.6

Table 4.4: Input parameters used to perform Blum calculation

Some additional factors to be taken into account for the calculation:

- the anchor is modelled as if it makes an angle of 90° with the wall. Therefore the resulting anchor force has been increased to correct for the actual angle of 45°.
- the coefficients of lateral soil pressure are determined using the theory of Müller-Breslau, which is valid for friction angles $\phi' \leq 30^\circ$ (see Ch28.2 of D-Sheet manual). This results in a small underestimation of the passive soil strength for the Pleistocene sand layer.
- The top load as presented in Figure 4.4 is for the calculation represented as a uniform load of 20 kN/m², because Blum's theory looks only at the soil stresses right next to the wall.
- No leveling of pore pressures due to different water table at left/right side of wall

Results

The results of the calculations are presented in Table 4.5. The calculated anchor force and bending moments are later compared with the results found by D-Sheet and Plaxis.

Variable	Value
Anchor Force	2238 kN
M_{\max}	1583 kNm/m ¹
Required embedding depth wall	24.8 m - NAP

Table 4.5: Results of Blum calculation

4.4 Designs based on conventional design approach

Design using D-Sheet Piling

In this section the design of the Amazonehaven quay wall, based on the current design practices, is presented. For this design, a model of the quay wall and soil profile is build in D-Sheet Piling. The structural properties presented in Chapter 4.2 and the soil profile given in Table 4.1 have been used as input for the calculations. This way the calculations coincide with those performed for the actual design of the Amazonehaven. For the existing design calculations, the tangent option (1 branch) in D-Sheet has been used to describe the stiffness of the soil. Since only 1 curve for the spring characteristic is used, the soil behavior is assumed to have a bi-linear stress-strain relationship.

A more accurate result can be obtained using the secant option, which takes into account the stress-dependency of the soil stiffness. Assuming that the soil properties of the different soil layers are constant along the quay wall, the values for the modulus of subgrade reaction have been derived using the report of the design for cross section A3 (see Figure 4.2). The values found are presented in Table 4.6.

Layer nr.	k_1 [kN/m ² /m ¹]	k_2 [kN/m ² /m ¹]	k_3 [kN/m ² /m ¹]
1	16000	8000	4000
2	30000	15000	7500
3	16000	8000	4000
2	30000	15000	7500
5	16000	8000	4000
7	20000	10000	5000
8.1	12000	6000	4000
8.2	16000	8000	4000
8.1	12000	6000	3000
9	2000	800	500
10	40000	20000	10000
11	6000	4000	2000
10	40000	20000	10000

Table 4.6: Overview of the values for modulus of subgrade reaction using the secant method. Based on geotechnical report of Amazonehaven quay wall section A3

The results of the calculations are presented in Table 4.9, at the end of this section. More detailed information about the design calculations is presented in Appendix C.

Design using Plaxis

In this section the design of the Amazonehaven quay wall is presented using a Finite Element Method. A model of the quay wall and soil profile has been made in Plaxis. Again, the structural properties presented in Chapter 4.2 and the soil profile given in Table 4.1 are used as input for the model. This has resulted in the following list of input parameters:

Layer	Top of layer [m NAP]	Material model	$\gamma_{dry}/\gamma_{sat}$ [kN/m ³]	ϕ' [°]	C [kPa]	ψ [°]	R_{inter}
1	+5.0	Sand	17.2 / 19.2	30	0	0	0.66
2	-1.5	Sand	17.4 / 19.4	32.5	0	2.5	0.66
3	-2.7	Sand	17.2 / 19.2	30.0	0	0	0.66
2	-4.7	Sand	17.4 / 19.4	32.5	0	2.5	0.66
5	-5.5	Sand	17.2 / 19.2	30.0	0	0	0.66
7	-11.8	Sand	17.2 / 19.2	32.5	0	2.5	0.66
8.1	-13.3	Sand	17.0 / 19.0	27.5	0	0	0.66
8.2	-16.3	Sand	17.2 / 19.2	30.0	0	0	0.66
8.1	-17.5	Sand	17.0 / 19.0	27.5	0	0	0.66
9	-19.6	Clay	15.0 / 15.0	17.5	10	0	0.5
10	-21.2	Sand	18.0 / 20.0	32.5	0	2.5	0.66
11	-29.5	Clay	17.0 / 17.0	22.5	5	0	0.5
10	-30.0	Sand	18.0 / 20.0	32.5	0	2.5	0.66

Table 4.7: Normative soil profile and strength parameters inserted in Plaxis.

Layer	Top of layer [m NAP]	E_{50}^{ref}	E_{oed}^{ref}	E_{ur}^{ref}	m
1	+5.0	25	25	100	0.5
2	-1.5	30	30	120	0.5
3	-2.7	25	25	100	0.5
2	-4.7	30	30	120	0.5
5	-5.5	24	24	96	0.5
7	-11.8	30	30	120	0.5
8.1	-13.3	22	22	88	0.5
8.2	-16.3	25	25	100	0.5
8.1	-17.5	22	22	88	0.5
9	-19.6	2.5	2.0	5.7	1.0
10	-21.2	40	40	160	0.5
11	-29.5	16	8	40	1.0
10	-30.0	40	40	160	0.5

Table 4.8: Stiffness parameters inserted in Plaxis. The values presented in red are estimates since no data was available.

The calculations are performed according to the flowchart presented in Figure 3.4.

Results

The final results of the calculations using D-Sheet and Plaxis, using the conventional design approach, are presented in Table 4.9. In section 4.6 these results are compared with the outcome of the calculations using the new approach.

	N_{anchor} [kN]	M_{max} [kNm/m]	V_{max} [kN/m]	$w_{\text{max,top}}$ [mm]	$w_{\text{max,field}}$ [mm]
D-Sheet tangent method	1538 / 1532	1980	477	9	-64
D-Sheet secant method	1562 / 1533	2125	486	15	-70
Plaxis HS	2122 / 1794	2926	587	-91	-195

Table 4.9: Results of calculations applying conventional design approaches. The table gives from left to right: axial force in both anchors, maximum bending moment and shear force in the wall, and the maximum wall displacements at the top of the wall and in the field. The displacements w are the horizontal displacements, where a negative value corresponds with a displacements towards the water.

4.5 Design based on alternative design approach using cssm

In this section the design of the quay wall is presented, using the new design method using critical state soil mechanics theory. Because of the soil profile, consisting of mostly sandy soil layers, the analysis is performed using purely drained response, and the undrained analysis using the Shansep theory is not applied here.

Again, calculations have been performed in both D-Sheet and Plaxis.

Based on the analyzed data of the soil investigation of soil layers 5, 9 and 10, a trend can be observed. For the layers 5 and 11, both dense sand, a ϕ'_{cv} had been found which is 3-4 degrees less than $\phi'_{2\%}$, where $\phi'_{2\%}$ stands for the friction angle of the soil at an axial strain level of 2%. This trend has been used to estimate the critical state friction angles for the other soil layers consisting of sand, for which no data was available.

For clay, the value found for soil layer 9 is also used for soil layer 11 (both on larger depth so comparable stress levels.)

With respect to the designs using the conventional design approach, the structural specifications and load specifications have not changed. The modified strength parameters of the soil are given in Table 4.10.

Layer	Top of layer [m NAP]	Material model	$\gamma_{dry}/\gamma_{sat}$ [kN/m ³]	ϕ' [°]	C [kPa]	ψ [°]
1	+5.0	Sand	17.2 / 19.2	27	0	0
2	-1.5	Sand	17.4 / 19.4	29	0	0
3	-2.7	Sand	17.2 / 19.2	27	0	0
2	-4.7	Sand	17.4 / 19.4	29	0	0
5	-5.5	Sand	17.2 / 19.2	28	0	0
7	-11.8	Sand	17.2 / 19.2	29	0	0
8.1	-13.3	Sand	17.0 / 19.0	24	0	0
8.2	-16.3	Sand	17.2 / 19.2	27	0	0
8.1	-17.5	Sand	17.0 / 19.0	24	0	0
9	-19.6	Clay	15.0 / 15.0	32	0	0
10	-21.2	Sand	18.0 / 20.0	31	0	0
11	-29.5	Clay	17.0 / 17.0	32	0	0
10	-30.0	Sand	18.0 / 20.0	31	0	0

Table 4.10: Normative soil profile and strength parameters based on critical state theory, according to Rijkswaterstaat (2017).

4.5.1 Design using D-Sheet

Only changes made are the values for the friction angle and the cohesion. Modulus of subgrade reaction have been held the same as for the conventional design approach, using a multi-linear stress-displacement diagram.

Layer nr.	k_1	k_2	k_3
	[kN/m ² /m ¹]	[kN/m ² /m ¹]	[kN/m ² /m ¹]
1	16000	8000	4000
2	30000	15000	7500
3	16000	8000	4000
2	30000	15000	7500
5	16000	8000	4000
7	20000	10000	5000
8.1	12000	6000	4000
8.2	16000	8000	4000
8.1	12000	6000	3000
9	2000	800	500
10	40000	20000	10000
11	6000	4000	2000
10	40000	20000	10000

Table 4.11: Values of modulus of subgrade reaction in the D-Sheet calculations

4.5.2 Design using Plaxis

Strength parameters of the critical state are used, see Table 4.10. Constant volume of the soil, soil can still shear but no volume change anymore. Therefore dilatancy angles equal to zero. Stiffness parameters same as for the conventional design approach, see Table 4.8.

Results

The results of the calculations using both design methods are presented in Table 4.12.

	Anchor Forces	M_{\max}	V_{\max}	$w_{\max, \text{top}}$	$w_{\max, \text{field}}$
	[kN]	[kNm/m]	[kN/m]	[mm]	[mm]
D-Sheet sec	1735 / 1608	2695	561	19	-95
Plaxis (HS)	2355 / 1947	3359	658	-124	-243

Table 4.12: Results of calculations applying the new design approach

4.6 Results

In this section the outcome of case study 1 is analyzed and discussed.

In the Figures 4.6 up to 4.9 the results of the calculations in terms of forces and displacements of the wall are given, for both the conventional and alternative design approach.

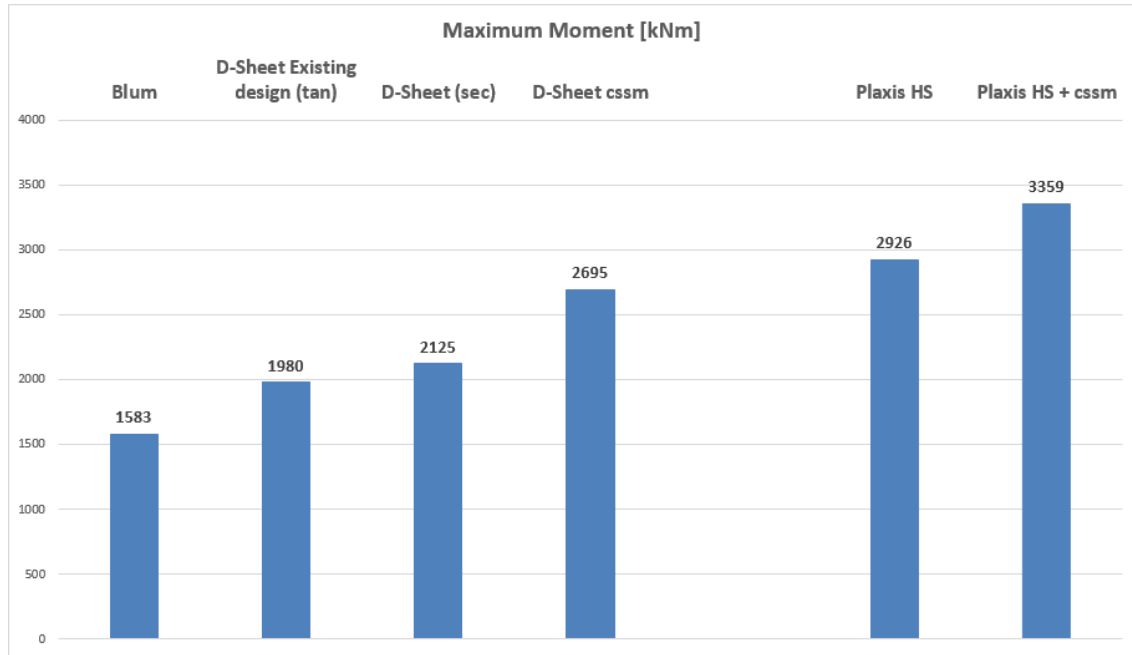


Figure 4.6: Overview of the maximum bending moments in the wall found using the different design approaches and design methods.

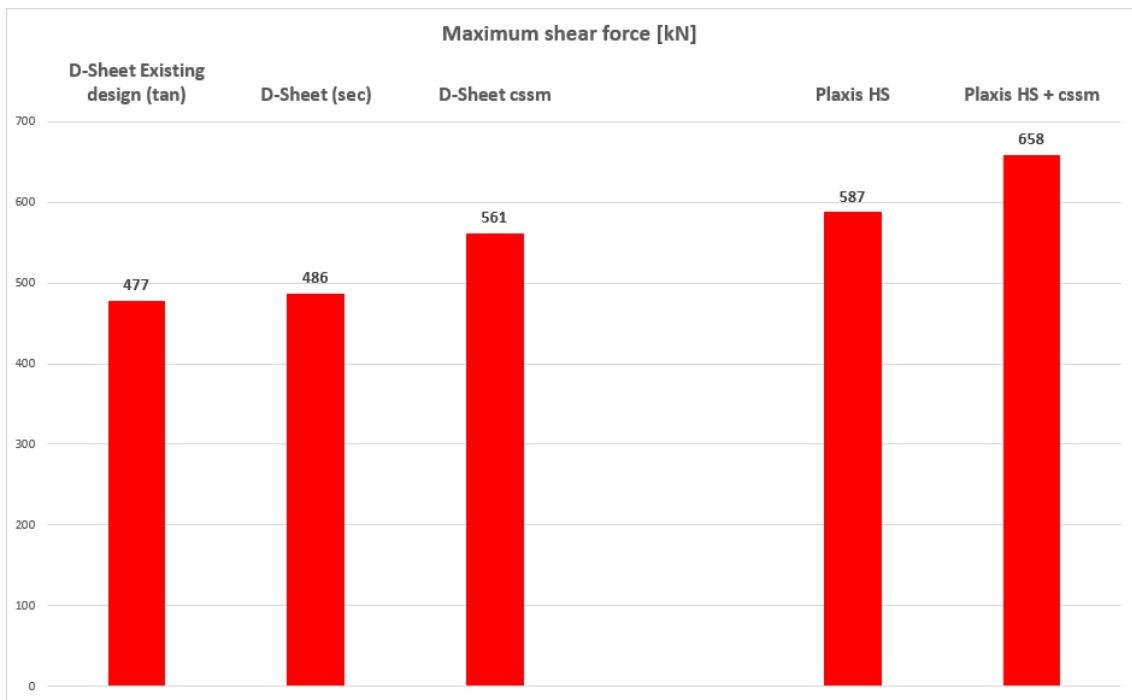


Figure 4.7: Overview of the maximum shear force in the wall found using the different design approaches and design methods.

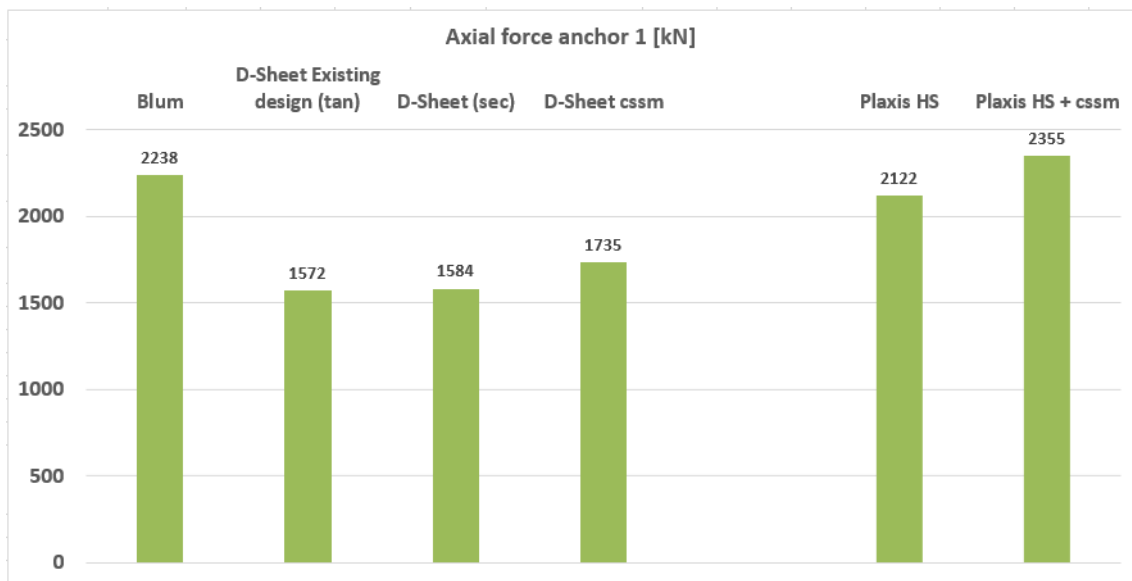


Figure 4.8: Overview of the anchor forces found using the different design approaches and design methods.

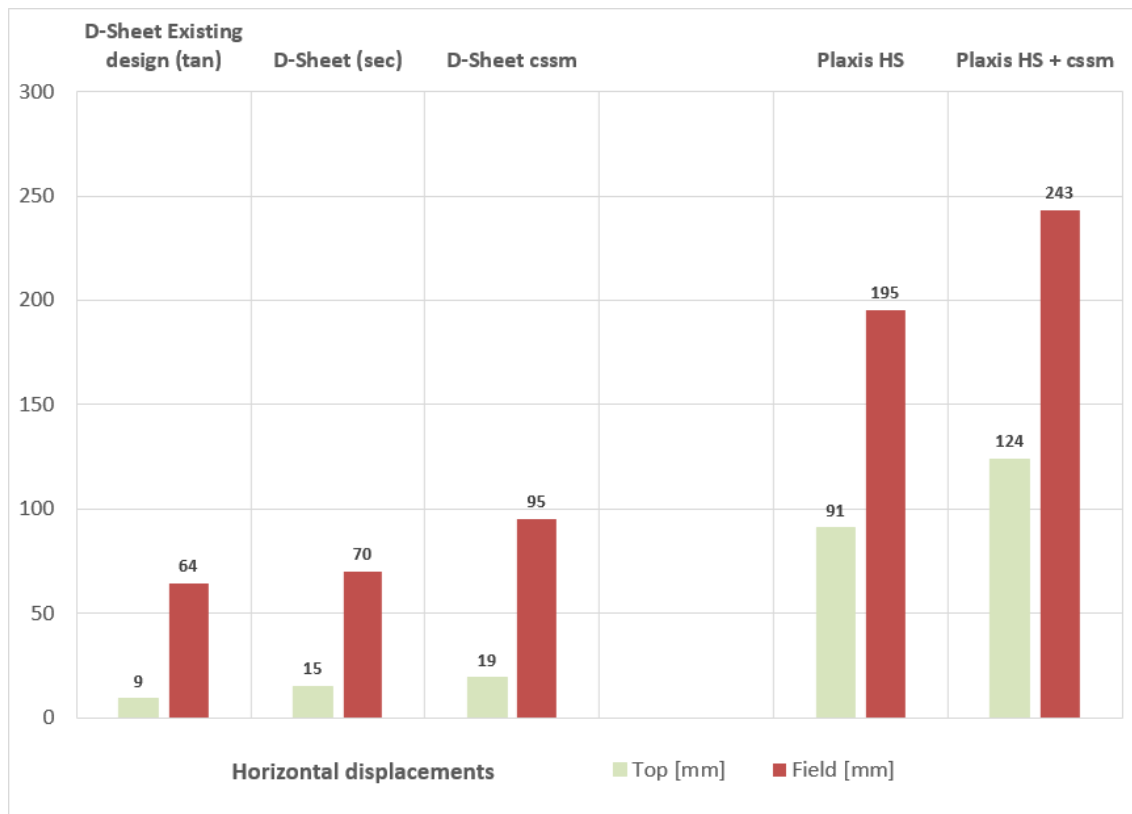


Figure 4.9: Overview of the maximum horizontal displacements of the wall, found using the different design approaches and design methods. Only absolute values are presented.

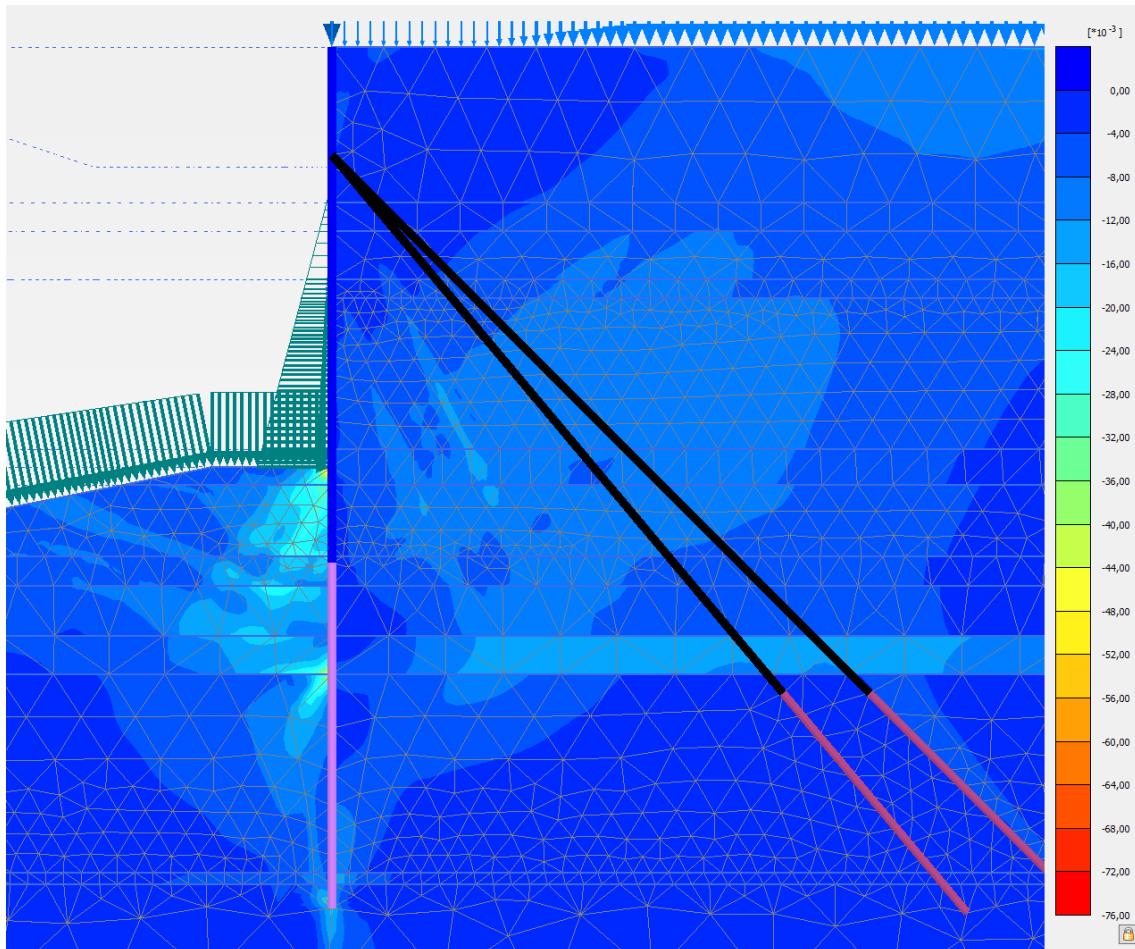


Figure 4.10: Overview of the generated principle axial strains ε_1 in case of the new design approach. The scale on the right varies from 0.0 % (dark blue) till 8.0 % (red).

Interpretation of the results

Based on the results presented in the figures above, two phenomena stand out. First of all, the results generated using Plaxis gives higher values in terms of both forces and displacements compared to the results generated using D-Sheet. This is especially clear for the displacements of the wall, which are around 2-3 times as high.

Secondly, the new design approach produces higher values in terms of both sectional forces and displacements compared to the results of the conventional design approach. This is the case for both D-Sheet calculations and Plaxis calculations. It can be explained by the smaller friction angles for the sand layers at the critical state, which results in a decrease of shear strength mobilization compared to the conventional design approach. The clay layers can mobilize more shear strength due to higher friction angles, but since there are only two small clay layers present this results in a minor contribution.

The calculation results of both design methods (see Table 4.9 and Table 4.12) show inconsistent values regarding w_{max}^{top} . This can be explained by the differences in calculation method regarding the anchor forces and prestressing between D-Sheet Piling and Plaxis. The relative difference between the two design approaches is presented in Table 4.13.

	$F_{\text{anchor},1}$	$F_{\text{anchor},2}$	M_{max}	V_{max}	$w_{\text{max,top}}$	$w_{\text{max,field}}$
D-Sheet	1.27	1.15	1.27	1.36	1.10	1.09
Plaxis	1.15	1.12	1.36	1.25	1.11	1.09

Table 4.13: Relative difference between the outcome of the conventional and alternative design approach, for both D-Sheet and Plaxis calculations. The ratio is calculated by dividing the value of the alternative design approach by the value of the conventional design approach.

Possible explanation for the discrepancy in displacements between D-Sheet and Plaxis results: the assumed stiffness parameters for Plaxis calculation are quite conservative, in relation to the average values for soils with the same density / cone resistance as presented in NEN9997-1. Also, the stiffness parameters are determined using data from only 1 or 2 triaxial tests on prepared samples of sand. Using a correlation between stiffness and density of soil can give more accurate results in terms of displacements of the wall.

4.6.1 Discussion

The new design approach as presented in the WBI2017 is derived specifically for the assessment of slope stability. It is assumed that when sliding of the soil occurs, high strain levels develop and the critical state of the soil is reached. In this case study however, there is no sliding plane development of the soil as can be seen in Figure 4.10. The soil is retained by the wall and can mobilize sufficient shear strength. The maximum principal axial strain levels reached is 7.3% which means the critical state of the soil is not reached, even locally. It is questionable if the current application of csm is a suitable approach for determining the strength of the soil in case of a retaining wall.

Regarding the critical state friction angle: ϕ'_{cv} is the end state of the soil, and this should be independent of the packing (initial state) of the soil. For very loose soil, the critical state friction angle is likely to be higher than $\phi'_{2\%}$, and for dense soil the critical state friction angle is lower than $\phi'_{2\%}$.

The accuracy of the comparison between the results, and the conclusions following the comparison, are dependent on the efficiency of the design using the conventional design approach.

4.6.2 Conclusion

Based on the quantitative results of this case study, the alternative design approach will produce significantly higher values for both sectional forces and displacements of the quay wall. This would lead to more conservative design outcomes. Furthermore is the application of the alternative design method not suitable in the case of a solely sandy soil profile.

Case study 2 - Amazonehaven modified with normally consolidated clay layer

This chapter comprises the analysis of a quay wall with a soil profile consisting a normally consolidated (NC) clay layer. The properties of the clay layer are based on soil investigation data from the construction project of the quay wall for the Container Transfer Alblasserdam (CTA). This quay wall is located along the canal *Noord* between the cities of Rotterdam and Dordrecht. This area is known to contain sizable layers of soft to very soft soil.

The properties of the new soil profile used for this case study, and the accompanying soil parameters are presented in section 5.1. The sections 5.2 and 5.3 give the starting points for the design calculations and results of both conventional and new design approach. An analysis of the results and conclusions based on the results of this case study is presented in section 5.4.2.

5.1 Parameters / Boundary conditions

In this case study, the Holocene part of the soil profile consists of sand and soft clay. The characteristics of the soft clay are based on the soil investigation data obtained during the construction project Container Terminal Alblasserdam.

5.1.1 Type of soil response

As in compliance with section 2.2.4, an undrained soil response can be assumed if the hydrodynamic period satisfied the criterion $T < 0.01$, using Equation 2.5. This criterion is checked for both the soft clay and the peat. For these soil types, a variety of drainage lengths and load durations have been taken into account to create an overview which shows for which conditions an undrained response of the soil can be expected.

For the clay layer the hydrodynamic period is plotted against the duration of the loading. For varying thickness of the clay layer multiple graphs of the hydrodynamic period T versus load duration are presented in Figures 5.1 and 5.2. Here the two straight horizontal lines represent the boundary values for which a clear drained or undrained response can be expected according to Vermeer and Meier (1998), see also section 2.2.4. For the area in between these lines such a clear distinction cannot be made and the soil response will be partially drained, partially undrained.

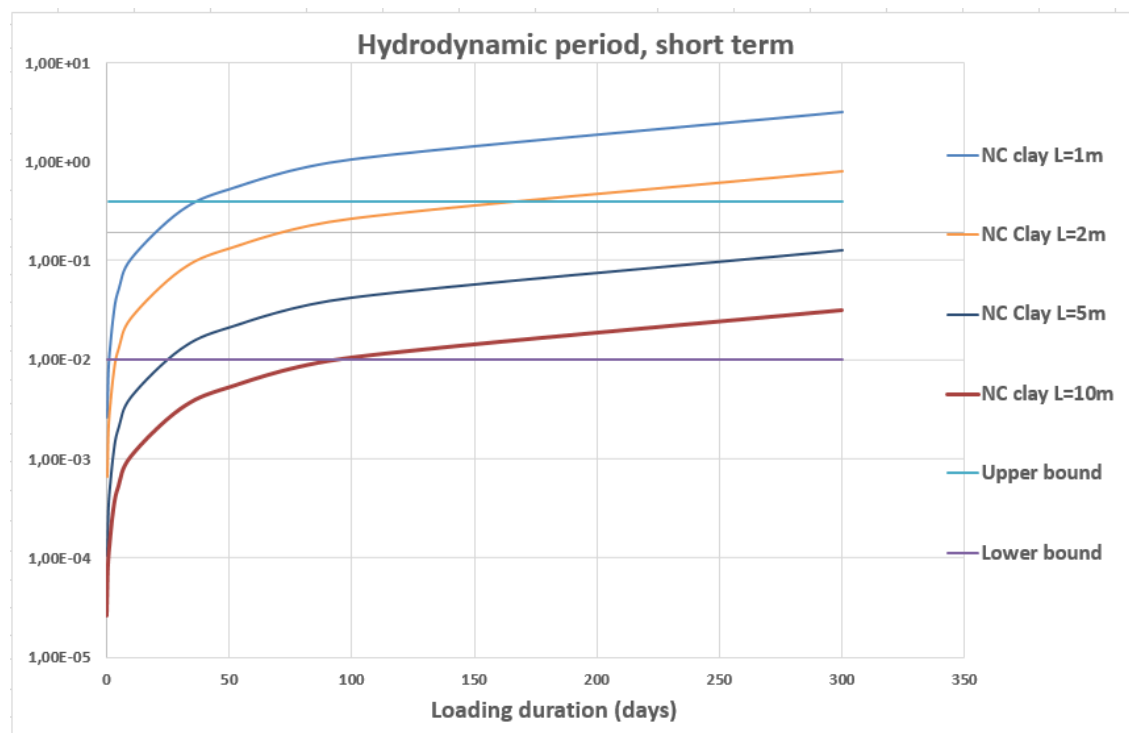


Figure 5.1: Short-term analysis of the hydrodynamic period (log-scale) versus loading duration for different thickness of the clay layer

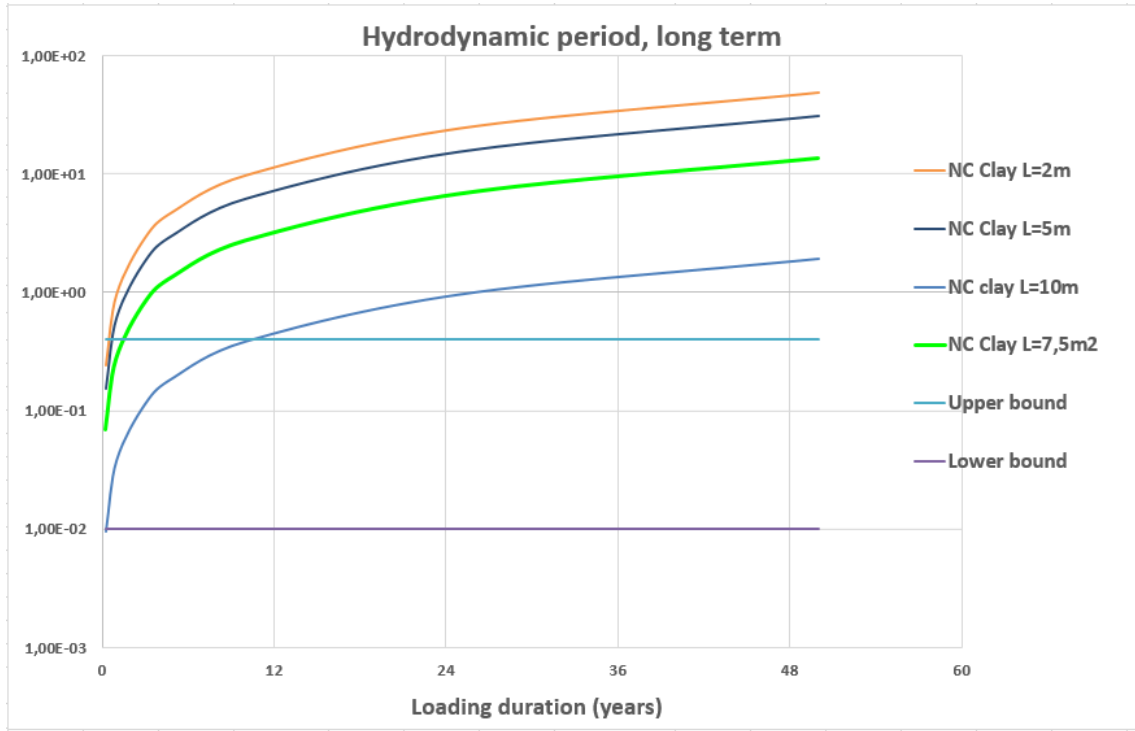


Figure 5.2: Long-term analysis of the hydrodynamic period (log-scale) versus loading duration for different thickness of the clay layer

5.1.2 Soil profile

For this case study, a soil profile consisting a normal consolidated clay layer and multiple sand layers is generated. As shown in the figures above, the clay layer should be modelled using an undrained analysis for short term loads, and both undrained and drained analysis for long term loads. The characteristics of this soil profile are presented in Table 5.1.

Layer	Top of layer [m NAP]	Soil type	$\gamma_{dry}/\gamma_{sat}$ [kN/m ³]	ϕ [°]	C [kPa]	k [m/day]
1	+5.0	Sand	17.5 / 19.5	30	0.1	0.86
2	0.0	Clay	15 / 16.5	17.5	12	2.2E-5
3	-18.0	Sand, Pleistocene	18 / 20	32.5	0.1	0.86

Table 5.1: Build-up of the soil profile. For each soil layer, the location and properties are given.

5.1.3 Different scenarios regarding the timing of construction and loading of the wall

After the dredging of the soil in front of the quay wall, the construction phase is finished and the quay wall can be made ready to use. In case of high demand for quay wall space, the quay wall will be taken into function as soon as possible, and it is possible that the design loads of the user phase do occur very soon after construction. In this case the undrained soil response caused by the dredging of the soil is followed by the undrained soil response caused by the surcharge behind the quay wall. However, it is also possible that the quay wall will not be used in the near future due to a lack of demand. Now the

soil has time to consolidate and the excess pore pressures will slowly dissipate. To model both possibilities, the following two scenarios have been used:

- Scenario 1: a fully undrained analysis of the soil response for all construction stages.
- Scenario 2: a drained analysis of the soil response for the construction stages up to dredging of the soil, and an undrained analysis of the final construction stage where the design loads are being applied.

5.2 Designs based on conventional design approach

5.2.1 Design using Plaxis

For the conventional design method a Plaxis model is constructed. The choice which material model is used for each soil layer is based on the recommendations given in (Plaxis, 2018). The clay layer are modelled using the Soft Soil material model. The sand layers are modelled with the hardening soil material model. Since the clay layer shows an undrained soil response, it is modelled using the undrained (A) function.

The strength and stiffness parameters of the different soil layers that are used in the calculations are presented in Tables 5.2 and 5.3.

Layer	Top of layer [m NAP]	Soil Type	Material model	Drainage Type	$\gamma_{dry}/\gamma_{sat}$ [kN/m ³]
1	+5.0	Sand	HS	Drained	17.5 / 19.5
2	0.0	Clay	HS	Undrained (A)	15 / 16.5
3	-18.0	Sand	HS	Drained	18 / 20

Table 5.2: General info of soil profile used in Plaxis

Layer	ϕ' [°]	C [kPa]	ψ [°]	E_{50}^{ref}	E_{oed}^{ref}	E_{ur}^{ref}	m	R_{inter}	POP [kPa]
1	30	1	0	25	25	100	0.5	0.66	0
2	17.5	12	0	1.6	3.2	12.8	1.0	0.5	0
3	32.5	0.1	2.5	40	40	160	0.5	0.66	0

Table 5.3: Strength and stiffness parameters of the soil layers.

A schematization of the model in Plaxis is given in Figure 6.3. In this figure, the final situation is depicted, including the acting design loads on the structure.

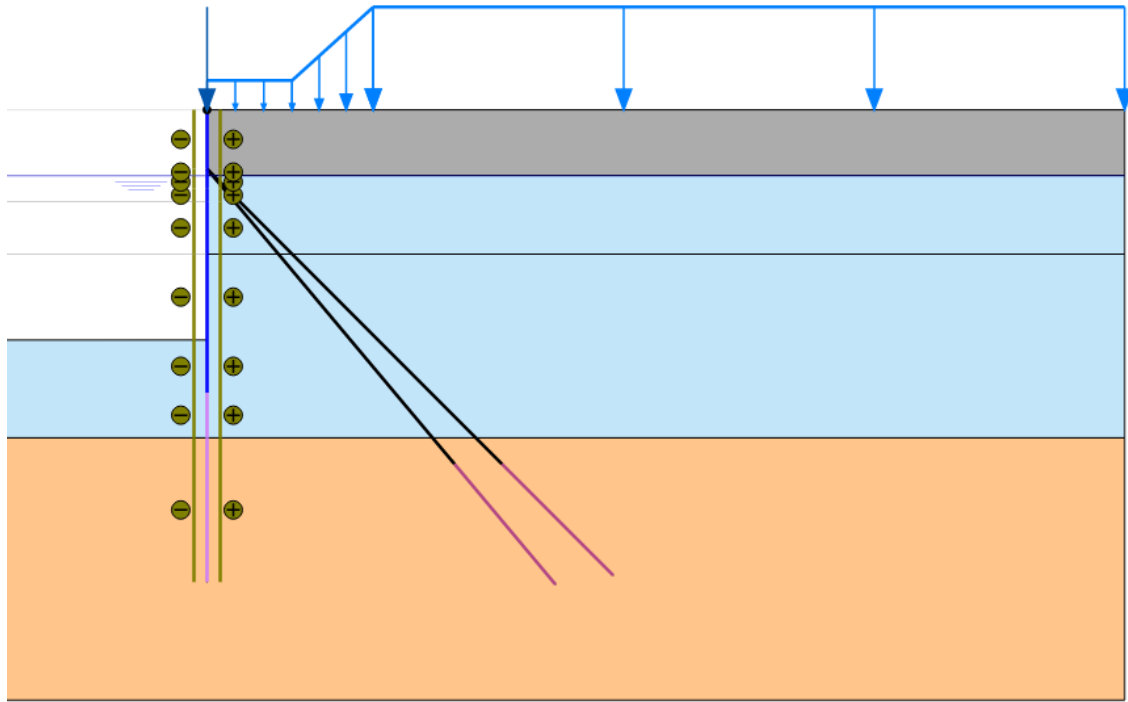


Figure 5.3: Plaxis model of the final construction phase for case study 2. The grey layer represent moderately dense sand, the light blue layer represents the normally consolidated clay and the orange layer represents Pleistocene sand.

Results

The final results of both the D-Sheet and Plaxis calculations are presented in Table 5.4.

	Anchor Forces [kN]	M_{\max} [kNm/m]	V_{\max} [kN/m]	$w_{\max, \text{top}}$ [mm]	$w_{\max, \text{field}}$ [mm]
Plaxis HS scenario 1	2968 / 2702	3685	725	-175	-249
Plaxis HS scenario 2	3235 / 2972	4280	955	-141	-253

Table 5.4: Results of calculations applying conventional design approaches. The displacements w are the horizontal displacements, where a negative value corresponds with a displacement towards the water.

5.3 Design based on alternative design approach using undrained analysis combined with cssm

As shown in section 5.1, a soil layer consisting of normally consolidated clay with a drainage length of 10 meters shows an undrained response for loading situations up to a duration of multiple years. The undrained behavior of the clay layer is modelled in Plaxis using the User Defined material model *Shansep NGI-ADP*. A list of input parameters required for this model is given in Table 5.5. The model parameters are derived using the correlations presented in section 3.2.

Model parameters	Symbol	Value	Unit
Normalized stiffness	G/s_u^A	70	-
Failure shear strain in compression	γ_f^C	10.5	%
Failure shear strain in extension	γ_f^E	15.7	%
Failure shear strain in direct simple shear	γ_f^{DSS}	13.1	%
Reference undrained shear strength in active mode	$s_u^A{}_{ref}$	108	kN/m ²
Reference depth	$vert_{ref}$	-4	m - NAP
Increase of undrained shear strength over depth	$s_u^A{}_{inc}$	4	kN/m ² /m
Ratio between passive and active shear strength	s_u^P/s_u^A	0.45	-
Initial mobilized shear strength	τ_0/s_u^A	0.5	-
Ratio between shear strength in DSS and active mode	s_u^{DSS}/s_u^A	0.73	-
Poissons ratio	ν	0.15	-
Poissons ratio undrained	ν_u	0.495	-
Ratio between s_u^A and σ'_v in case of virgin loading (S)	alpha	0.27	-
Power. Indicates the dependency of s_u on OCR	m	0.8	-
Minimum value of undrained shear strength	$s_{u,min}$	3.0	kN/m ²

Table 5.5: Shansep NGI-ADP model parameters and the corresponding values for soft clay in the Rhine river delta

Symbol	Value	Unit
$E_{oed}{}^{ref}$	15.0 E3	kN/m ²
c'_{ref}	1.0	kN/m ²
ϕ	10.0	°
ψ	0	°
UD-Power	1.0	-
UD-P ref	100	kN/m ²

Table 5.6: Shansep NGI-ADP interface parameters of soft clay

Input values extracted from soil investigation data (see Appendix D):

Parameter	Symbol	Value	Unit
Undrained secant stiffness	E_{50}^u	22.7	MPa
Original depth of soil sample	d_{sample}	-7.8	m below surface
Undrained shear strength at depth d_{sample}	s_u^A	108	kN/m ²
Axial failure strain in compression	ε_f^C	10.5	%
Primary compression index	C_c	0.053	-
Secondary compression index	C_s	0.015	-
Critical state friction angle	ϕ'_{cv}	34	°

Table 5.7: Input used to determine the model parameters of the NGI-ADP Shansep model

Results

In the following table the final results of the design calculations of the alternative design method are presented. For the two scenarios described in section 5.1.3 the sectional forces of the wall, the anchor forces and the displacements are given in the following table.

	Anchor Forces [kN]	M_{max} [kNm/m]	V_{max} [kN/m]	$w_{max,top}$ [mm]	$w_{max,field}$ [mm]
NGI-ADP Shansep Scenario 1	2623 / 2431	2595	608	-137	-189
NGI-ADP Shansep Scenario 2	2822 / 2640	2898	715	-134	-186

Table 5.8: Results of calculations using the alternative design approach including the NGI-ADP Shansep model

5.4 Results

In this section the outcome of case study 2 is presented and analyzed. In the Figures 5.4 up to 5.7 the results of the calculations in terms of forces and displacements of the wall are given, for both the conventional and alternative design approach. Also, the relative difference between the outcomes of both approaches for each quantity is given in Table 5.9.

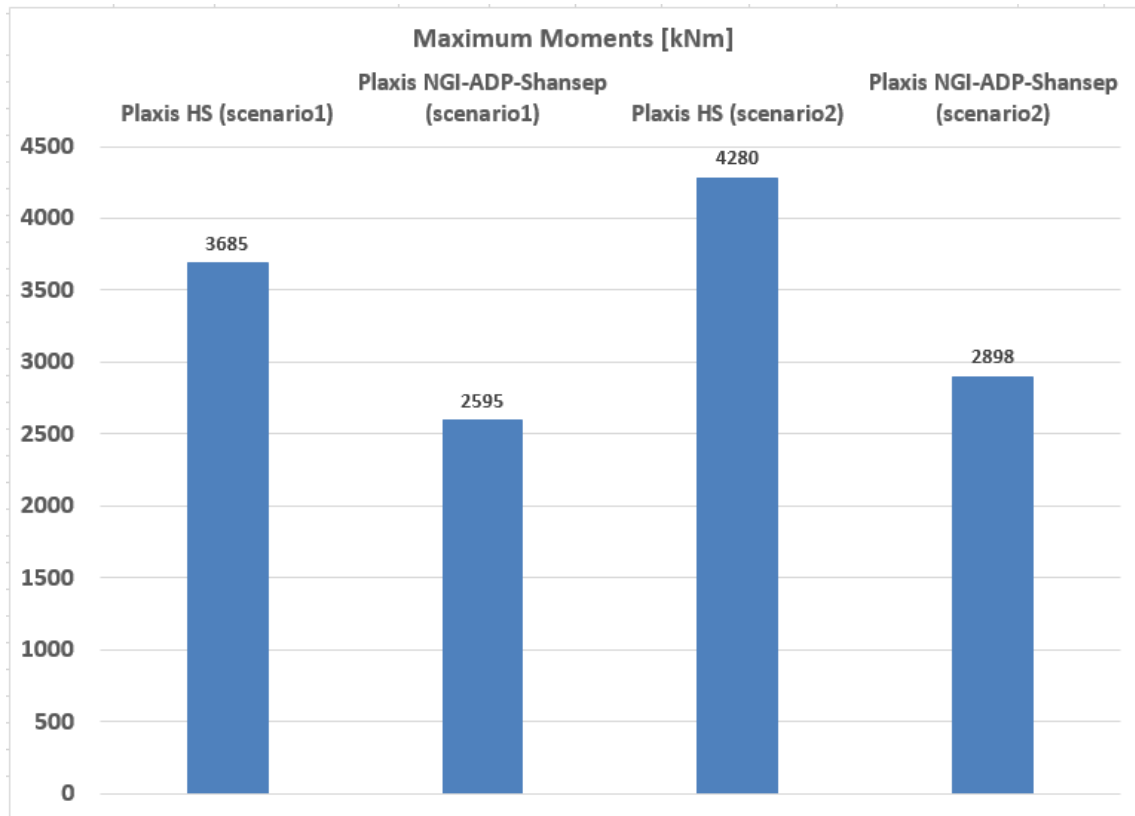


Figure 5.4: Overview of the calculated maximum bending moments in the wall for the two design approaches.

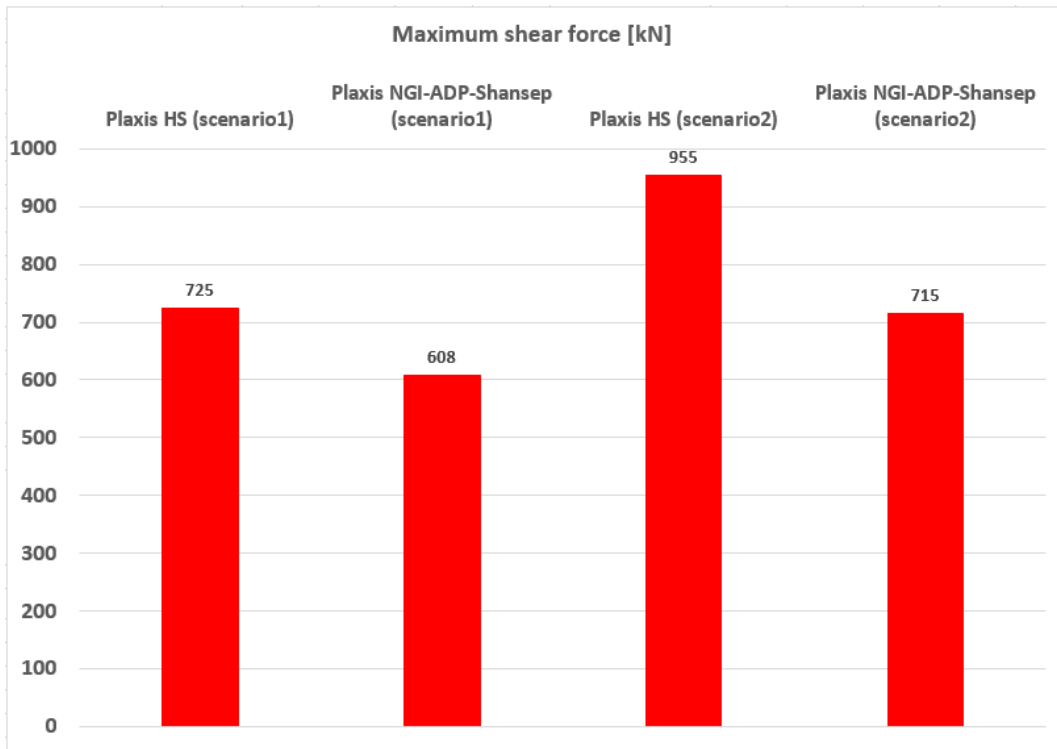


Figure 5.5: Overview of the calculated maximum shear force in the wall for the two design approaches.

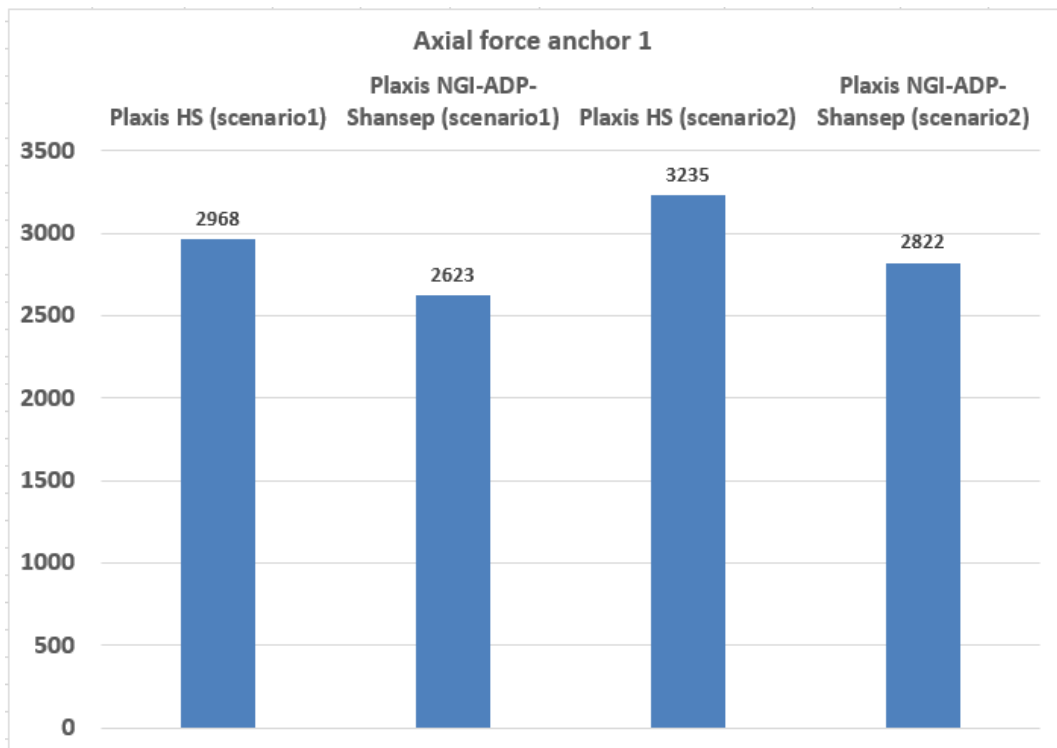


Figure 5.6: Overview of the calculated anchor forces for the two design approaches.

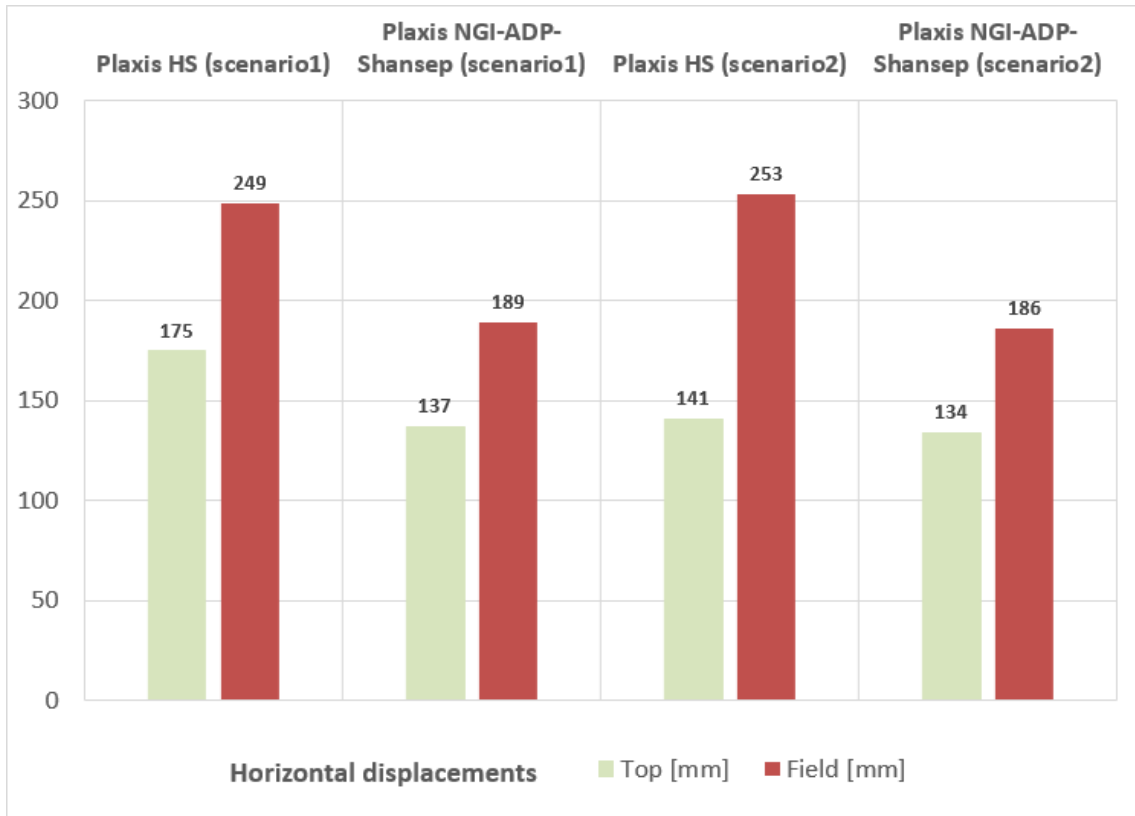


Figure 5.7: Overview of the calculated maximum horizontal displacements of the wall for the two design approaches.

	$F_{\text{anchor},1}$	$F_{\text{anchor},2}$	M_{max}	V_{max}	$w_{\text{max,top}}$	$w_{\text{max,field}}$
Scenario 1	0.88	0.90	0.70	0.84	0.78	0.76
Scenario 2	0.87	0.89	0.68	0.75	0.95	0.74

Table 5.9: Relative difference between the outcome of the two design approaches. The ratio is calculated by dividing the value of the alternative design approach by the value of the conventional design approach.

From the results presented in the figures and table above the following can be observed: The calculated forces and displacements using the conventional design approach (Plaxis Hardening soil model, undrained (A)) are larger than the values found using the alternative design approach (Plaxis NGI-ADP Shansep model). The difference between the two approaches ranges from 10% for the anchor forces up to 30% for the maximum moment and field displacement of the wall. This holds for both loading scenarios.

5.4.1 Discussion

For this case study, no calculations using the method of Blum or D-Sheet piling are performed. These methods are not capable to model the undrained behavior of the clay layer with the same level of accuracy compared to Plaxis and are therefore excluded from the analysis. Also, there are no triaxial extension test results available for the soil layers of this case study. The same holds for DSS test results. The ratios between the shear strain at failure of other clayey soils with similar characteristics like volumetric weight and nor-

malized stiffness (Post and Luijendijk, 2018) have been used. This has resulted in a ratio of 1 : 1.25 : 1.5 for $\gamma_f^C : \gamma_f^{DSS} : \gamma_f^E$. The value of γ_f^C is determined using the results of available laboratory tests.

5.4.2 Conclusion

Based on the quantitative results of this case study, the alternative design approach produces smaller forces and displacements compared to the conventional design approach. It could be that the actual stress state of the clay layer is relatively large in this specific situation. The alternative design method explicitly takes into account the effective stress levels when calculation the undrained shear strength. However, no direct explanation has been found for this outcome.

Case study 3 - Quay wall situated in overconsolidated clay layer

6.1 Introduction

This chapter comprises the analysis of a quay wall with a soil profile consisting, among others, an overconsolidated (OC) clay layer. The OC clay is typical for the northern part of the Netherlands, and is called boulder clay. Here, the Holocene soil layers have been subjected to large ice loads in the past. For an overview of the soil profile of this case study, see Figure 3.3. The soil investigation data has been gathered from the construction project of the new hospital AZG. For this project a deep excavation and construction pit with retaining walls have been applied (Dijkstra, 2002).

The characteristics of the overconsolidated clay layer, along with an analysis into undrained soil behavior for different soil types, are presented in section 6.2. In sections 6.3 and 6.4 the starting points for the design calculations plus the results of both the conventional and new design approach are presented. In section 6.5 the effects of the magnitude of the load history of the soil is being investigated. Finally, section 6.6 gives an overview of all the results combined with an analysis and conclusions of this case study.

Relevance of this case

The data of this case study does not originate an actual quay wall design, but from a building pit in the city center of Groningen. However, in the ports of Delfzijl and also in the Eemshaven, these quay walls do exist or could be build in the future. Therefore also a case with this soil type is elaborated.

In Appendix E some lab results are added that form the basis for the derivation of several model parameters used in the calculations.

6.2 Parameters and Boundary conditions

For the purpose of this research, a soil profile is constructed so that an undrained response of the soil is expected. However, whether a drained or undrained soil response will occur, depends on several factors such as soil type, permeability and the thickness of the soil layers. Therefore first the type of soil response for a number of scenarios is analyzed. The outcome of this is used to construct a soil profile to which an undrained analysis using the alternative design method can be applied. The soil profile still represents a realistic case that can occur in reality.

6.2.1 Type of soil response

As in compliance with section 2.2.4, an undrained soil response can be assumed if the hydrodynamic period satisfied the criterion $T < 0.01$, using Equation 2.5. This criterion is checked for both the original clay layers of the Amazonehaven as well as the boulder clay, where a variety of drainage lengths and load durations have been taken into account.

Soil layer	Drainage length [m]	Permeability [m/s]	Hydrodynamic period
Boulder clay	0.5	1.94E-11	1.67E-2
Boulder clay	1	1.94E-11	4.17E-3
Boulder clay	2	1.94E-11	1.04E-3
Clay (layer 9)	0.3	9.7E-11	1.68E-1
Clay (layer 11)	0.25	8.0E-11	2.65E-1
Sand (layer 5)	3.15	1.0E-5	7.83E+0

Table 6.1: Hydrodynamic period of different soil layers, duration = 3days

For sand layers, the permeability is relatively high and an undrained response of the soil for typical loading conditions of quay walls is therefore unlikely. This is confirmed by the value for T of soil layer 5, see Table 6.1. Due to the large drainage length of this layer in comparison to the other sand layers, it can be seen as representative for all sand layers present at the location of the Amazonehaven. The sand layers therefore are excluded from the undrained analyses, and will be modelled using a drained analysis.

For the cohesive soil layers the hydrodynamic period is plotted against the duration of the loading. A number of scenarios are presented in Figures 6.1 and 6.2. Here the two straight horizontal lines represent the boundary values for which a clear drained or undrained response can be expected according to Vermeer and Meier (1998), see also section 2.2.4. For the area in between these lines such a clear distinction cannot be made and the soil response will be partially drained, partially undrained.

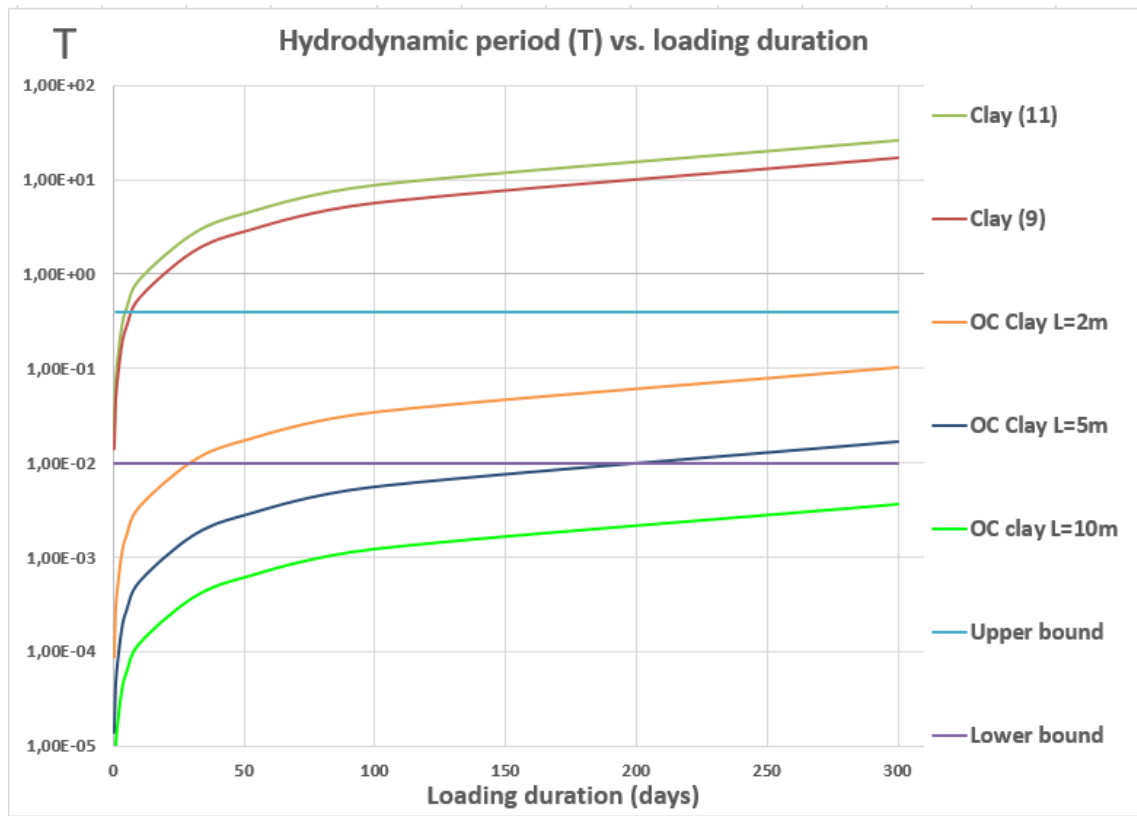


Figure 6.1: Short-term analysis of the hydrodynamic period versus loading duration for different soil layers. The values of T are presented on logarithmic scale.

From Figure 6.1 it can be seen that the soil layers 9 & 11, which represent existing clay layers at the location of the Amazonehaven, can be modelled by a drained soil response, with the exception of very short loading durations up to one week. These layers have a very small thickness and therefore also very small drainage length, see Table 6.1.

The overconsolidated clay layers however, do show an undrained response for a loading duration up to several months or years, depending on the thickness of the layer. The OC clay $L=10$ graph for example, shows the hydrodynamic period for boulder clay with a drainage length $L=10$ m, and thus a thickness of the layer of 20 meters. For loading durations up to 300 days, the soil response is still expected to be undrained. From Figure 6.2 it can be seen that a fully undrained response can be expected for loading durations till approximately 2 years, and a partially drained partially undrained response for loading situations up to 50 years, which is the technical lifetime of a quay wall structure.

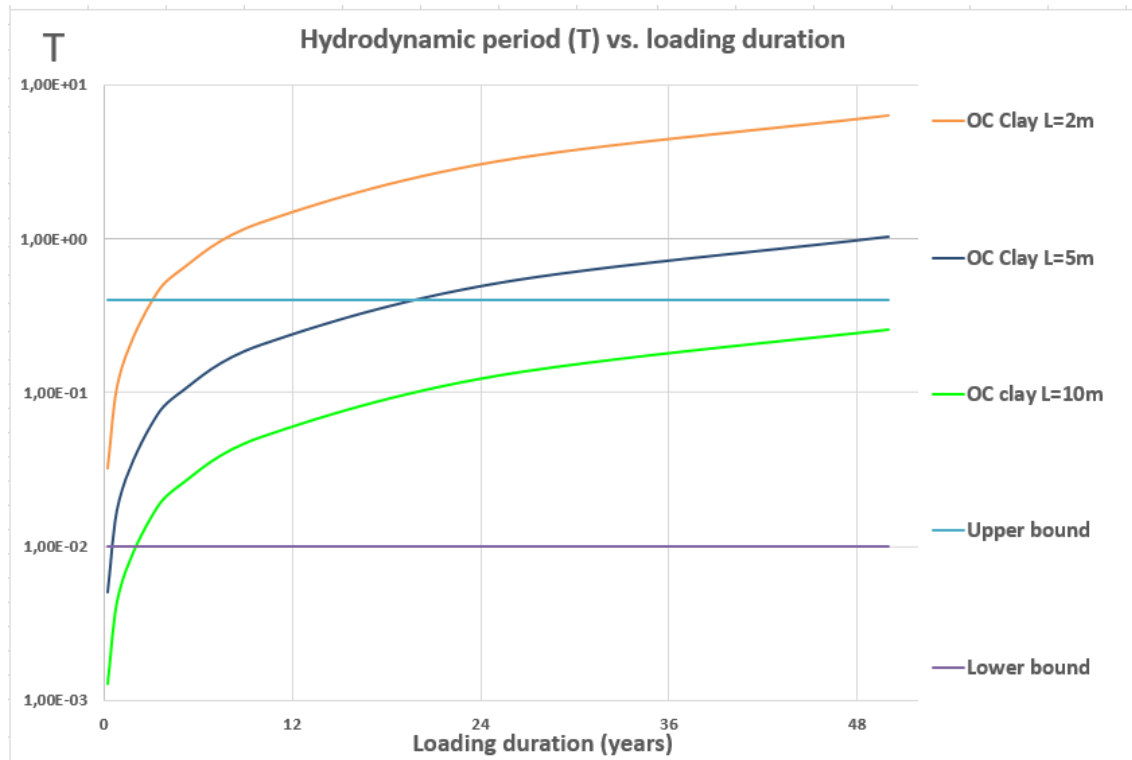


Figure 6.2: Long-term analysis of the hydrodynamic period versus loading duration for different soil layers. The values of T are presented on logarithmic scale.

6.2.2 Soil profile

For this case study, a soil profile with an OC clay layer of 25 meters is used. Due to the large thickness of the OC clay layer, it should be modelled using an undrained analysis for short term loads, and both undrained and drained analysis for long term loads. The characteristics of this soil profile are presented in Table 6.2.

Layer	Top of layer [m NAP]	Soil type	$\gamma_{dry}/\gamma_{sat}$ [kN/m ³]	ϕ [°]	C [kPa]	k [m/day]
1	+5.0	Boulder clay	17.7 / 17.7	16	34	1.68E-6
2	-20.0	Sand, Pleistocene	18.0 / 20.0	32.5	0.1	0.86

Table 6.2: Soil profile. The properties of the sand layer are the same as those of the Pleistocene sand in Chapter 4.

6.3 Designs based on conventional design approach

In this section the input parameters and results of the conventional design approach are presented. First a preliminary design calculation performed using the method of Blum is given. Next, the detailed design calculations are presented. Here a plaxis calculation is performed where the Hardening Soil material model is used to model the boulder clay. The option Undrained (A) is used to model the undrained soil behavior of the clay layer during construction and loading of the quay wall.

6.3.1 Preliminary design based on theory of Blum

Parameters

The input parameters used for this case are presented in Table 6.3. These properties are in accordance with the soil profile given in Table 6.2.

Top of layer [m NAP]	Bottom of layer [m NAP]	$\gamma_{dry}/\gamma_{sat}$ [kN/m ³]	ϕ' [°]	c' [kPa]	δ [°]
+5.0	-20	17.7 / 17.7	16	34	8
-20	-40	18 / 20	32.5	0	21.7

Table 6.3: Input parameters used to perform Blum calculation

Results

The results of the calculations are presented in Table 6.4.

Variable	Value
Anchor Force	2626 kN
M_{max}	2065 kNm/m ¹
Required embedding depth wall	30.0 m - NAP

Table 6.4: Results of Blum calculation

6.3.2 Design using Plaxis

For the conventional design method a Plaxis model is constructed where both the boulder clay and the Pleistocene sand layer have been modelled using the hardening soil material model. Because of the over-consolidation of the clay layer, the HS material model can in this case be used for clay as well. (Plaxis, 2018)

However, the clay layer shows an undrained response for the loading situations examined in this case study. The boulder clay is modelled using the drainage type Undrained (A) in Plaxis. The strength and stiffness parameters used for the different soil layers are presented in Tables 6.5 and 6.6.

Layer	Top of layer [m NAP]	Soil Type	Material model	Drainage Type	$\gamma_{dry}/\gamma_{sat}$ [kN/m ³]
1	+5.0	Clay, OC	HS	Undrained (A)	17.7 / 17.7
2	-20.0	Sand	HS	Drained	18.0 / 20.0

Table 6.5: General info soil profile as used in Plaxis

Layer	ϕ' [°]	C [kPa]	ψ [°]	E_{50}^{ref}	E_{oed}^{ref}	E_{ur}^{ref}	m	R_{inter}	POP [kPa]
1	16	34	0	8.3	8.3	33.2	1.0	0.5	39
2	32.5	0.1	2.5	29.7	29.7	118.8	0.5	0.66	39

Table 6.6: Strength and stiffness parameters used for the soil layers modelled with the Hardening Soil model

A schematization of the model in Plaxis is given in Figure 6.3. In this figure, the final situation is depicted, including the acting design loads on the structure.

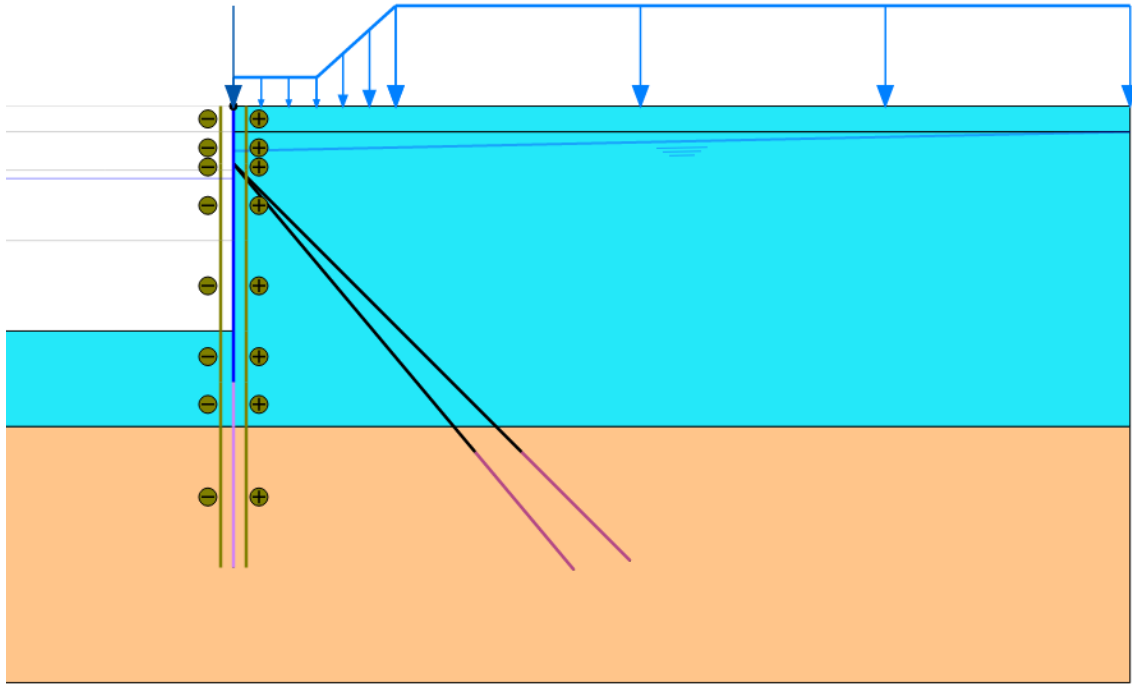


Figure 6.3: Plaxis model of the final construction phase for case study 3. Blue soil layer is boulder clay, orange layer is Pleistocene sand.

Results

The final results of the Plaxis calculations are presented in Table 6.7.

	Anchor Forces [kN]	M_{\max} [kNm/m]	V_{\max} [kN/m]	$w_{\max, \text{top}}$ [mm]	$w_{\max, \text{field}}$ [mm]
Plaxis HS scenario 1	2498 / 2244	2419	663	-125	-173
Plaxis HS scenario 2	2856 / 2592	2913	763	-134	-196

Table 6.7: Results of calculations applying conventional design approach. The displacements w are the horizontal displacements, where a negative value corresponds with a displacement towards the water.

6.4 Design based on alternative design approach using undrained analysis combined with cssm

Design using Plaxis

As shown in section 6.2, a soil layer consisting of boulder clay with a drainage length of 10 meters shows an undrained response for loading situations up to a duration of multiple years. The undrained behavior of the clay layer below the phreatic surface is modelled in Plaxis using the User Defined material model *Shansep NGI-ADP*.

Layer	Top of layer [m NAP]	Soil Type	Material model	Drainage Type	$\gamma_{dry}/\gamma_{sat}$ [kN/m ³]
1	+5.0	Clay, OC	HS	Undrained (A)	17.7 / 17.7
2	0.0	Clay, OC	NGI-ADP Shansep	Undrained (A)	17.7 / 17.7
3	-20.0	Sand	HS	Drained	18.0 / 20.0

Table 6.8: Soil profile as specified in Plaxis for the alternative design approach

A list of input parameters used to model soil layer 2 using the NGI-ADP Shansep material model is given in Table 6.9.

More information about this material model can be found in section 2.5.

Model parameters	Symbol	Value	Unit
Normalized stiffness	G/s_u^A	110.1	-
Failure shear strain in compression	γ_f^C	3.6	%
Failure shear strain in extension	γ_f^E	9.4	%
Failure shear strain in direct simple shear	γ_f^{DSS}	6.5	%
Reference undrained shear strength in active mode	$s_{u,ref}^A$	115	kN/m ²
Reference depth	$vert_{ref}$	-10.8	m - NAP
Increase of undrained shear strength over depth	$s_{u,inc}^A$	7	kN/m ² /m
Ratio between passive and active shear strength	s_u^P/s_u^A	0.798	-
Initial mobilized shear strength	τ_0/s_u^A	0.7	-
Ratio between shear strength in DSS and active mode	s_u^{DSS}/s_u^A	0.90	-
Poissons ratio	ν	0.2	-
Poissons ratio undrained	ν_u	0.495	-
Ratio between s_u^A and σ'_v in case of virgin loading (S)	alpha	0.28	-
Power. Indicates the dependency of s_u on OCR	m	0.8	-
Minimum value of undrained shear strength	$s_{u,min}$	1.0	kN/m ²

Table 6.9: Shansep NGI-ADP model parameters and the corresponding values for boulder clay

For a number of parameters of the Shansep NGI-ADP material model, correlations have been determined in the case of insufficient available soil investigation data. See also section 3.2.1. Input values extracted from soil investigation data (see Appendix E):

Parameter	Symbol	Value	Unit
Undrained secant stiffness	E_{50}^u	62.4	MPa
Original depth of soil sample	d_{sample}	-15.8	m below surface
Undrained shear strength at depth d_{sample}	s_u^A	189	kN/m ²
Axial strain in compression	ε_1^C	2.4	%
Primary compression index	C_c	0.05	-
Secondary compression index	C_s	0.02	-
Critical state friction angle	ϕ'_{cv}	16	°

Table 6.10: Input used to determine the parameters of the NGI-ADP Shansep material model

Some notes:

1. There are no triaxial extension test results available for the soil layers of this case study. The same holds for DSS test results. The ratios between the shear strain at failure of other clayey soils with similar characteristics like volumetric weight and normalized stiffness (Post and Lujendijk, 2018) have been used as reference. This has resulted in a ratio of 1 : 1.8 : 2.6 for γ_f^C : γ_f^{DSS} : γ_f^E . The value of γ_f^C is determined using the results of available triaxial compression tests.

Results

In the following table the final results of the design calculations of the alternative design method are presented. For the two scenarios described in section 5.1.3 the sectional forces of the wall, the anchor forces and the displacements are given in the following table.

	Anchor Forces [kN]	M_{\max} [kNm/m]	V_{\max} [kN/m]	$w_{\max, \text{top}}$ [mm]	$w_{\max, \text{field}}$ [mm]
NGI-ADP Shansep Scenario 1	2651 / 2412	2379	686	-138	-180
NGI-ADP Shansep Scenario 2	3044 / 2781	2905	820	-140	-196

Table 6.11: Results of calculations where the alternative design approach including the NGI-ADP Shansep model is used

6.5 Sensitivity analysis for historic loads

Because the magnitude of historic load and thereby preconsolidation is explicitly taken into account in the Shansep model, an additional analysis has been performed to look specifically at the effects of the loading history. Here, for both the conventional and alternative design approach calculations have been performed using varying values of the pre-overburden pressure for the clay layer. The relative difference of both design approaches is plotted versus the POP values in Figures 6.4 and 6.5.

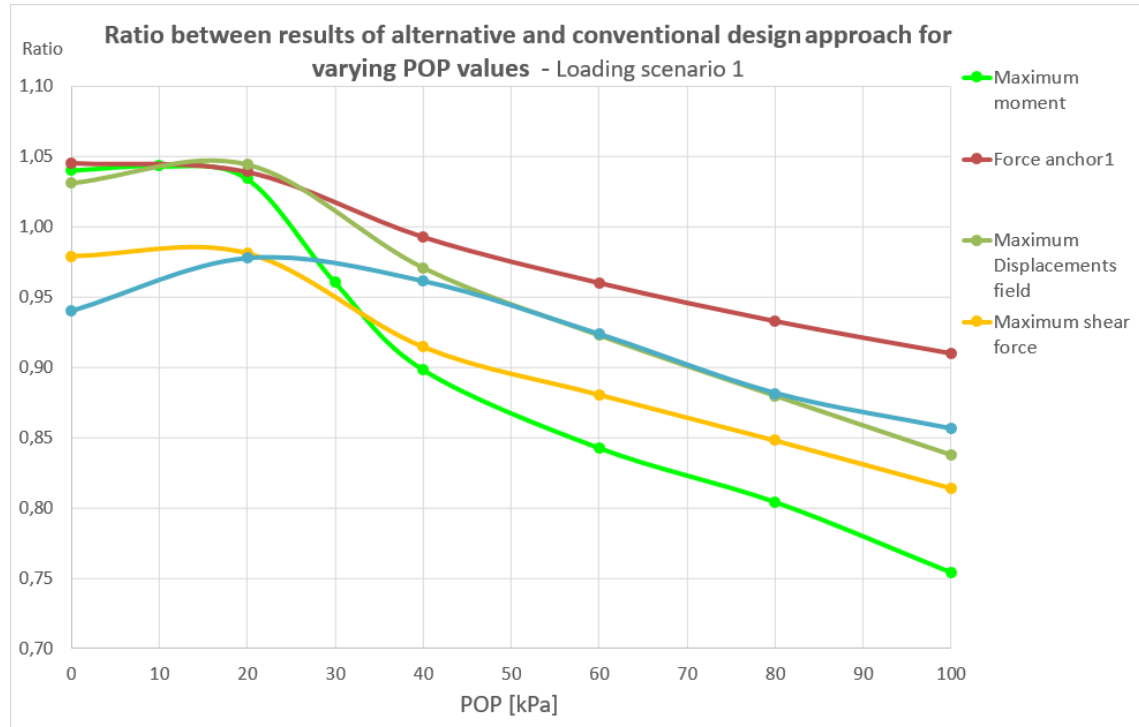


Figure 6.4: For each quantity the quotient alternative value over conventional value is plotted against loading history, presented for loading scenario 1.

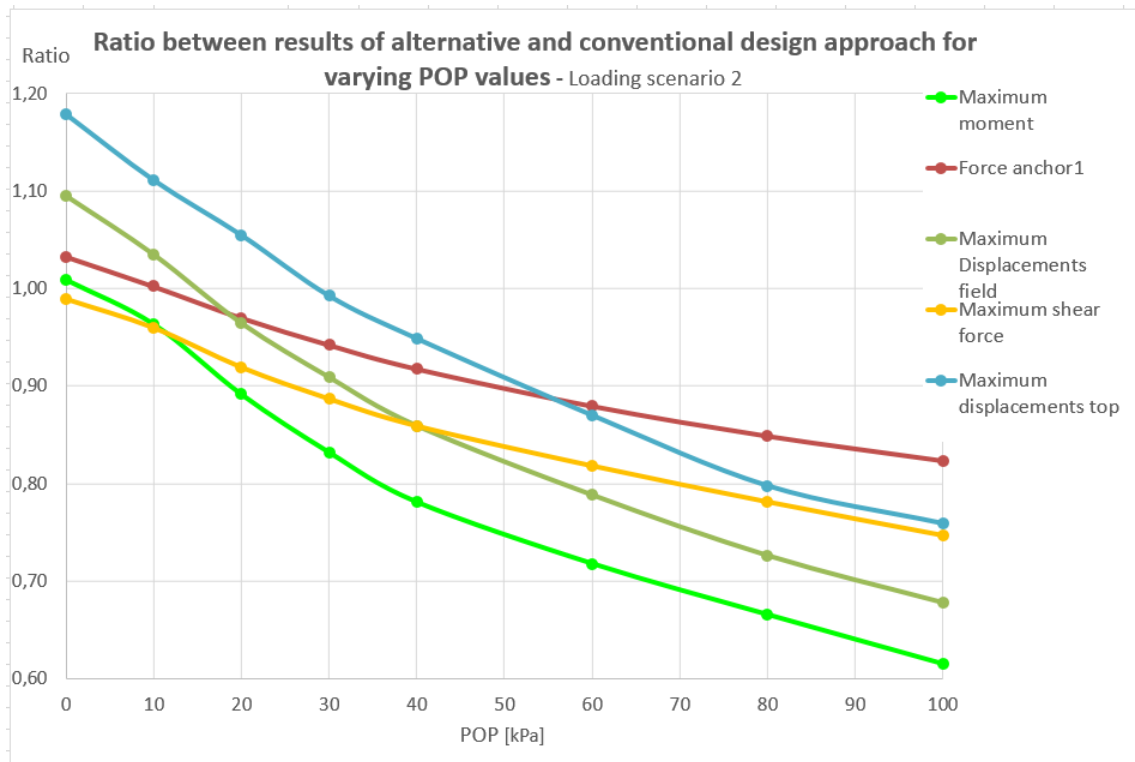


Figure 6.5: For each quantity the quotient alternative value over conventional value is plotted against loading history, presented for loading scenario 2.

In case of no load history, the alternative design approach will produce the same order of magnitude for the sectional forces and displacements of the wall, as indicated by a ratio close to 1. For increasing values of the pre-overburden pressure, the ratio decreases and the alternative design approach produces lower values than the conventional design approach.

6.6 Results

In this section the outcome of case study 3 is analyzed and discussed.

In the Figures 6.6 up to 6.9 the results of the calculations in terms of forces and displacements of the wall are given, for both the conventional and alternative design approach.

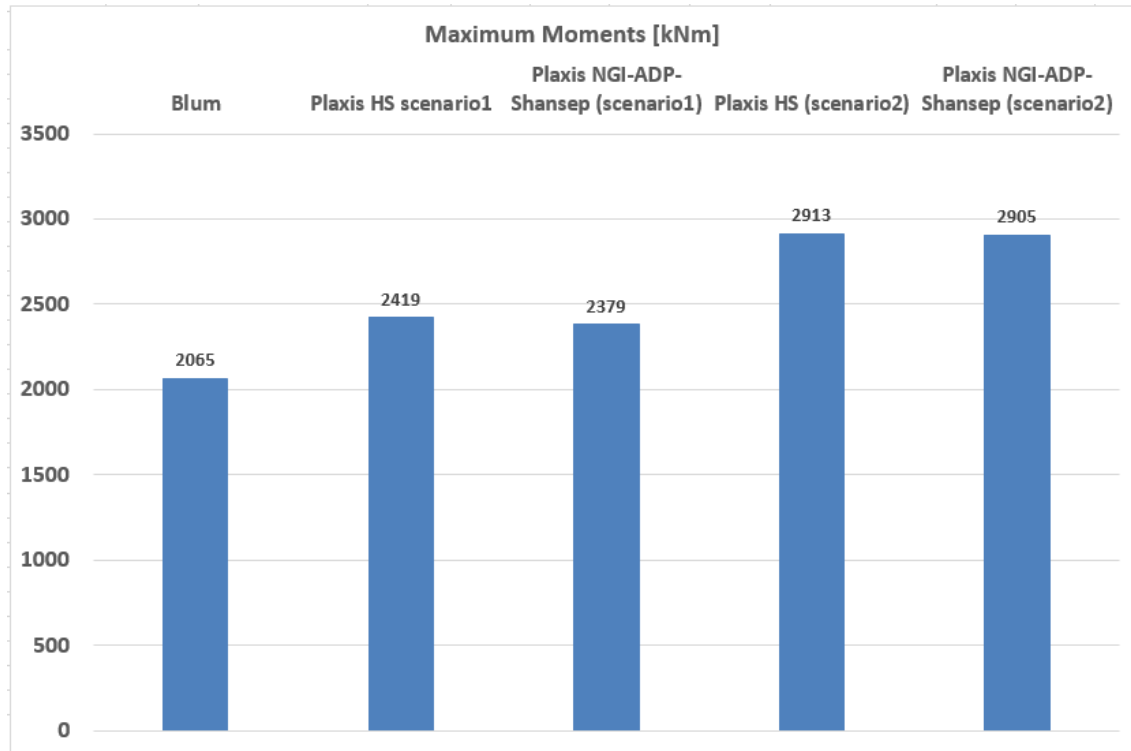


Figure 6.6: Overview of the maximum bending moments in the wall found using the different design approaches and design methods.

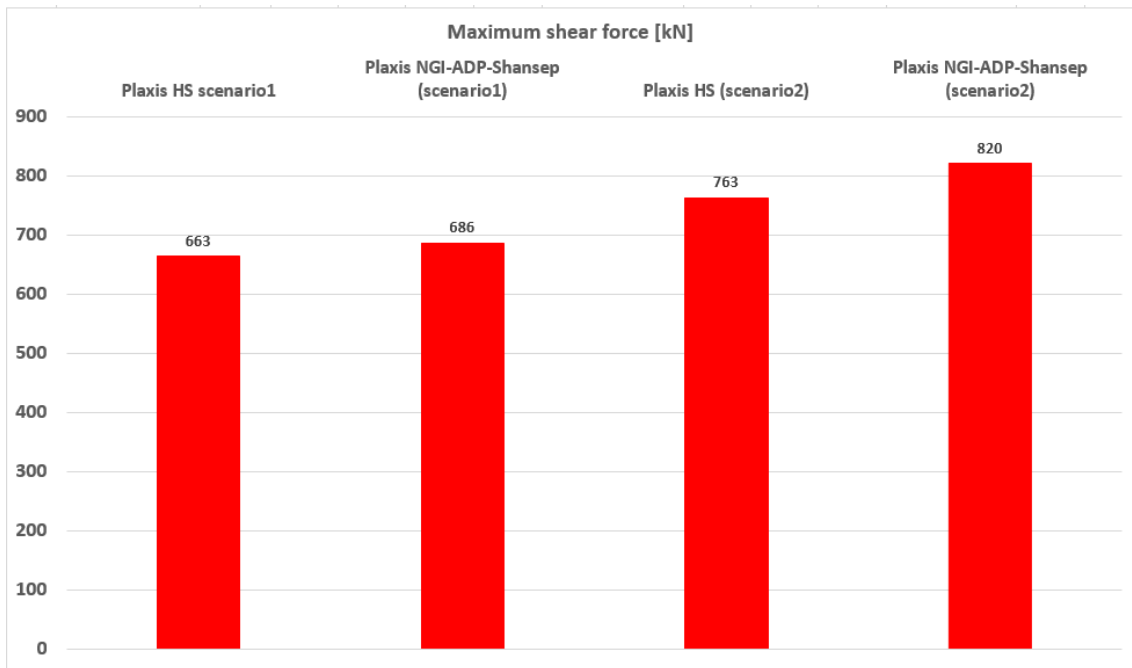


Figure 6.7: Overview of the maximum shear force in the wall found using the different design approaches and design methods.

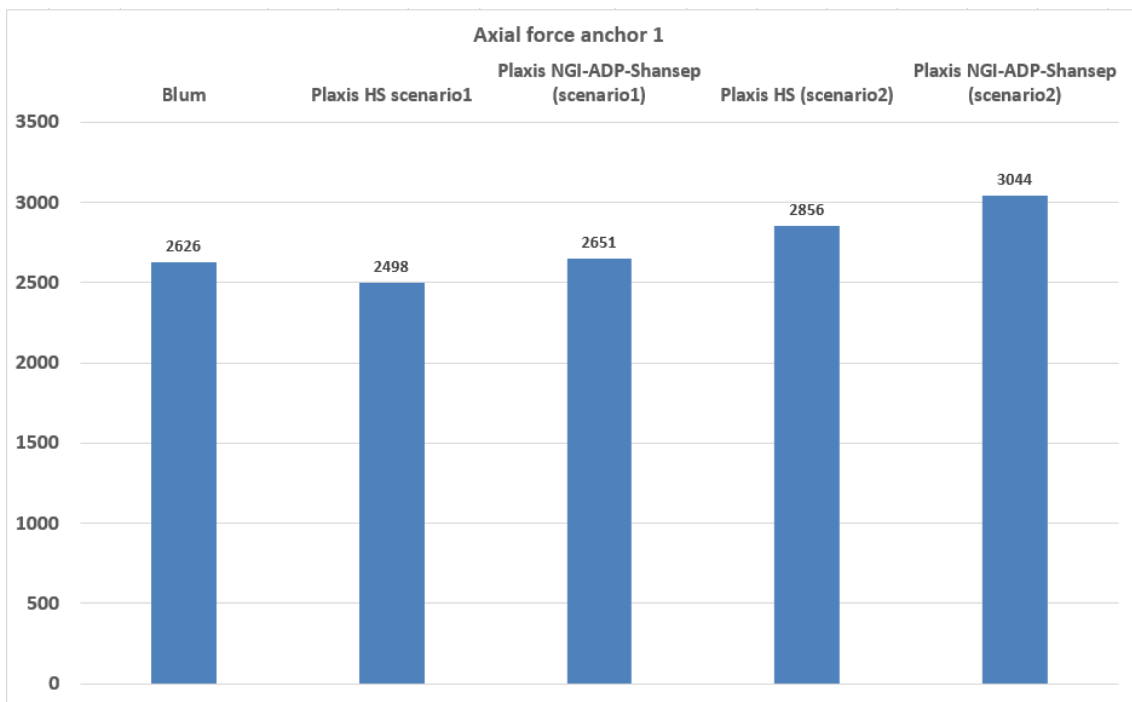


Figure 6.8: Overview of the anchor forces found using the different design approaches and design methods.

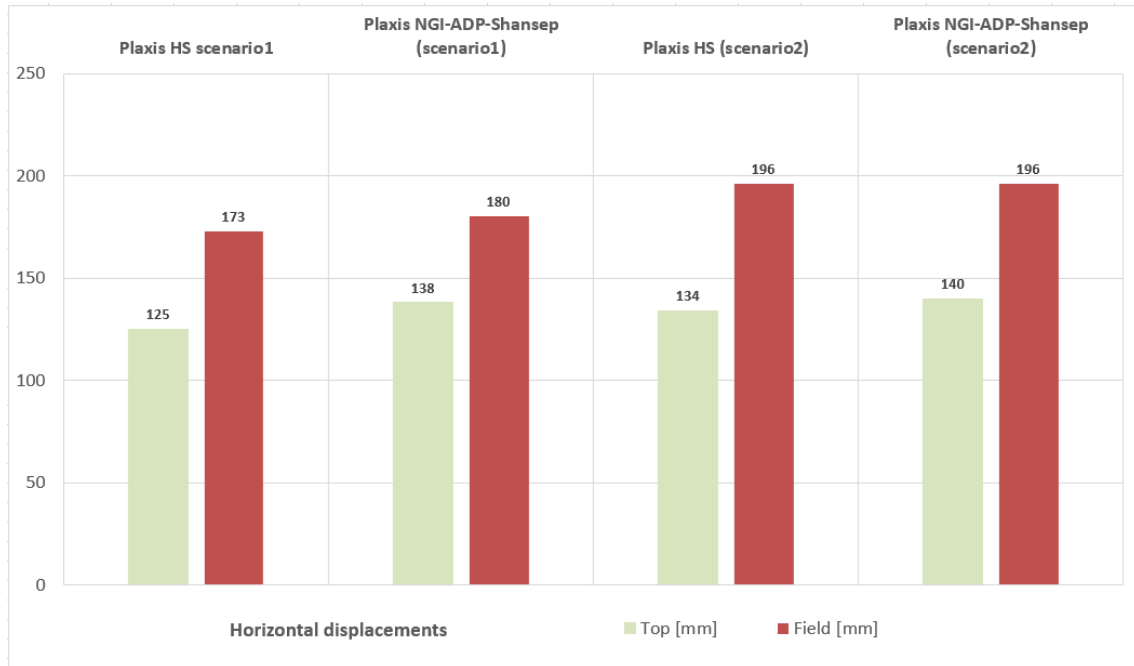


Figure 6.9: Overview of the maximum horizontal displacements of the wall, found using the different design approaches and design methods.

From the results of the figures and table above the following trends can be observed:

- For both loading scenarios, the differences in outcome between the conventional design approach (Plaxis HS) and the alternative design approach (Plaxis NGI-ADP Shansep) are small, The differences between the two methods are given in Table 6.12.
- There is a difference between the results of loading scenario 1 and 2. This suggests that whether drained or undrained behavior of the soil occurs, does influence the soil stresses and strains that will occur during the lifetime of this quay wall. The results of scenario 1, where undrained soil behavior is taken into account for the complete lifetime of the structure, including construction, shows slightly smaller displacements and smaller forces compared to scenario 2.

	$F_{\text{anchor},1}$	$F_{\text{anchor},2}$	M_{max}	V_{max}	$w_{\text{max,top}}$	$w_{\text{max,field}}$
Scenario 1	1.06	1.07	0.98	1.03	1.10	1.04
Scenario 2	1.07	1.07	1.00	1.07	1.04	1.00

Table 6.12: Relative difference between the outcome of the two design approaches. The ratio is calculated by dividing the value of the alternative design approach by the value of the conventional design approach.

6.6.1 Discussion

For this case study, the results of both the method of Blum and D-Sheet are not comparable with the results of the Plaxis calculations due to the fact that all plaxis calculations do include at least partially undrained behavior. The results of Blum and D-Sheet do reflect a fully drained analysis. Also, the assumption that during sliding of the soil very large strains do occur (for clay 25%) and that the soil is in critical state does not hold for this

case study. The quay wall will prevent full sliding of the soil, and the maximum shear strains reached for this case study are in the order of 8% reached at the passive side of the quay wall.

For the sensitivity analysis of loading history, only the parameter for POP is changed in the calculations. In reality, a soil that has experienced a lower or higher maximum pre-overburden pressure in the past, also possesses different strength and stiffness parameters. This has not been included in the calculations, which makes the outcome unreliable.

6.6.2 Conclusion

Based on the quantitative results of this case study, the difference in outcome between the conventional and alternative design approaches is between -2 and 10% for the quantities displacements and sectional forces. This difference in outcome is not significant when taking into account the uncertainty that is introduced by 1) the theoretical models used, 2) laboratory results of soil experiments and 3) correlations for model parameters.

In this chapter the results and approach of the research are discussed. First, in Table 7.1 an overview of the relative difference of the design approaches for each design method is given.

	D-Sheet	Plaxis
Case 1	1.10 - 1.36	1.11 - 1.36
Case 2	Not applicable	0.68 - 0.95
Case 3	Not applicable	0.98 - 1.10

Table 7.1: Overview of relative differences of the design approaches for each design method, presenter for each case study.

The table shows that the ratios of case 1 and case 3 are equal to or larger than 1. This can be explained due to the fact that the circumstances and boundary conditions of case 1 and also to less extend case 3, do not reflect the conditions for which the alternative design method originally was developed.

However, case 2 does not fit in this trend. Here the results of the alternative design approach are lower than those of the conventional design approach. As mentioned before in section 5.4.2, a direct explanation for this has not been found. Further research in the direction of local stress states of the soil should be performed to clarify this. Also, the applicability of the Hardening soil model for soft clay layers such as those in case study 2 can be analysed further.

Based on the results and conclusions of this research, the following remarks and recommendations can be used as input for further research. First, the new design method incorporates the different locations along a sliding plane, i.e. active shear, direct shear and passive shear. In case of a quay wall, the slip surface of the soil next to the wall is either active (on the land side) or passive (on the water side). Only for global slope failure a full sliding plane is developed and the analogy used in the method for dikes is representative. However, the method is also used in case of a structural element inside the dike body to increase stability.

Second, the laboratory tests are not executed according the prescribed standards. Most

notable point is the prescribed strain levels for triaxial compression tests and triaxial extension tests. These prescribed levels have not been reached in the tests, making the test results not a reliable reflection of the soil properties at critical state. This results in less reliable model parameters that serve as input for the design calculations. A possible measure to overcome some of this uncertainty is the use of in-situ measurements of the displacements of the wall. This data can be used to validate which model better represents the reality.

Third, the case study with a normal consolidated clay layer indicates that in the absence of pre-overburden pressure, the alternative design approach produces lower values for both sectional forces and displacements. The results of case study 3 with an overconsolidated clay layer show, for a POP value of zero, larger values for the alternative design approach compared to the conventional design approach. These two outcomes contradict each other. No direct explanation has been found for this.

The objective of this research is to investigate the possibilities to use an alternative design approach, taking into account anisotropy and loading history of the soil during undrained circumstances, for modelling soil behavior in the design processes of a quay wall. Using the results of the case studies and literature review, the main research question can be answered.

Can critical state soil mechanics in combination with undrained analysis of the soil be applied for the design of quay walls, and what are the effects for the prediction of strength and stability?

Based on the results of the three case studies elaborated in this report, the alternative design approach applied in this report is not a valid option for a quay wall in sandy soil due to the absence of undrained soil conditions. For the cases where a clay layer is present, the hydrodynamic period indicates whether undrained soil behavior will occur. In those situations the alternative design method could be used.

The new design approach for dikes is developed under the condition that a specific set of soil investigation data and laboratory tests on the soil samples is being executed. Using the results of these tests, the model parameters can be determined with more certainty and the results become more reliable. This approach has to be implemented for quay walls into further research. Furthermore, the comparability of the failure mechanisms assessed in this research with respect to those of dikes is limited, due to the absence of a structural element in dikes.

The results of the case studies show that for a sandy soil profile, the alternative design approach produces larger values for sectional forces and displacements of the wall than the conservative design approach. In case of a quay wall situated in a predominantly clayey soil, the alternative design approach produces results with the same order of magnitude for sectional forces and displacements of the wall compared to the conventional design approach. The magnitude of preconsolidation of the soil plays an important role here, where with increasing values of pre-loading, the results of the alternative design approach are decreasing in comparison to those of the conventional design approach.

Finally, the new assessment approach for dikes is specifically developed for slope stability of a dike body in case of a flood wave, where excess pore pressures develop inside the dike body. For retaining structures, the alternative design approach is only valid if an undrained response of the soil can be expected. This is assessed by determining the hydrodynamic period of each soil layer, where the duration of the load acting on the wall is taken into account. Also, since new design approach is specifically developed for the assessment of slope stability, the calculations using Plaxis will enable the assessment of global (slope) stability of the wall, and local shearing and displacements of the soil. Regarding the assessment of sectional forces of both wall and soil anchors, values for these quantities are generated by Plaxis which can be used as input for additional calculations to determine structural safety and stability of the wall.

List of Figures

2.1	The left figure shows stress paths of a dilatant soil, the right figure shows stress paths of a contractant soil. (Verruijt, 2012)	14
2.2	Schematization of Blum for a situation with homogeneous soil profile. In the left figure the internal stresses in the wall are shown. The right figure shows the pressures due to soil and groundwater, acting on the wall. (Verruijt, 2012)	16
2.3	Example of a retaining wall in D-Sheet Piling	18
2.4	General overview of dike showing the most important elements. Source: Jonkman et al. (2018)	20
2.5	Example of a dike with a stability screen. In this case there are grout anchors applied along the screen, to provide more horizontal support if the soil body starts shearing. Source: POVM	21
2.6	Shear strength according to CSSM. (Rijkswaterstaat, 2017)	22
2.7	Hyperbolic stress-strain relation of sand in primary loading for a standard drained triaxial test. (Plaxis, 2018)	24
2.8	Stress-strain relation of clay and peat. The three curves represent the results of an undrained triaxial compression test (s_u^A), an undrained triaxial extension test (s_u^P) and a Direct Simple Shear test (s_u^{DSS}). G_{ur} defines the isotropic elasticity of the soil. (Naves and Lengkeek, 2017)	25
3.1	Overview of soil layers and soil types for case study 1.	28
3.2	Overview of soil layers and soil types for case study 2.	28
3.3	Overview of soil layers and soil types for case study 3.	29
3.4	Overview of construction phases used in the calculations	30
3.5	Stress-strain diagram of an CRS test. The blue line represents the test results. The red line through points A and B represents the tangent line of the primary loading branch of the diagram. Source: Rijkswaterstaat (2017)	34
4.1	Location of the Amazonehaven in the Port of Rotterdam. Source: Google Inc.	37
4.2	Overview Amazonehaven with different quay walls. 'Kade A1' and 'Kade A2' are indicated with the solid green respectively purple line. The dotted yellow line indicates the old quay wall, which has been demolished afterwards. Source: Gemeentewerken Rotterdam (2011a)	37

4.3	Cross section of quay wall A1. Source: Gemeentewerken Rotterdam	39
4.4	Schematization of the variable load behind the quay wall	40
4.5	Geotechnical length profile of the Amazonehaven quay wall part A1. Source: Gemeentewerken Rotterdam	41
4.6	Overview of the maximum bending moments in the wall found using the different design approaches and design methods.	50
4.7	Overview of the maximum shear force in the wall found using the different design approaches and design methods.	51
4.8	Overview of the anchor forces found using the different design approaches and design methods.	51
4.9	Overview of the maximum horizontal displacements of the wall, found using the different design approaches and design methods. Only absolute values are presented.	52
4.10	Overview of the generated principle axial strains ε_1 in case of the new design approach. The scale on the right varies from 0.0 % (dark blue) till 8.0 % (red).	53
5.1	Short-term analysis of the hydrodynamic period (log-scale) versus loading duration for different thickness of the clay layer	56
5.2	Long-term analysis of the hydrodynamic period (log-scale) versus loading duration for different thickness of the clay layer	57
5.3	Plaxis model of the final construction phase for case study 2. The grey layer represent moderately dense sand, the light blue layer represents the normally consolidated clay and the orange layer represents Pleistocene sand.	60
5.4	Overview of the calculated maximum bending moments in the wall for the two design approaches.	63
5.5	Overview of the calculated maximum shear force in the wall for the two design approaches.	64
5.6	Overview of the calculated anchor forces for the two design approaches.	64
5.7	Overview of the calculated maximum horizontal displacements of the wall for the two design approaches.	65
6.1	Short-term analysis of the hydrodynamic period versus loading duration for different soil layers. The values of T are presented on logarithmic scale.	69
6.2	Long-term analysis of the hydrodynamic period versus loading duration for different soil layers. The values of T are presented on logarithmic scale.	70
6.3	Plaxis model of the final construction phase for case study 3. Blue soil layer is boulder clay, orange layer is Pleistocene sand.	73
6.4	For each quantity the quotient alternative value over conventional value is plotted against loading history, presented for loading scenario 1.	76
6.5	For each quantity the quotient alternative value over conventional value is plotted against loading history, presented for loading scenario 2.	77
6.6	Overview of the maximum bending moments in the wall found using the different design approaches and design methods.	78
6.7	Overview of the maximum shear force in the wall found using the different design approaches and design methods.	79
6.8	Overview of the anchor forces found using the different design approaches and design methods.	79

6.9	Overview of the maximum horizontal displacements of the wall, found using the different design approaches and design methods.	80
A.1	Example	93
A.2	α represents the inclination of the CSL. ϕ_i' is the critical state friction angle. Source: Appendix F Rijkswaterstaat (2017)	94
D.1	Results of lab tests onto soft clay from borehole Container Terminal Alblasserdam, part1	99
D.2	Results of lab tests onto soft clay from borehole Container Terminal Alblasserdam, part2	100
D.3	Results of lab tests onto soft clay from borehole Container Terminal Alblasserdam, part3	101
D.4	Results of lab tests onto soft clay from borehole Container Terminal Alblasserdam, part4	102
D.5	Results of CU triaxial tests onto soft clay from borehole Container Terminal Alblasserdam, part1	103
D.6	Results of CU triaxial tests onto soft clay from borehole Container Terminal Alblasserdam, part2	104
E.1	Overview of borehole B1,part1	106
E.2	Overview of borehole B1,part2	107
E.3	Results of triaxial compression test of boulder clay, sample B1S7	108
E.4	Results of triaxial compression test of boulder clay, sample B1S7	109
E.5	Results of triaxial compression test of boulder clay, sample B1S7	110
E.6	Results of a uniaxial compression test of boulder clay, sample B1S7	111
E.7	Settlement curve of boulder clay, sample B1S7	112
E.8	Z - log p curve of boulder clay, sample B1S7	113

List of Tables

2.1	Shansep NGI-ADP model variables. (Brinkgreve and Panagoulas, 2017) . . .	25
3.1	Similarities and differences of modelling choices and boundary conditions for the case studies	31
3.2	Strength and stiffness parameters of the interface of boulder clay for the Shansep NGI-ADP model	35
4.1	Normative soil profile and parameters of quay wall part A1, profile1. In the 3 rd column the volumetric weights of the soil in both dry and saturated state are given. The 4 th and 5 th column give the friction angle and cohesion of the soil for an axial strain level of 2%, based on historical data & triaxial tests.	42
4.2	Structural parameters of quay wall used in Plaxis models	42
4.3	Structural parameters of grout anchor used in Plaxis models	43
4.4	Input parameters used to perform Blum calculation	44
4.5	Results of Blum calculation	45
4.6	Overview of the values for modulus of subgrade reaction using the secant method. Based on geotechnical report of Amazonehaven quay wall section A3	45
4.7	Normative soil profile and strength parameters inserted in Plaxis.	46
4.8	Stiffness parameters inserted in Plaxis. The values presented in red are estimates since no data was available.	46
4.9	Results of calculations applying conventional design approaches. The table gives from left to right: axial force in both anchors, maximum bending moment and shear force in the wall, and the maximum wall displacements at the top of the wall and in the field. The displacements w are the horizontal displacements, where a negative value corresponds with a displacements towards the water.	47
4.10	Normative soil profile and strength parameters based on critical state theory, according to Rijkswaterstaat (2017).	48
4.11	Values of modulus of subgrade reaction in the D-Sheet calculations	49
4.12	Results of calculations applying the new design approach	49

4.13	Relative difference between the outcome of the conventional and alternative design approach, for both D-Sheet and Plaxis calculations. The ratio is calculated by dividing the value of the alternative design approach by the value of the conventional design approach.	54
5.1	Build-up of the soil profile. For each soil layer, the location and properties are given.	57
5.2	General info of soil profile used in Plaxis	59
5.3	Strength and stiffness parameters of the soil layers.	59
5.4	Results of calculations applying conventional design approaches. The displacements w are the horizontal displacements, where a negative value corresponds with a displacement towards the water.	60
5.5	Shansep NGI-ADP model parameters and the corresponding values for soft clay in the Rhine river delta	61
5.6	Shansep NGI-ADP interface parameters of soft clay	61
5.7	Input used to determine the model parameters of the NGI-ADP Shansep model	62
5.8	Results of calculations using the alternative design approach including the NGI-ADP Shansep model	62
5.9	Relative difference between the outcome of the two design approaches. The ratio is calculated by dividing the value of the alternative design approach by the value of the conventional design approach.	65
6.1	Hydrodynamic period of different soil layers, duration = 3days	68
6.2	Soil profile. The properties of the sand layer are the same as those of the Pleistocene sand in Chapter 4.	70
6.3	Input parameters used to perform Blum calculation	71
6.4	Results of Blum calculation	71
6.5	General info soil profile as used in Plaxis	72
6.6	Strength and stiffness parameters used for the soil layers modelled with the Hardening Soil model	72
6.7	Results of calculations applying conventional design approach. The displacements w are the horizontal displacements, where a negative value corresponds with a displacement towards the water.	73
6.8	Soil profile as specified in Plaxis for the alternative design approach	74
6.9	Shansep NGI-ADP model parameters and the corresponding values for boulder clay	74
6.10	Input used to determine the parameters of the NGI-ADP Shansep material model	75
6.11	Results of calculations where the alternative design approach including the NGI-ADP Shansep model is used	75
6.12	Relative difference between the outcome of the two design approaches. The ratio is calculated by dividing the value of the alternative design approach by the value of the conventional design approach.	80
7.1	Overview of relative differences of the design approaches for each design method, presenter for each case study.	82
B.1	Correlations to find stiffness parameter for different soil types	95

B.2 Ratios of stiffness parameters in Plaxis for different soil types. (CUR2003-7,
2003) 96

 Info about current practise CSSM in dikes and embankments

A.1 Approach for determining the critical state friction angle

The shear strength of the soil according to the critical state soil mechanics, is described using

$$t_{max} = s' \sin \phi'_{cv} \quad (\text{A.1})$$

where:

- t_{max} the maximum mobilized shear strength,
- s' the mean effective stress $\frac{1}{2}(\sigma'_v + \sigma'_h)$,
- ϕ'_{cv} the critical state friction angle

According to Rijkswaterstaat (2017) the critical state friction angle can be found using a triaxial test where either:

- the consolidation stress is higher than the yield stress of the soil specimen, or
- the consolidation stress equals the in-situ vertical stress in the soil

The triaxial test has to be performed up to an axial strain level of at least 25% for sand and clay, and 40% for peat.

In Figure A.1 an example of a stress-strain diagram is given. The diagram gives the results of an consolidated, undrained triaxial test on a clay specimen of soil layer 9. The triaxial test is performed up to an axial strain level of 18%. In this example there is a decreasing trend with increasing axial strain. The value for ϕ'_{cv} is therefore probably a little overestimated if the stress-strain values at 18% axial strain are used.

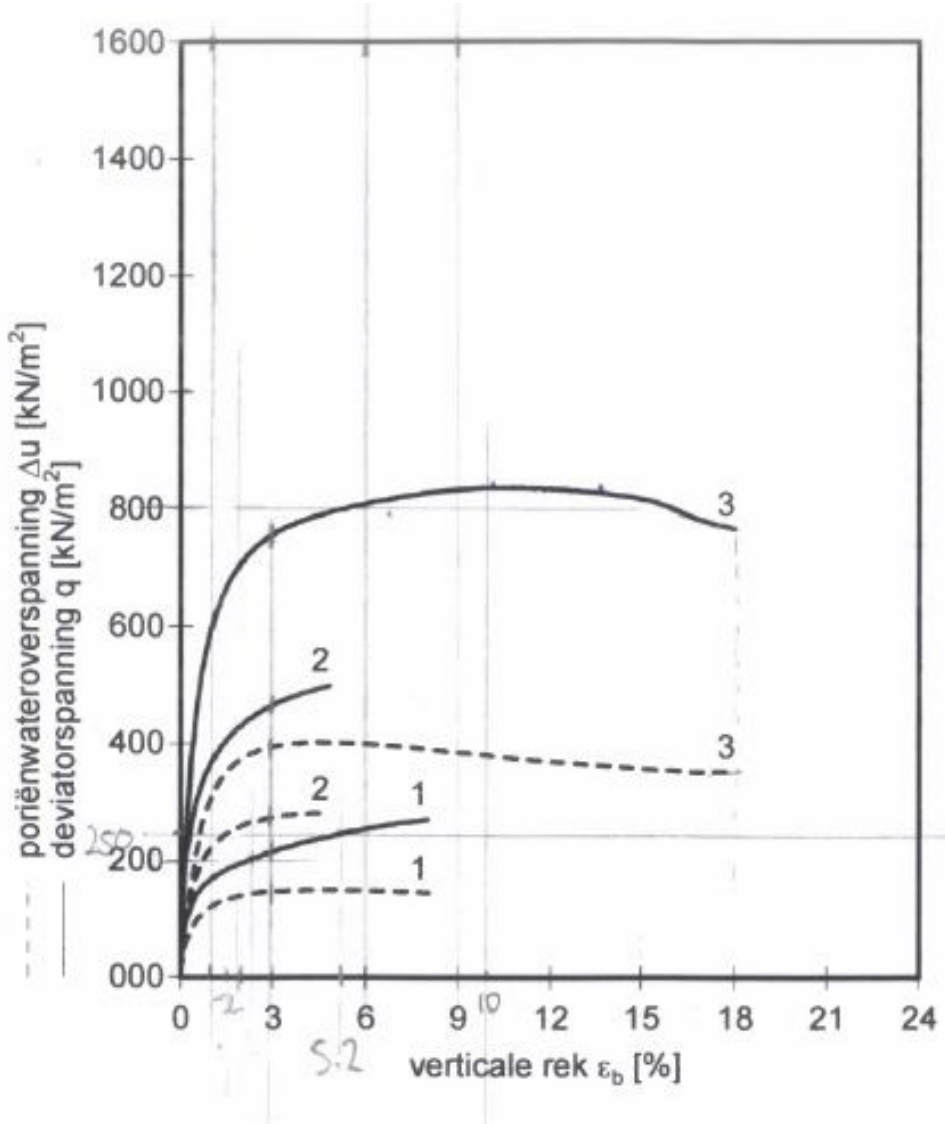
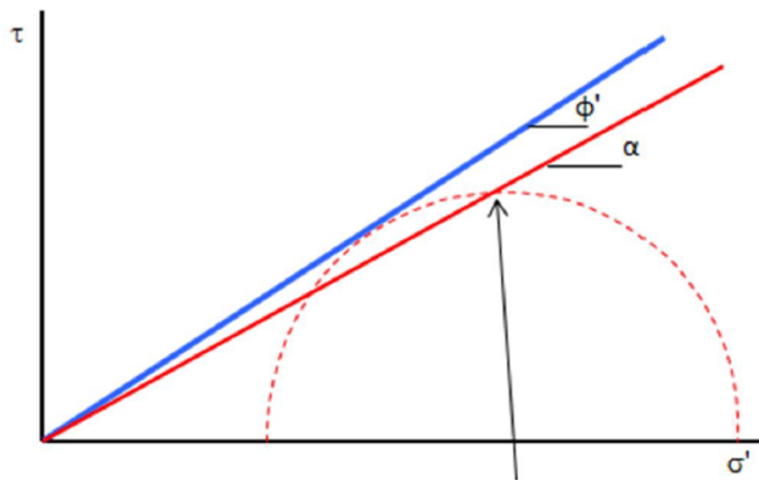


Figure A.1: Example

The result of these test, and other available data are used to determine the critical state friction angles. For this, Mohr's Circle is used. Figure A.2 shows the relation between the critical state friction angle and the angle of the critical state line.



Top of Mohr's Circle is the stress state at failure. This point is located on the CSL

Figure A.2: α represents the inclination of the CSL. ϕ_i' is the critical state friction angle. Source: Appendix F Rijkswaterstaat (2017)

Correlations provided by CUR166 (2008), CUR211 (2014), CUR2003-7 (2003) and Plaxis (2018) that have been used to determine model parameters for the design calculations:

Stiffness parameters based on triaxial tests

The stiffness parameters are derived using available soil investigation data, where the values of the secant stiffness E_{50} and oedometer stiffness E_{oed} are given. Using the relations presented in Equations B.1 and B.2, the values for the reference stiffness are determined (Plaxis, 2018).

$$E_{50} = E_{50}^{ref} \left(\frac{c \cos \phi - \sigma'_3 \sin \phi}{c \cos \phi + p^{ref} \sin \phi} \right)^m \quad (\text{B.1})$$

$$E_{oed} = E_{oed}^{ref} \left(\frac{c \cos \phi - \frac{\sigma'_3}{K_0^{nc}} \sin \phi}{c \cos \phi + p^{ref} \sin \phi} \right)^m \quad (\text{B.2})$$

Stiffness parameters based on correlations

In Tables B.1 and B.2 some empirical formulas are given which can be used to determine the stiffness parameters, in case triaxial test results are not (sufficiently) available.

Soil type	E_{oed}^{ref}
Clay (OCR = 1)	$\frac{50000}{I_p}$
Clay (OCR > 1)	$\frac{50000}{I_p}$
Sand (OCR = 1)	$3q_c \sqrt{\frac{p^{ref}}{\sigma_{v0}}}$

Table B.1: Correlations to find stiffness parameter for different soil types

Soil type	E_{50}^{ref}	E_{oed}^{ref}	E_{ur}^{ref}
Clay (OCR = 1)	2	1	5-8
Clay (OCR > 1)	1	1	4
Sand (OCR = 1)	1	1	4

Table B.2: Ratios of stiffness parameters in Plaxis for different soil types. (CUR2003-7, 2003)

Additional information case study 1: Amazonehaven

In this appendix additional and more detailed information of the Amazonehaven is given. This includes more comprehensive descriptions of input values, design calculations and assumptions made for the calculations.

C.1 D-Sheet calculations

In this section, additional information about the calculations performed in D-Sheet is given.

D-Sheet options

- Reduce delta friction angles according to CUR: yes
- For the wall friction angle δ , the relationships $\delta = 2/3 \cdot \phi$ for sand and $\delta = 1/3 \cdot \phi$ for clay have been used, according to CUR166 (2008).
- For the vertical balance check, the following parameters are used in the sheet piling window:
 - Height: 1524mm & 1524mm
 - Coating area: 2.23 & 1.42 mm²/mm²
 - Section area: 193 & 78 cm²/m
 - Max. point resistance: 0 MPa, see p.61 of PDF Gemeentewerken Rotterdam (2011a)
 - Xi-factor: 0.75

Additional information case study 2: soft soil consisting of clay and peat

In this appendix additional information and details about the soil investigation data of case study 2 is given.

D.1 Soil investigation data

In the following figures the results of laboratory tests on soil samples of the reference project CTA in Alblasserdam are given.

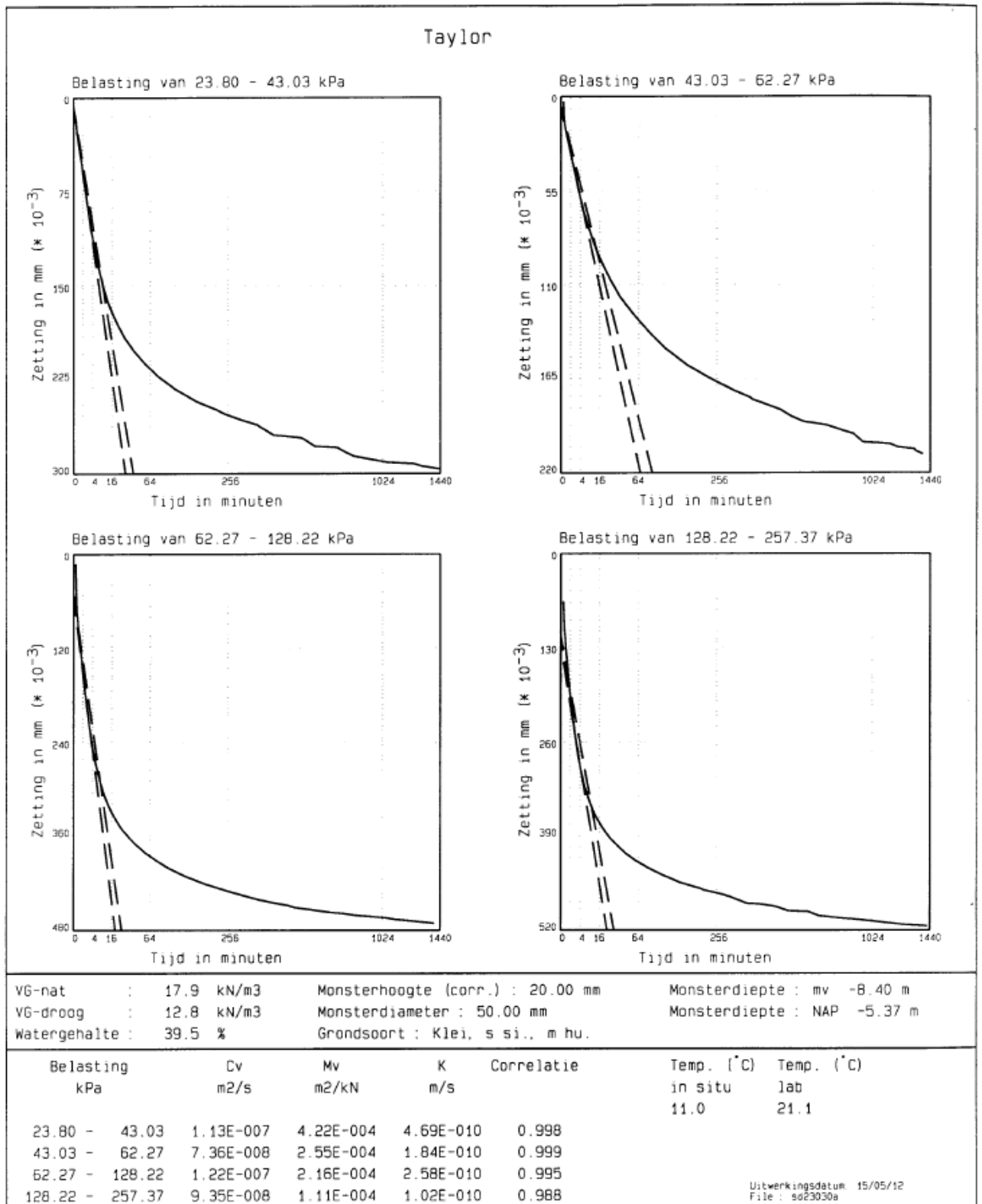


Figure D.1: Results of lab tests onto soft clay from borehole Container Terminal Alblasserdam, part1

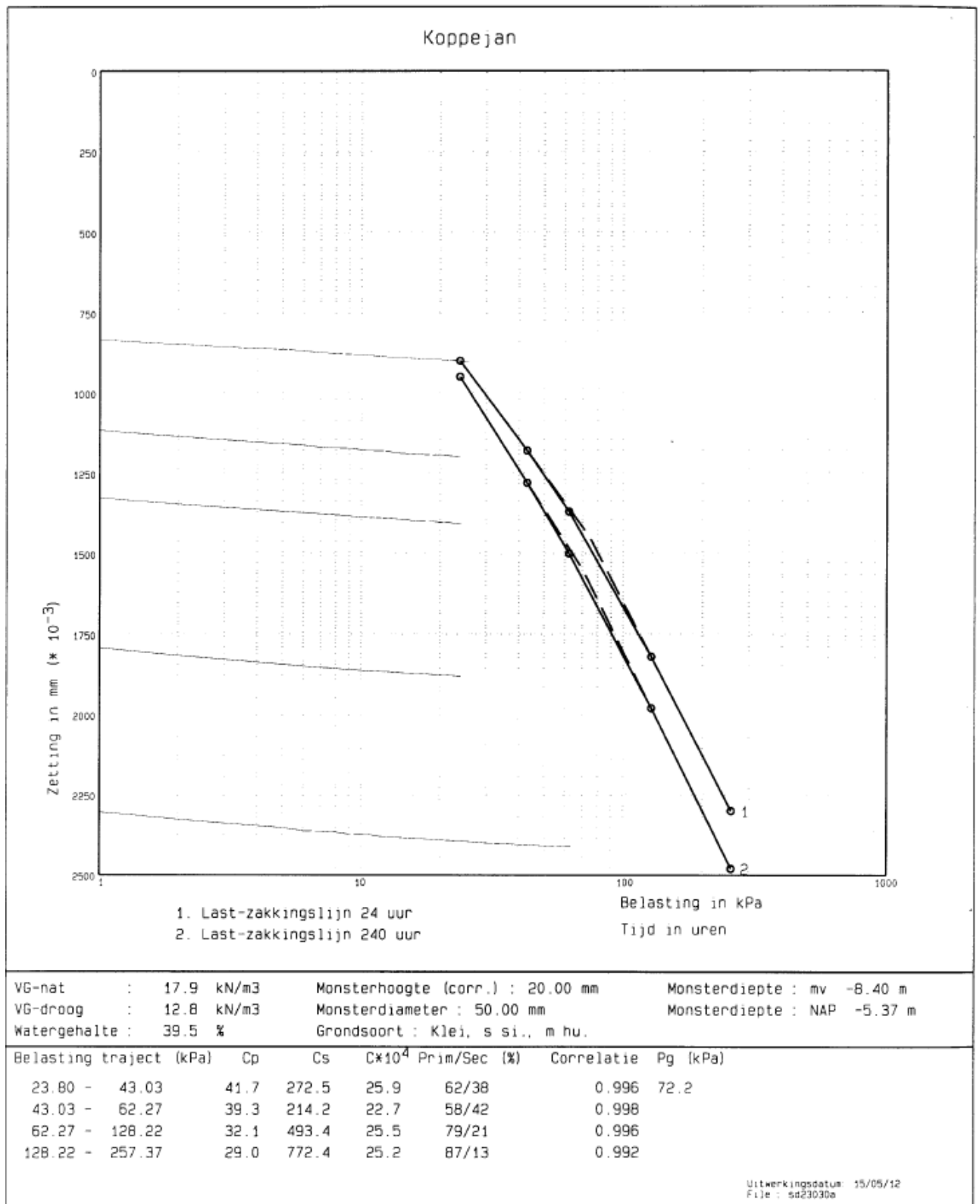


Figure D.2: Results of lab tests onto soft clay from borehole Container Terminal Alblaserdam, part2

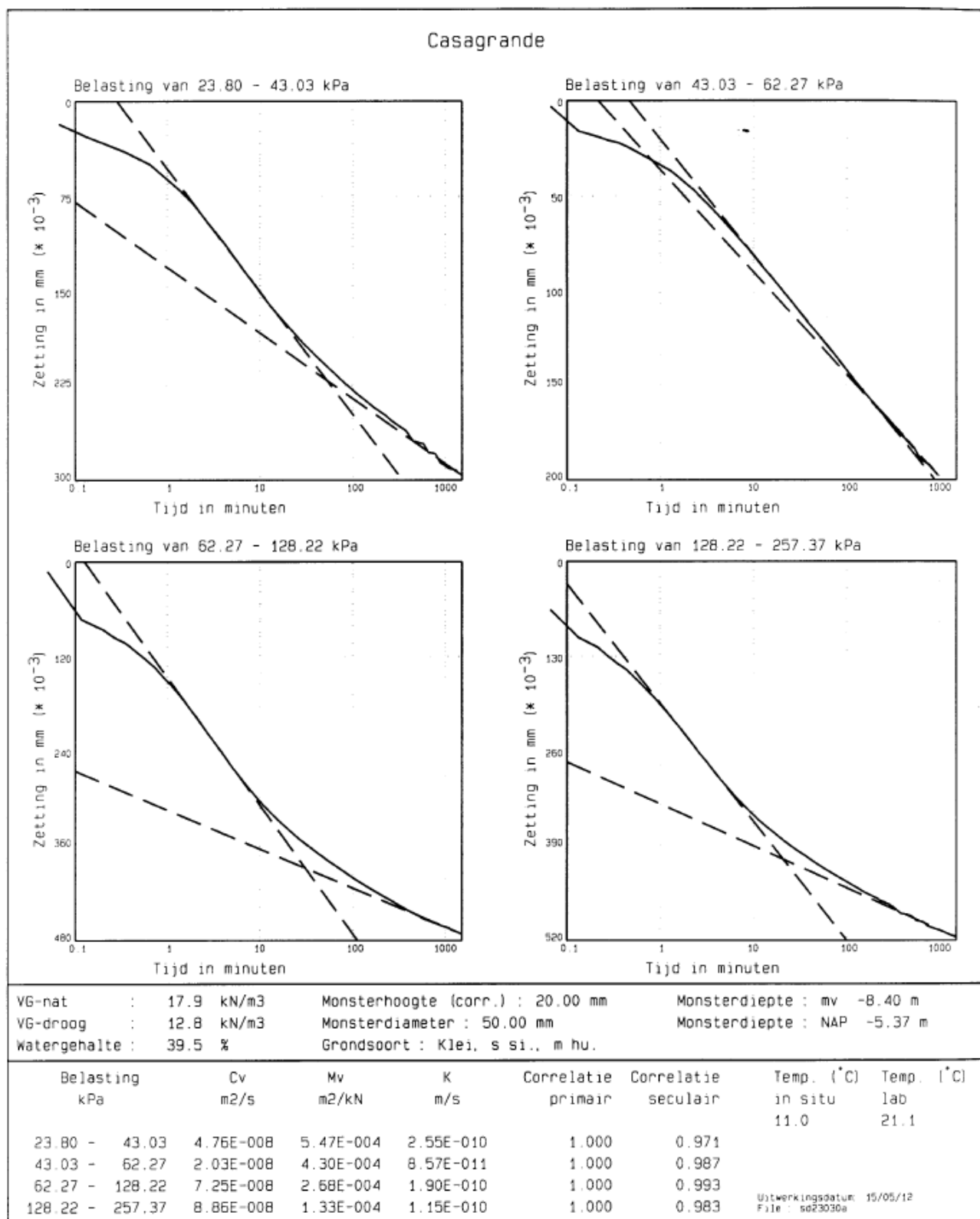


Figure D.3: Results of lab tests onto soft clay from borehole Container Terminal Alblasserdam, part3

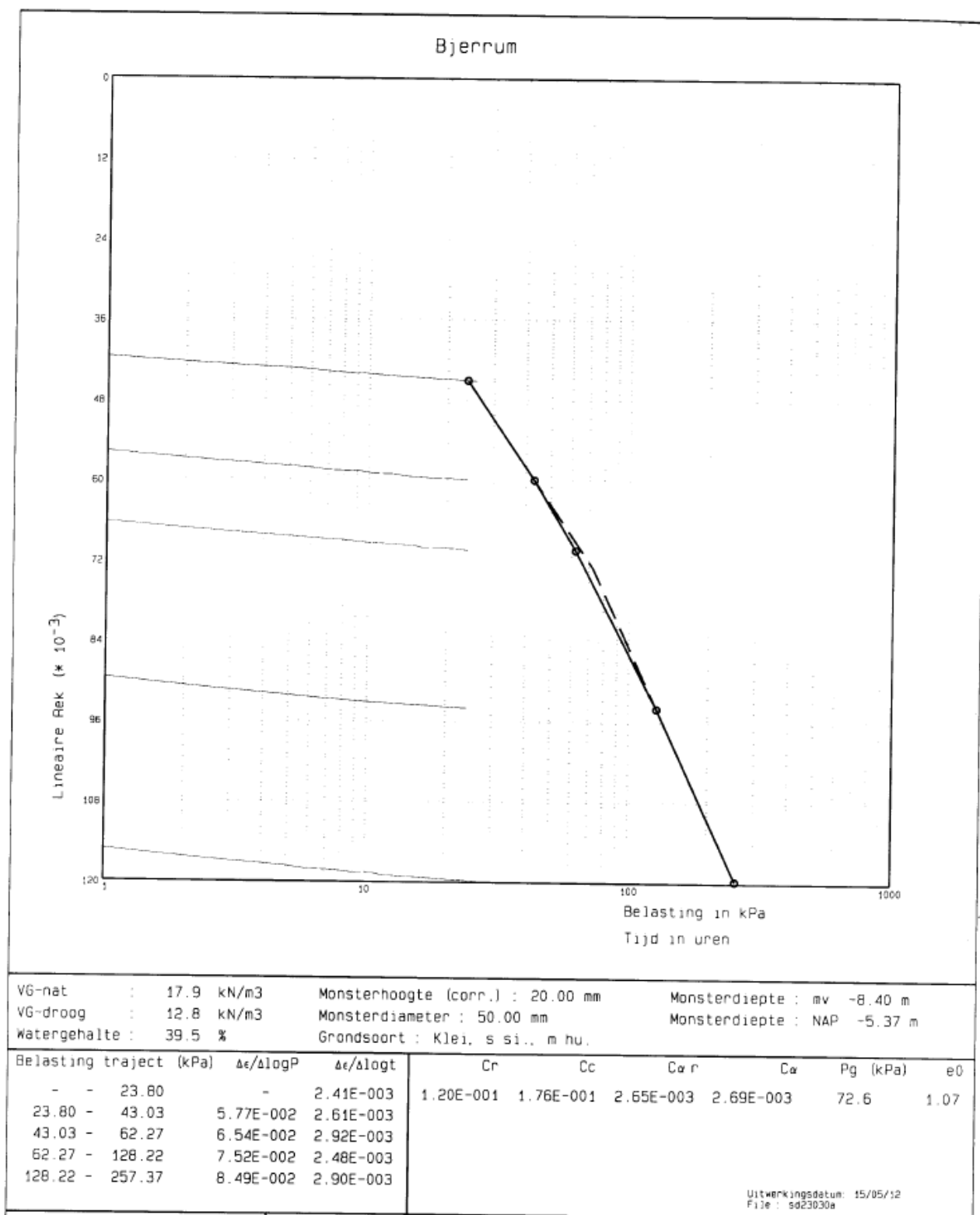


Figure D.4: Results of lab tests onto soft clay from borehole Container Terminal Alblaserdam, part4

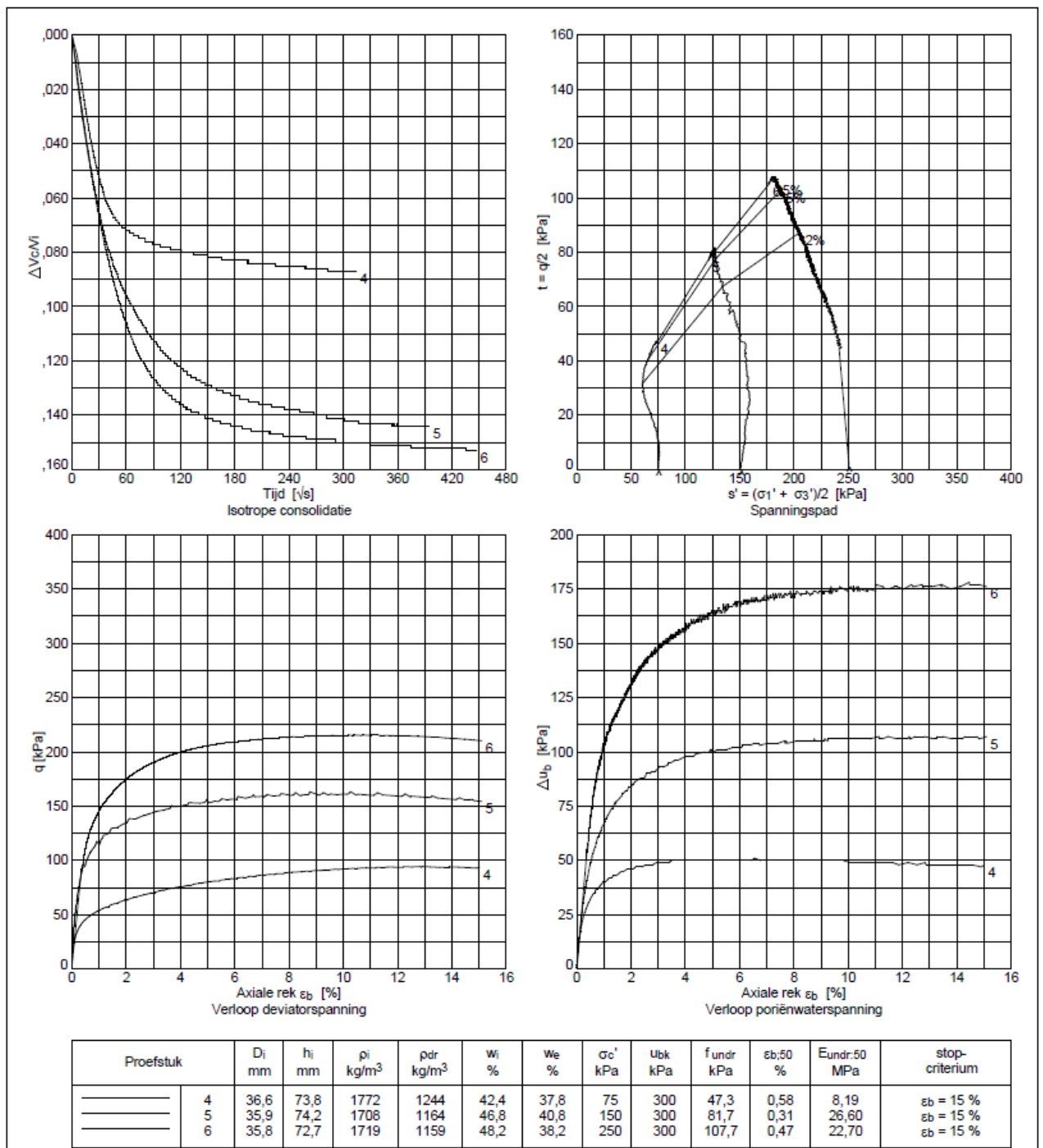


Figure D.5: Results of CU triaxial tests onto soft clay from borehole Container Terminal Alblaserdam, part 1

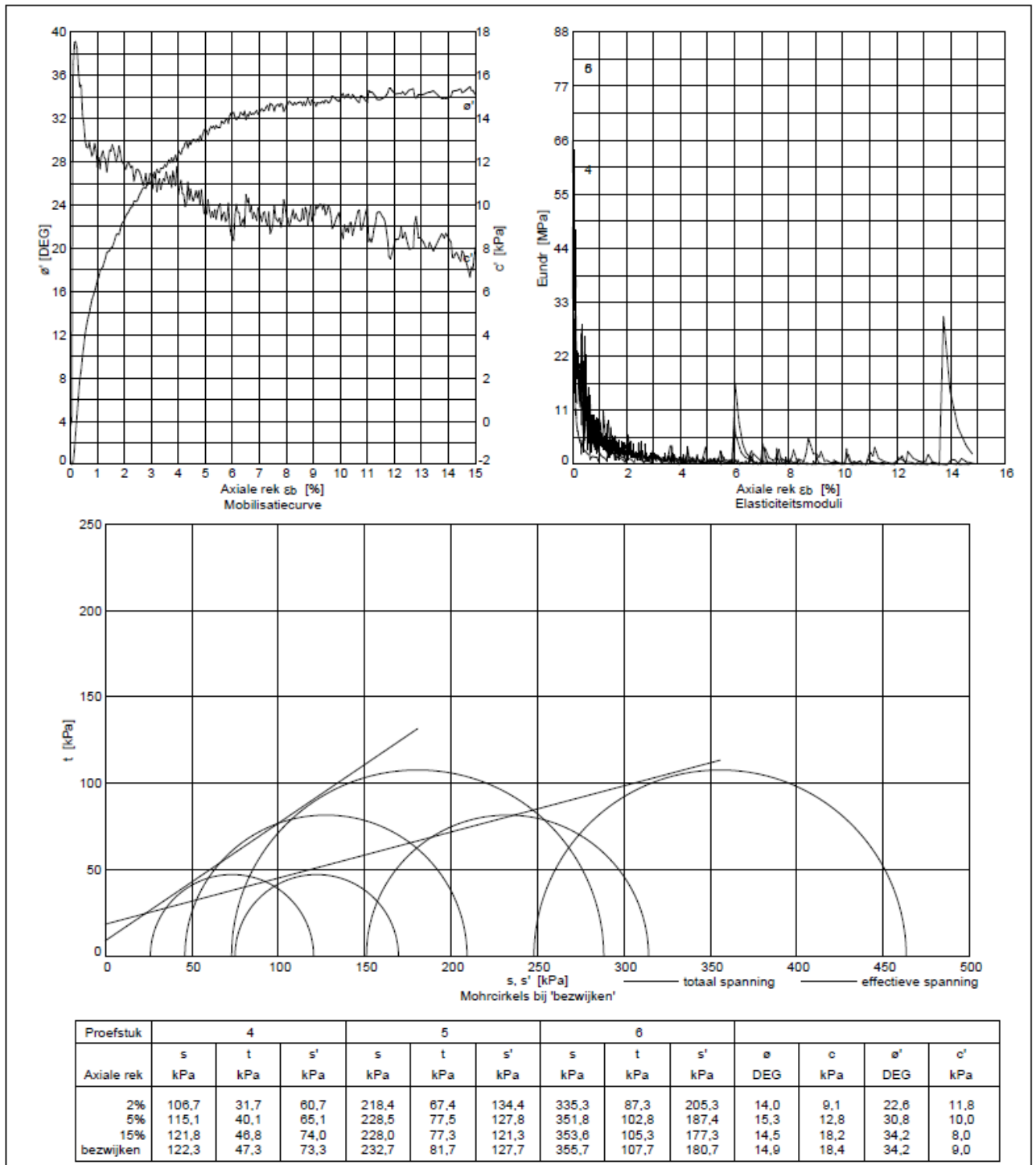


Figure D.6: Results of CU triaxial tests onto soft clay from borehole Container Terminal Ablasserdam, part2

Additional information case study 3: Boulder clay

In this appendix additional information and details about the soil investigation data of case study 3 is given.

E.1 Soil investigation data

In the following figures the results of one borehole of the reference project AZG in Groningen is given. The properties of the boulder clay are of particular interest for this research. Also, for one triaxial compression test the lab results that are used for the parameter determination are presented here.

ONSTER NR	DIEPTE t.o.v. NAP [m]	BODEM PROFIEL	BESCHRIJVING BODEM PROFIEL	DIEPTE TEST t.o.v. NAP [m]	VOLUMIEK GEWICHT			WATER-GEHALTE w [massa %]	PORIEN-GEHALTE n [%]	VERZAD. GRAAD S [%]	ONGEDR. SCHUIFSTERKTE f undr [kPa]	HOEK INWENDING ϕ [°]	COHESIE c' [kPa]
					γ [kN/m ³]	VERZAD. γ_{sat} [kN/m ³]	DROOG γ_{dr} [kN/m ³]						
1	1,0	[diagram]	1,00 Zand (matig fijn), bruin		19,9		16,6	19,9	36,2	93,3			
	0,0		0,20 Klei (vast), grijs										
2	-1,0	[diagram]	-2,50 Zand (zeer fijn), grijs		20,2		17,2	17,6	34,0	90,7			
	-2,0												
	-3,0												
	-4,0												
3	-5,0	[diagram]	-5,00 Zand (fijn), grijs		18,6		14,5	28,1	44,1	94,4			
	-6,0												
	-7,0												
4	-8,0	[diagram]	-8,00 Zand (fijn), zwak grindig, grijs		18,2		14,1	28,9	45,8	90,8			
	-9,0												
	-10,0		-10,50 Zand (fijn), matig siltig, grijs										
	-11,0												
	-12,0												
	-13,0												

Uitvoering : 15.12.1998 Boring bij : DKM123 MV : NAP : 1,00 m. GHG : MV : m.
Pelling PB : Boormaster : Bkh Gemeen GWS : MV : -1,56 m. GLG : MV : m.

BORING VOLGENS NEN 5119
AZG NOORDPUNT GRONINGEN

Figure E.1: Overview of borehole B1,part1

MONSTER NR	DIEPTE t.o.v. NAP [m]	BODEM PROFIEL	BESCHRIJVING BODEM PROFIEL	DIEPTE TEST t.o.v. NAP [m]	VOLUMIEK GEWICHT			WATER-GEHALTE w [massa %]	PORIEN-GEHALTE n [%]	VERZAD. GRAAD s [%]	ONGEDR. SCHUIFSTERKTE f undr [kPa]	HOEK INWEND. WRIJVING ϕ [°]	COHESIE c' [kPa]					
					γ [kN/m ³]	γ_{sat} [kN/m ³]	γ_{dr} [kN/m ³]											
5 6 7 8 9 10	-13,0		-13,00 Klei (vast), donkergrijs, (Potklei)															
	-14,0												17,7	12,5	41,6	51,9	100,0	120,0
	-15,0																	90,0
	-16,0												17,0	11,8	43,5	54,5	96,4	110,0
	-17,0																	
	-18,0												17,7	12,6	40,5	51,5	100,0	130,0
	-19,0																	
	-20,0												17,6	12,6	39,4	51,5	98,3	100,0
	-21,0																	
	-22,0												17,9	13,2	35,1	49,1	96,4	110,0
-23,0																		
-24,0			-24,00 Einde boring															

Uitvoering : 15.12.1998 Boring bij : DKM123 MV : NAP 1,00 m. GHG : MV - m.
 Peiling FB : Boormeester : Dkh Gemeten GWS : MV - 1,50 m. GLG : MV - m.

BORING VOLGENS NEN 5119
AZG NOORDPUNT GRONINGEN

Figure E.2: Overview of borehole B1,part2

ALGEMENE INFORMATIE

Boring	: B1	Proefstuk	: Ongeroerd
Monster	: 7	Monsterklasse	: 1
Diepte	: 16.80 m	Test Methode	: CUMS isotroop

VISUELE CLASSIFICATIE

KLEI zwak siltig zwak humeus zwart

INITIELE EIGENSCHAPPEN	TRAP 1	TRAP 2	TRAP 3	
Hoogte	100.0			mm
Diameter	50.0			mm
Volumiek gewicht	17.5			kN/m ³
Droog volumiek gewicht	12.6			kN/m ³
Vochtgehalte	39.0			%
B-factor	0.80			-
Dichtheid van het korrelmateriaal (geschat)	2.65			t/m ³
NA VERZADIGING				
Verzadigingsspanning	300	300	300	kPa
Droog volumiek gewicht	12.4			kN/m ³
Vochtgehalte	43.5			%
B-factor	0.96			-
NA CONSOLIDATIE				
Horizontale consolidatie spanning	130	260	520	kPa
Verticale consolidatie spanning	130	260	520	kPa
Droog volumiek gewicht	12.8	13.0	13.4	kN/m ³
Vochtgehalte	41.0	39.5	37.5	%
AFSCHUIFFASE				
Axiale reksnelheid	4.0	4.0	4.0	%/uur
Bij maximale deviator spanning				
Effective horizontale spanning	66	158	347	kPa
Effective verticale spanning	215	395	726	kPa
Axiale rek	2.8	2.1	2.4	%
f _{undr}	74	118	189	kPa
ε ₅₀	0.2	0.2	0.3	%
E _{undr;50}	36.6	50.3	62.4	MPa
Bij maximum hoofdspanningsverhouding σ₁'/σ₃'				
Effective horizontale spanning	65	158	347	kPa
Effective verticale spanning	212	395	726	kPa
Axiale rek	2.5	2.1	2.4	%
f _{undr}	73	118	189	kPa
ε ₅₀	0.2	0.2	0.3	%
E _{undr;50}	37.3	50.3	62.4	MPa
EIND CONDITIES				
Bezwijkvorm proefstuk			Meerv. afschuifvlak	
Droge dichtheid			13.4	kN/m ³
Vochtgehalte			37.5	%
BEZWIJK OMHULLENDE				
	maximale deviator spanning	maximale spanningsverhouding	maximale rek alle belastingtrappen	
Effectieve hoek van inwendige wrijving	17	17	17	°
Effectieve cohesie	37	37	36	kPa

Figure E.3: Results of triaxial compression test of boulder clay, sample B1S7

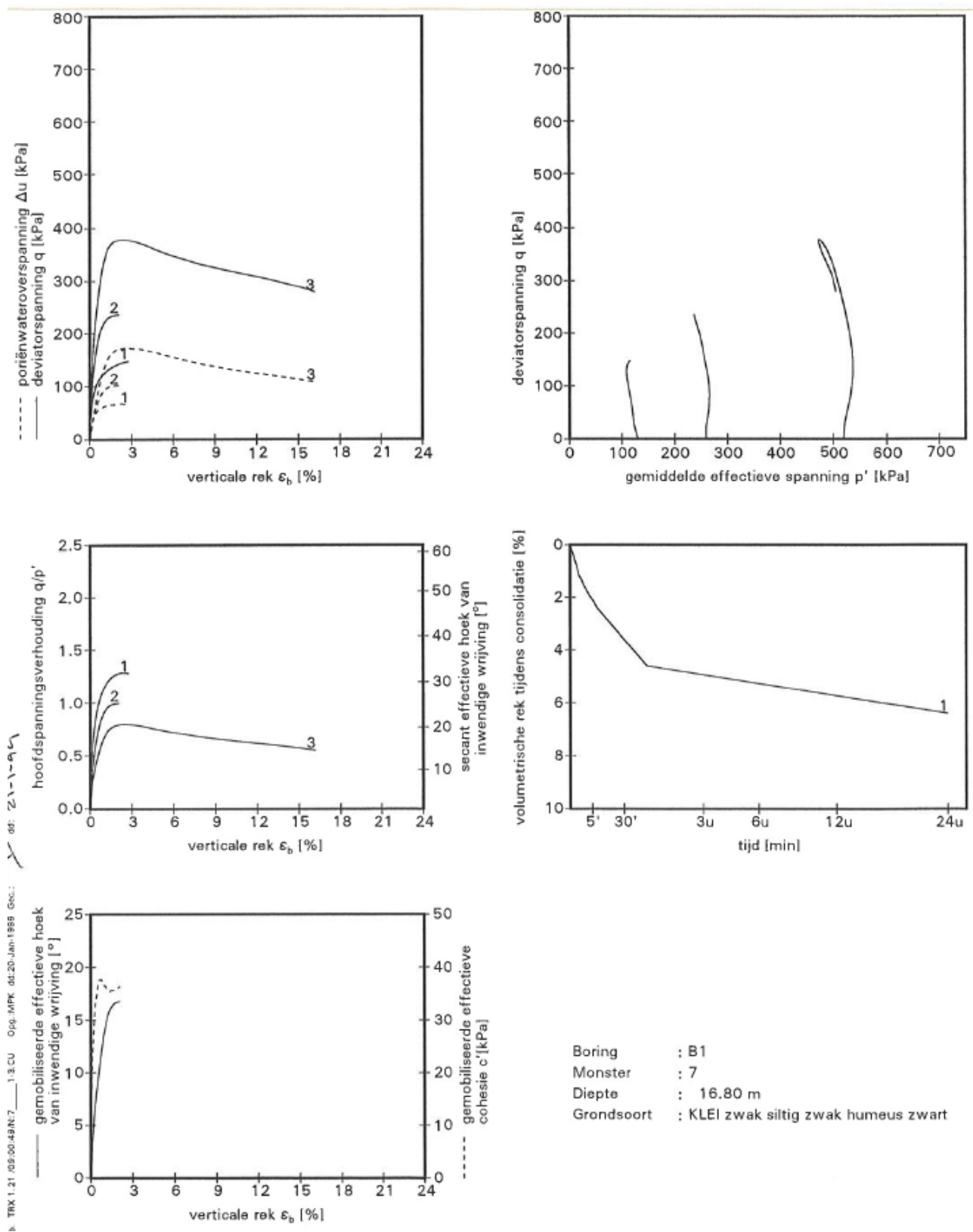
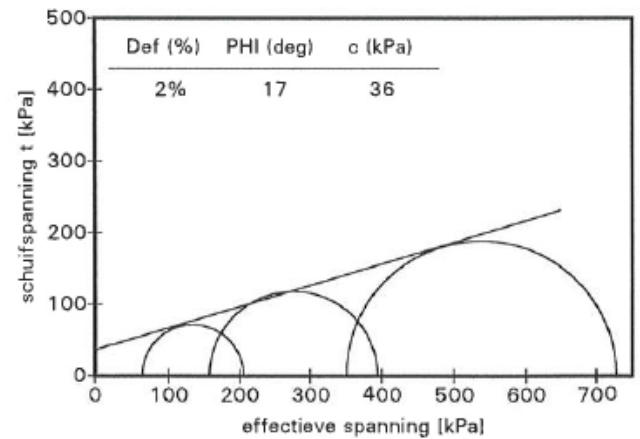
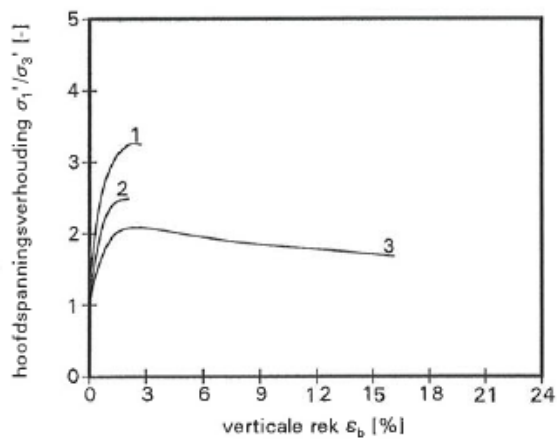
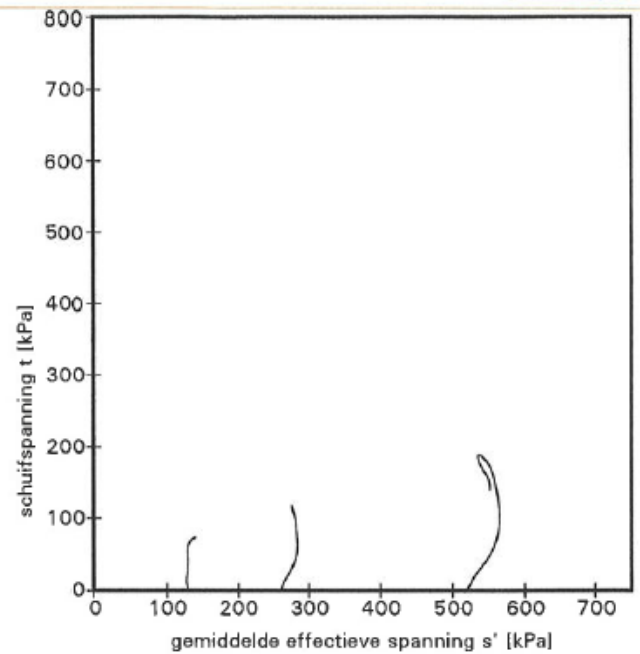


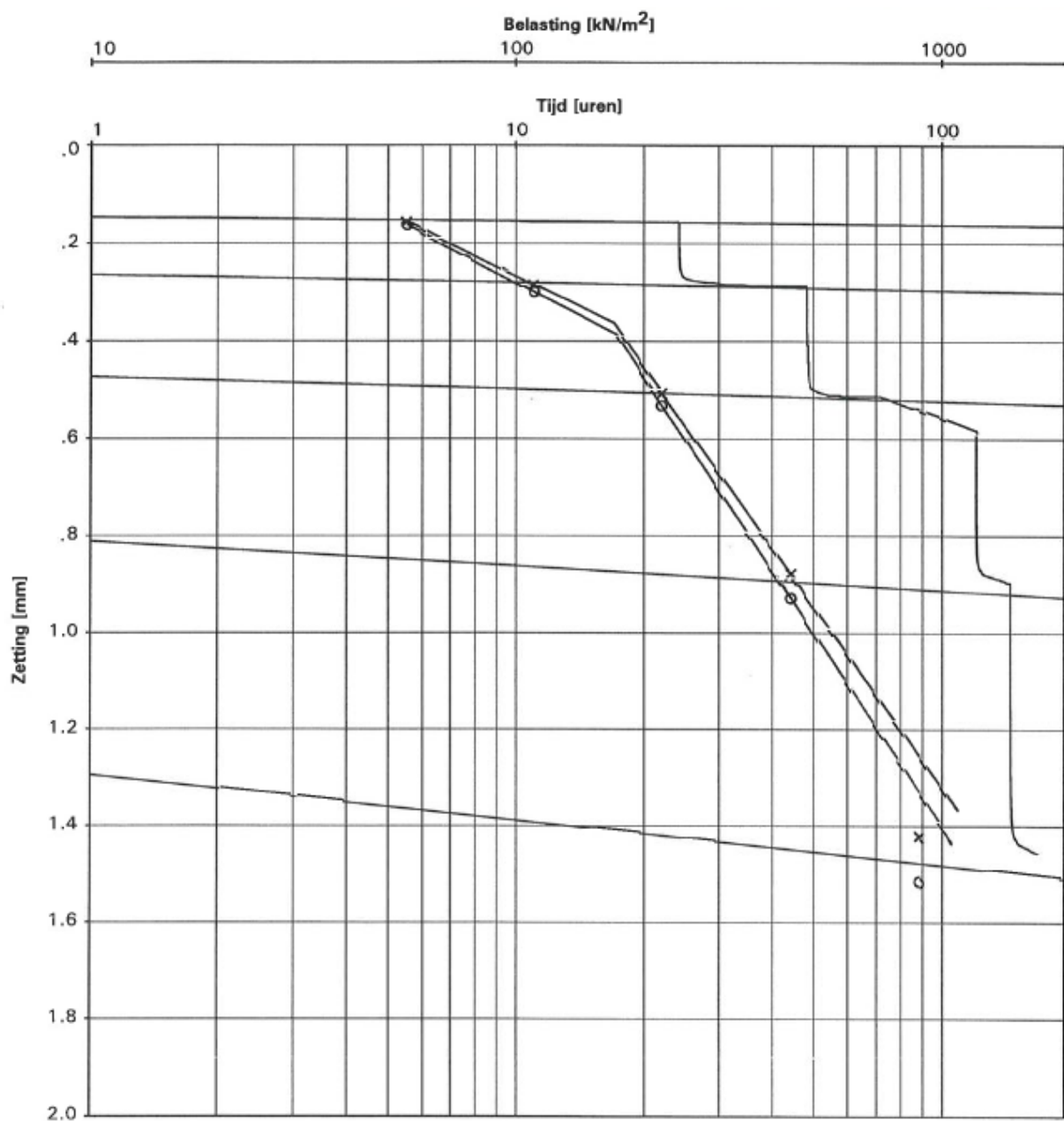
Figure E.4: Results of triaxial compression test of boulder clay, sample B1S7

Axiale rek	Eff. hoek van inwendige wrijving [ϕ']	Eff. cohesie [c'] kPa
0.5%	9	36
1.0%	14	37
1.5%	16	36
2.0%	17	36
3.0%	-	-
4.0%	-	-
6.0%	-	-
Max Def 2.0%	17	36



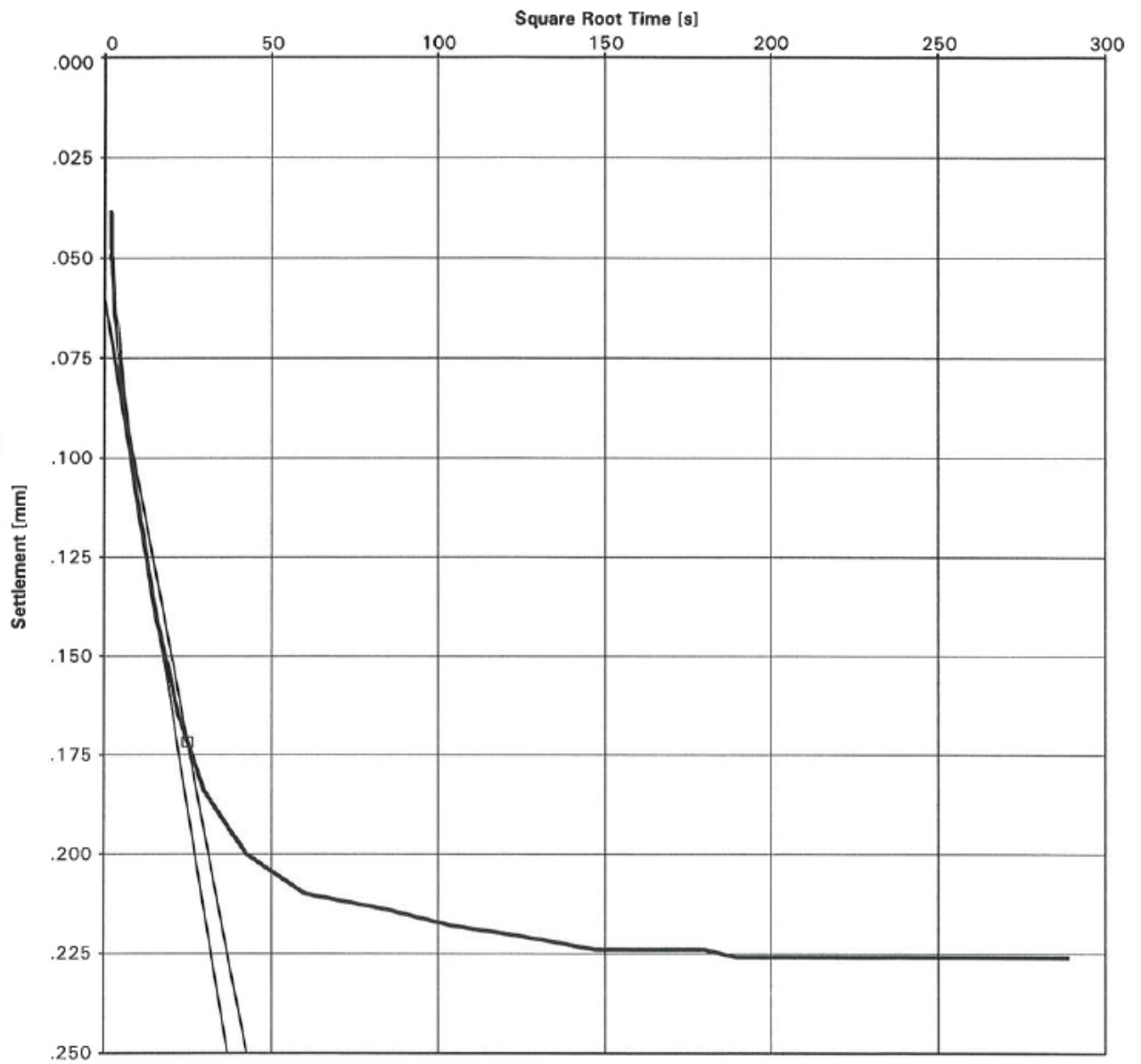
Boring : B1
 Monster : 7
 Diepte : 16.80 m
 Grondsoort : KLEI zwak siltig zwak humeus zwart

Figure E.5: Results of triaxial compression test of boulder clay, sample B1S7



Boring	: B1	C1	=	81.6
Monster	: 7	C2	=	27.5
Diepte-MV	: 16.75 m	Pg	=	171 kPa
Grondsoort	: KLEI, zwak siltig, zwak humeus zwart (potklei)	1/Cp1	=	,0098
		1/Cs1	=	,0006
Vg nat	= 17.0 kN/m ³	1/Cp2	=	,0284
Vg droog	= 11.9 kN/m ³	1/Cs2	=	,0020
Watergehalte	= 42.6 %			
		Hoogte	=	19.0 mm
		Diameter	=	50.0 mm

Figure E.6: Results of a uniaxial compression test of boulder clay, sample B1S7

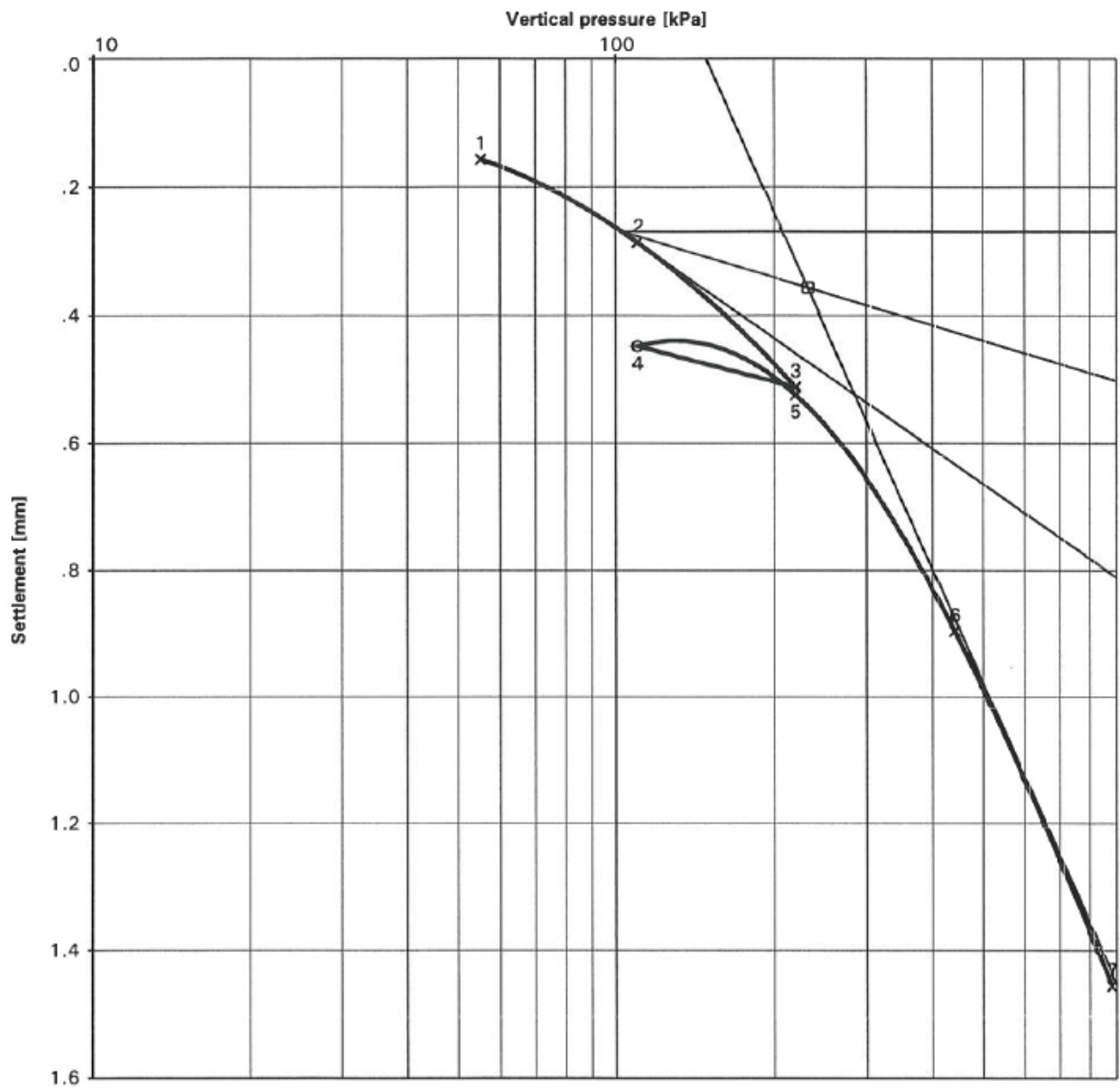


Borehole : B1
 Sample : 7
 Depth : 16.75 m
 Soil type : KLEI, zwak siltig, zwak humeus zwart (potklei)

 Test stage : 3
 Stress P : 220. kPa
 Stress dP : 110. kPa
 Height : 18.714 mm

Consolidation		50	90	%
H	=	.062	.112	mm
H100	=	.124	.124	mm
t	=	146	626	s
c_v	=	1.2E-07	1.2E-07	m ² /s
m_v	=	6.0E-02	6.0E-02	m ² /MN
k_v	=	7.0E-11	7.0E-11	m/s

Figure E.7: Settlement curve of boulder clay, sample B1S7



Borehole : B1
 Sample : 7
 Depth : 16.75 m
 Soil type : KLEI, zwak siltig, zwak
 humeus zwart (potklei)

Wet unit weight = 17.0 kN/m³
 Dry unit weight = 11.9 kN/m³
 Watercontent = 42.6 %

Max. preconsolidation
 pressure P'_c = 231 kPa
 Compression index C_c
 at loads < P'_c = .05
 at loads > P'_c = .21
 Swell index C_s 3- 4 = .02
 Height = 19.0 mm
 Diameter = 50.0 mm

Figure E.8: Z - log p curve of boulder clay, sample B1S7

Bibliography

- BAM Infra. Final design Amazonehaven southside quay wall A1. Document code: 2009-613, 2009.
- BAM Infratechniek Midden-Wet bv. Drawing of location CPT's, boreholes and monitoring wells. Technical drawing belonging to, 2009.
- M. Bolton. The strength and dilatancy of sands. *Geotechnique*, 36(1):65–78, 1986.
- R. Brinkgreve. Selection of soil models and parameters for geotechnical engineering application. *Soil Constitutive Models: Evaluation, Selection, and Calibration*, 1(1):69–98, 2005.
- R. Brinkgreve and S. Panagoulas. Shansep NGI-ADP Material Manual. Technical report, POVM, 2017.
- CUR166. 'Handboek Damwandconstructies'. Technical report, SBRCURnet, 2008.
- CUR2003-7. Determination Geotechnical Parameters. Technical report, Stichting CUR, 2003.
- CUR211. Handbook Quay Walls, Second Edition. Technical report, SBRCURnet, 2014.
- Deltares. D-Sheet Piling User Manual. Technical report, Deltares, 2017.
- O. Dijkstra. Special solutions for construction AZG Groningen. Educom, 2002.
- Fugro GeoServices B.V. Geotechnical investigation broadening Amazonehaven Rotterdam. Reportnr.: 1010-0204-000, 2011.
- Fugro Ingenieursbureau B.V. Drawing of location CPT's, boreholes and monitoring wells. Part of 1010-0204-000, 2010.
- A. Gaba, S. Hardy, L. Doughty, W. Powrie, and D. Selemetas. Guidance on embedded retaining wall design. Technical report, CIRIA, 2017.
- Gemeentewerken Rotterdam. Final design Amazonehaven southside quay wall A1. HH2341-0026-RAP, 2011a.
- Gemeentewerken Rotterdam. Geotechnical report for Amazonehaven quay wall part A1. HH2341-0030-RAP, 2011b.
- A. L. J. H. Grimstad, G. NGI-ADP: Anisotropic shear strength model for clay. *International Journal for Numerical and Analytical Methods in Geomechanics*, 36(666): 483–497, 2011.
- Helpdesk Water. About the legal assessment framework for the primary flood defenses. Accessed October 23rd, 2017a.
- Helpdesk Water. Failure mechanism of macro instability. Accessed October 23rd, 2017b.
- J. Jáky. Minimum value of earth pressure. *Proc. 2nd Int. Conf. Soil Mech. Found. Eng.*, 1948.

- S. Jonkman, R. Jorissen, T. Schweckendiek, and J. van den Bos. Flood Defenses. Technical report, Delft University of Technology, 2018.
- F. R. Ladd, C.C. New design procedure for stability of soft clays. *Journal of the Geotechnical Engineering Division*, 100(7):763–786, 1974.
- E. Meijer. Comparative analysis of design recommendations for Quay Walls. Technical report, Delft University of Technology, 2006.
- N. Mourillon. Stability analysis quay structure at the Amazonehaven, Port of Rotterdam. Technical report, Delft University of Technology, 2015.
- T. Naves and H. Lengkeek. Shansep NGI-ADP validation. Technical report, POVM, 2017.
- Plaxis. 2-D Material Models Manual. Technical report, Plaxis bv., 2018.
- M. Post and M. Luijendijk. POVM parameter determination FEM. Technical report, POVM, 2018.
- POVM BEEM. POVM calculation tools for FEM. Technical report, Deltares, 2018.
- Rijkswaterstaat. Schematiseringshandleiding macrostabiliteit. Technical report, Ministry of Infrastructure and Water Management, 2017.
- T. van Duinen. Back analyses of dikes that withstand a high water level. Technical report, Deltares, 2013.
- T. van Duinen. Undrained shear strength in the assessment of slope stability of water defenses. Presentation, 2016.
- T. van Duinen and H. van Hemert. Stabiliteitsanalyses met ongedraineerde schuifsterkte voor regionale waterkeringen. Educom, 2013.
- P. Vermeer and C. Meier. Stability and deformations in deep excavations in cohesive soils. *Darmstadt Geotechnics*, 1(4):177–192, 1998.
- A. Verruijt. *Soil Mechanics*. VSSD, 2012.
- D. M. Wood. *Soil behaviour and critical state soil mechanics*. Cambridge University Press, 2007.

